University of Alberta

Biological Fate of Chiral Organochlorine Contaminants

by

Nicholas Alexander Warner 

A thesis submitted to the Faculty of Graduate Studies and Research
in partial fulfillment of the requirements for the degree of Doctor of Philosophy

Department of Chemistry

Edmonton, Alberta
Spring 2008

Your file Votre référence
ISBN: 978-0-494-45621-7
Our file Notre référence
ISBN: 978-0-494-45621-7

Abstract

This dissertation discusses the fate of chiral organochlorine (OC) compounds, with particular focus on polychlorinated biphenyls (PCBs), within biological organisms.

Enantiomer enrichment of chiral PCBs was quantified within the Northwater Polynya arctic food web to examine enantioselective metabolisim (biotransformation) of chiral PCBs in arctic biota. No enantiomer enrichment was found in lower trophic level organisms; however, extensive enrichment was observed within seabirds and marine mammals at higher trophic levels, indicating enantioselective biotransformation had occurred. These findings provide insight into the metabolic capacity of arctic biota, which could not be previously determined using achiral techniques.

The fate of chiral PCBs was investigated in lower trophic level organisms to assess their contribution to enantiomer enrichment observed in higher trophic level organisms. Enantiomer enrichment of several chiral OC compounds was observed in the freshwater invertebrate, *Mysis relicta* after laboratory exposure to racemic chiral OC compounds. Enantioselective formation of chiral OC metabolites suggests these organisms have the metabolic capacity to degrade chiral OC compounds enantioselectively. These findings suggest that enantiomer enrichment within higher trophic level organisms may also be attributed to dietary uptake of lower trophic level organisms.

In vitro metabolism of chiral PCBs by rat and human cytochrome P-450 enzymes (CYP) was investigated to gain insight into the mechanism of enantiomer enrichment. Enantioselective degradation was observed for several chiral PCBs following incubation with rat CYP 2B1 and human CYP 2B6 isozymes. Unambiguous identification of hydroxylated metabolites (OH-PCBs) shows enantioselective degradation of chiral PCBs is due to

metabolism. Enantiomer enrichment observed for chiral PCBs *in vitro* is similar to enrichment found within rat and human tissues, suggesting that metabolism could be responsible for enantiomer enrichment observed within organisms. Analysis of individual enantiomer kinetics indicates that metabolism occurs for both enantiomers, but at different rates, resulting in enantiomer enrichment.

Acknowledgements

I would like to thank my supervisor, Dr. Charles S. Wong for his mentorship and guidance throughout my time spent here at the University of Alberta. My development as a young scientist in the area of environmental research has greatly benefited from his advice. I will always be appreciative for his time and effort spent on my training.

To my fellow colleague and good friend, Dr. Ross J. Norstrom, thank you for your sound advice and friendship which has helped me through the challenges that both graduate studies and life. I am very thankful of the friendship we have and will cherish it always.

The tremendous support provided by my family to help me find the strength to push through the hard times of my graduate studies. I would particularly like to thank my mother for always being an ear to listen to my problems and her advice to get me through those impossible days.

I would like to thank all of the Wong group members for their help and support through my dissertation. To my good friends B. A., M. R., C. G., B. Y. and M. N., thank you for all your support. My time in Edmonton would not have been the same without you. I particularly like to thank B. B. for her help and support through this difficult time.

Finally, I would like to thank the funding agencies that made that made the research presented within this dissertation possible: Natural Sciences and Engineering Research Council, the University of Alberta, and the 2003 Early Career Award for Applied Ecological Research presented to Dr. Charles Wong, cosponsored by the American Chemical Society and the Society of Environmental Toxicology and Chemistry (SETAC). I would also like to thank SETAC for awarding me travel awards, thus providing me the opportunity to present my research at their annual conference in 2003 and 2004.

Table of Contents

List of Figures

List of Tables

Abbreviations

PCB	polychlorinated biphenyl
DDT	dichlorodiphenyltrichloroethane
HCH	hexachlorocyclohexane
OC	organochlorine
$\Delta^{\ddagger}G$	rotational energy barrier
CYP	cytochrome P-450
$MeSO_2$-PCB	methyl sulfone polychlorinated biphenyl
OH-PCB	hydroxylated polychlorinated biphenyl
NOW	Northwater Polynya
LC	liquid chromatography
GC	gas chromatography
MDGC	multidimensional gas chromatography
MS	mass spectrometry
MS/MS	tandem mass spectrometry
GC/HRMS	gas chromatography high resolution mass spectrometry
ECD	electron capture detection
BMF	biomagnification factor
TMF	trophic magnification factor
GPC	gel permeation chromatography

Foreword

Persistent organic pollutants (POPs) are chemicals resistant to chemical and biological weathering processes, and can accumulate in various compartments within the environment upon their release [1]. One particular class of POPs that have been extensively studied is the synthetically produced organochlorine (OC) compounds, which were heavily used within the agricultural and industrial sectors. For example, chemicals such as DDT, chlordane, and hexachlorocyclohexane (HCH) were used as insecticides to protect crops and help prevent the spread of diseases such as malaria by insects [2]. Other chemicals such as polychlorinated biphenyls (PCBs) were utilized in many facets of industry ranging from additives in various products as well as dielectric and heat transfer fluids in industrial processes to increase their efficiency [3]. However, the ability of OC compounds to distribute globally [4, 5], and accumulate within biological organisms [6, 7] has led to decades of research in understanding their fate within the environment.

Within the last decade, chiral analysis has provided insight into the biological processing of OC compounds. Several OC compounds contain chiral centers or a plane of asymmetry, allowing them to exist as non-superimposable stereoisomers, or enantiomers under environmental and biological conditions [8, 9]. Enantiomers have the same atom connectivity, thus their physical and chemical properties will be identical; however, biological and toxicological properties can differ [10-13], making them powerful tracers of biological activity. The synthesis of chiral OC compounds was generally not a stereoselective process, thus production and subsequent release into the environment occurred in racemic proportions. However, enantiomer enrichment of chiral OC compounds has been reported in biological organisms, indicating that some form of biological processing

has occurred [9, 14-18]. Several processes such as metabolism (biotransformation), selective protein binding, and tissue transport may be responsible for enantiomer enrichment of chiral OCs within biota, but the mechanism(s) are still poorly understood. Although several chiral OC compounds exist within the environment in non-racemic proportions, the focus of this dissertation will be primarily on PCBs.

The hypothesis of this dissertation is that metabolism is responsible for enantiomer enrichment of chiral PCBs within biological organisms. Given the accumulation potential and the possible toxicity differences that exist between individual enantiomers, knowledge of the processes affecting enantiomer enrichment within organisms is needed.

Chapter 1 is a critical review of the literature regarding chiral PCBs. This chapter will discuss the analytical methodology for separation and detection of PCB enantiomers, fate within various environmental compartments, metabolism and enantioselective toxicity of chiral PCBs and their metabolites.

Chapter 2 discusses research investigating the fate of chiral PCBs within an arctic food web. Enantiomer enrichment quantified for chiral PCBs within organisms occupying various trophic levels of the food web is presented. Processes contributing to enantiomer enrichment such as enantioselective metabolism and dietary uptake in higher trophic level organisms (i.e., seabirds and marine mammals) are discussed. This study was a collaboration with Aaron Fisk and Ross Norstrom, who were responsible for sample collection and processing, with data analysis and interpretation by the author of this dissertation.

Chapter 3 discusses the enantiomer enrichment of chiral OC compounds within lower trophic level organisms. Laboratory experiments investigating enantioselective metabolism of chiral OC compounds within the fresh water invertebrate *Mysis relicta* are presented.

Metabolic capacity of lower trophic level organisms is discussed as well their contribution to enantiomer enrichment of chiral OC compounds within higher trophic level organisms.

Chapter 4 discusses the metabolism of chiral PCBs and the formation of their hydroxylated metabolites (OH-PCBs) *in vitro* using rat and human cytochrome P-450 (CYP) isozymes. The mechanism for enantioselective metabolism within rats and humans is discussed. Factors affecting metabolism and subsequent enantiomer enrichment are also discussed. Identification of unknown OH-PCBs produced from the metabolism of rat and human CYP enzymes is also presented.

Chapter 5 summarizes the findings of the research presented in this thesis and discusses future directions and considerations in regards to fate of chiral OC contaminants within biological organisms.

Chapter 1: Use of chirality in understanding the biochemical weathering of polychlorinated biphenyls[1]

History of Polychlorinated Biphenyls

Since their production began in 1929, polychlorinated biphenyls (PCBs) have historically been a class of chemicals heavily used in industry. These chemicals were manufactured as mixtures containing over 209 individual PCB congeners with varying degrees of chlorine substitution around the biphenyl core (Figure 1). Although several naming systems have been used to identify individual congeners and were recently reviewed by Mills et al. [19], the most commonly used system is that introduced by Ballschmiter and Zell (BZ system) [20]. This entailed sorting the congeners based on their degree of chlorine substitution (mono- to decachlorobiphenyls) and assigning each congener a number from 1-209. Various modifications and updates have occurred to the BZ system, which is more commonly referred to as the IUPAC system.

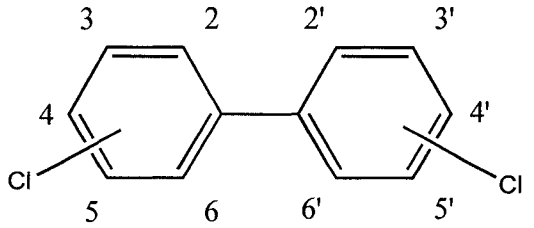

Figure 1. Structure of PCBs. Numbered carbon atoms represent possible sites of chlorine substitution

[1] A version of this chapter has been submitted for publication as part of an upcoming book chapter. Wong, C. S. and Warner, N. A. 2008. Chirality as an Environmental Forensics Tool, in *Persistent Organic Pollutants: Current Issues and Future Challenges* (Harrad, S. J. editor), Blackwell Publishing. Oxford, UK.

Desirable physical/chemical properties such as thermal/chemical stability and electrical insulating properties led to widespread use of PCB mixtures in industry as dielectric fluids, heat transfer and industrial fluids, flame retardants, and as additives within the polymer and paper industry [21]. Although these properties were advantageous for such industrial uses, they were disastrous from an environmental standpoint. The semi-volatile nature of PCBs allowed them to be transported great distances from their source of production through numerous volatilization and deposition steps [5]. After release into the environment, PCBs can partition to environmental compartments with higher organic content such as sediment/soil [22, 23], particulate matter [24], and biological organisms [6, 7, 25] due to their hydrophobic/lipophilic properties [26]. Once within these compartments, PCBs accumulate and persist due to their chemical stability towards environmental degradation processes. Though the production of PCBs halted in the late 1970s, these chemicals are still found today within the environment due to their extreme persistence. Studies have established that bioaccumulation of PCBs occurs within food webs [6, 7, 27, 28] due to their high affinity towards lipids, increasing lipid content within organisms, and continual environmental exposure, resulting in higher PCB contaminant burden at higher trophic levels which has been linked to various toxic effects reviewed by Safe et al. [29].

PCB Atropisomers

From the 209 PCB congeners that can be synthetically produced, 78 are asymetrically substituted about their long axis and can exist as non-superimposable stereoisomers, or enantiomers. Although these congeners exhibit axial chirality, only 19 of these congeners (atropisomers) are predicted to be stable under environmental and physiological conditions (Table 1) [8]. The stability of these atropisomers is attributed to the steric hindrance

provided by multiple *ortho*-substitution around the central carbon-carbon bond. Congeners having 3 to 4 *ortho*-substituted chlorine atoms greatly increase the rotational energy barrier ($\Delta^{\ddagger}G$ = 177 to 246 kJ/mol) [30, 31], thus preventing racemization and allowing atropisomers to exist in their non-planar conformations under environmental and physiological conditions.

Table 1. Stable PCB atropisomers at environmental and physiological conditions

PCB	Ring substitution
45	2,2′,3,6
84	2,2′,3,3′,6
88	2,2′,3,4,6
91	2,2′,3,4′,6
95	2,2′,3,5′,6
131	2,2′,3,3′,4,6
132	2,2′,3,3′,4,6′
135	2,2′,3,3′,5,6′
136	2,2′,3,3′,6,6′
139	2,2′,3,4,4′,6
144	2,2′,3,4,5′,6
149	2,2′,3,4′,5′,6
171	2,2′,3,3′,4,4′,6
174	2,2′,3,3′,4,5,6′
175	2,2′,3,3′,4,5′,6
176	2,2′,3,3′,4,6,6′
183	2,2′,3,4,4′,5′,6
196	2,2′,3,3′,4,4′,5,6′
197	2,2′,3,3′,4,4′,6,6′

At least 9 of the stable PCB atropisomers are considered to be environmentally relevant (Figure 2) due to their presence within commercially produced mixtures [32, 33] and their detection within environmental samples[17, 18, 34-57].

The synthesis of PCBs is not a stereoselective process. It involves reaction of biphenyl with chlorine gas under high temperature conditions [21]. The individual enantiomers of chiral PCBs will be produced in equal amounts; therefore initial

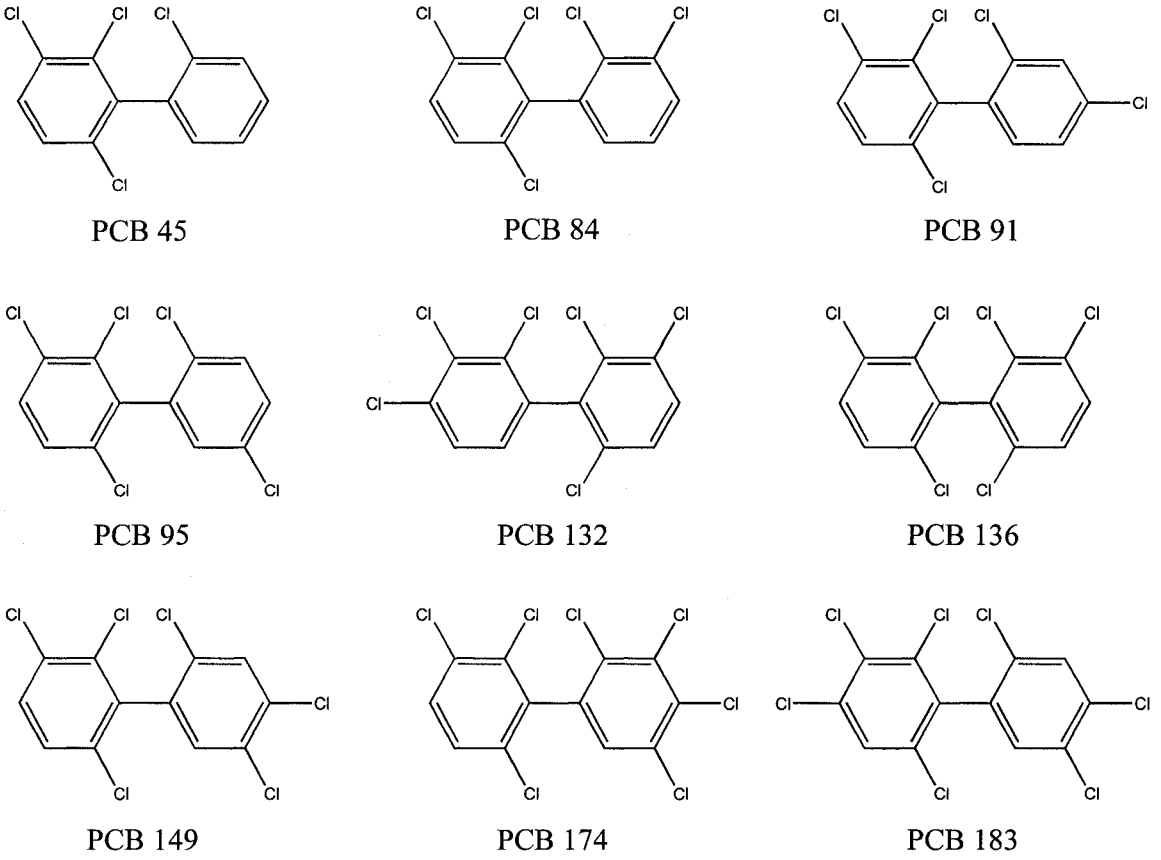

Figure 2. Environmentally relevant PCB atropisomers

contamination of chiral PCBs to the surrounding environment occurs as the racemate. The physical/chemical properties of the individual enantiomers will be the same (i.e., hydrophobicity, vapour pressure), thus their partitioning and uptake into environmental compartments will be identical; however, biological [12, 13] and toxicological [10, 11] properties between individual enantiomers might differ. Enantiomer enrichment of PCB atropisomers has been observed in various organisms within the surrounding environment [17, 18, 35, 36, 38-41, 43, 45-48, 50-54, 57, 58]. Therefore, understanding the fate of the

chiral PCBs is important to assess the exposure to the individual enantiomers that may pose a greater toxicological risk.

Analytical Separation, Detection, and Quantification of PCB Atropisomers

The first separation of PCB atropisomers was reported in 1985 by Mannschreck et al., where enantiomers of PCBs 88, 139, and 144 were separated using (+)-poly(tritylmethacrylate) and triacetylcellulose as sorbents by reversed-phase liquid chromatography (LC) [59]. Future development of new stationary phases saw dramatic improvement in the separation of PCB atropisomers, where studies by Haglund and co-workers were able to separate PCBs 84, 131, 132, 135, 136, 144, 149, 174, 175, 176, and 196 by LC using permethylated β-cyclodextrin derivatized silica (Nucleodex β-PM) and a (+)-polydiphenyl-2-pyridylmethylmethacrylate (Chiralpak OP(+)) as stationary phases [31, 60]. Future studies by Reich and Schurig separated the enantiomers of PCB 45 and 95 as well as improved the resolution between other PCB atropisomers using a β-cyclodextrin stationary phase (ChiraDex) [61]. Separation of the chiral PCB enantiomers by LC has produced enantiomer pure/enriched standards, which have been used to determine chromatographic elution order of the individual enantiomers based on their optical rotation [62] as well as study enantiomer specific toxicity within animals [10, 11].

Though LC has proven useful in the separation of PCB atropisomers, gas chromatography (GC) has been the preferred analytical technique due to its higher separation efficiency. Separation of PCB atropisomers by GC has primarily utilized cyclodextrin-based stationary phases. Cyclodextrins are cyclic oligosaccharides (Figure 3a) and can be distinguished based upon the number of glucose units (i.e., α-cyclodextrin with 6 glucose units, β-cyclodextrin with 7, and γ-cyclodextrin with 8) [63]. Hydrogen bonding between the

substituted hydroxyl groups at C_2 and C_3 of adjacent glucose units allows cyclodextrins to form a rigid toroid geometry (Figures 3b); however, due to their polarity and crystalline structure, cyclodextrins are not suitable as GC stationary phases in their native form. Partial derivatization of hydroxyl groups at C_2, C_3, and C_6 can decrease cyclodextrin polarity, making them amendable for use as GC stationary phases, but also alters the shape of the cyclodextrin. The distorted geometry of the modified cyclodextrin provides a cavity selective to the particular spatial orientations of an analyte and thus can discriminate between individual enantiomers [64]. Regioselective modification based on different chemical properties of the C_2, C_3, and C_6 hydroxyl groups can produce a vast number of cyclodextrin derivatives, each possessing its own unique enantioselectivity [65]. This has been observed within the literature, where the first reported gas phase separation of PCB atropisomers used octakis-(2,6 di-*O*-methyl-3-*O*-pentyl)-γ-cyclodextrin to separate PCBs 45, 95, and 139 [66]. Studies by Schurig and Glausch showed enantiomer separation could be achieved for PCBs 84, 91, 95, 132, 136, and 149 using a permethyl 2,3,6-tri-*O*-methyl β-cyclodextrin bonded to polysiloxane (Chirasil-Dex) [67], demonstrating the enantioselectivity differs between substituted cyclodextrins.

Commercially available cyclodextrin-based stationary phases can resolve most of the individual enantiomers of the chiral PCBs; however, other chromatographic challenges exist for the analysis of PCB atropismers within environmental samples. Environmental analysis of PCBs is not trivial because more than half of the 209 congeners persist within the surrounding environment. Due to this complexity, the chance of co-elution of the PCB atropisomers with other PCB congeners dramatically increases, making quantification of the individual enantiomers difficult. When one-dimensional GC fails in resolving the PCB

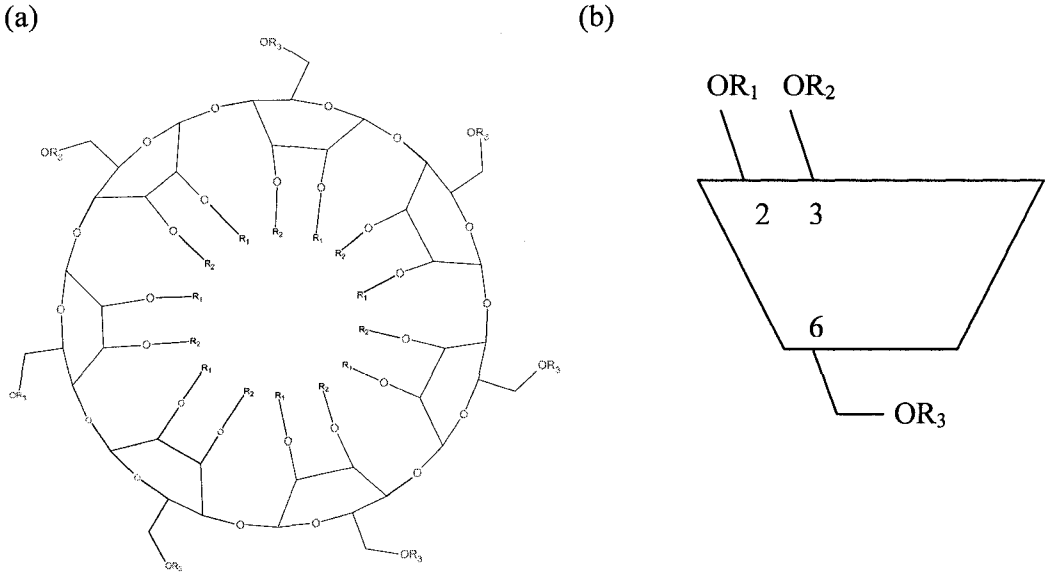

Figure 3. Structure of cyclodextrins. (a) General structure of a β-cyclodextrin. (b) 2D structure of cyclodextrin. Number designation 2, 3, and 6 represents C_2, C_3, and C_6, respectively.

atropisomers from other congeners, multidimensional GC (MDGC) has been used to improve resolution to quantify PCB atropisomers within environmental samples [17, 18, 36, 37, 52, 53]. Chiral separation by this technique is preceded by separation of the sample using an achiral column, where the appropriate chromatographic region from the achiral separation is diverted (heart-cutting) onto a chiral column to obtain enantiomer separation. This method drastically reduces the complexity of the sample diverted onto the chiral column providing confident peak assignment and quantification of individual enantiomers. However, lack of retention data for PCBs on various stationary phases, achiral retention time variability, accuracy of heart-cutting; long retention times, quantification by internal standards as well as cost poses challenges to using MDGC for environmental analysis [68].

Liquid chromatography combined with GC has also been used as a multidimensional technique. Fractionation of PCBs by LC followed by chiral GC analysis can drastically reduce the co-elutions that may occur with the PCB atropisomers and has been demonstrated within dolphin, porpoise, and human liver tissues [46, 47, 69]; however, more sample preparation time is need to perform chiral analysis by this method.

The use of multiple stationary phases with atropisomers is another means of eliminating co-elution problems. A comprehensive study by Wong and Garrison showed that 11 of the stable PCB atropisomers can be separated from other interferences using 6 different cyclodextrin-based stationary phases within commercial PCB mixtures and sediment [42]. Although this method does not require the use of costly multidimensional techniques, it does require multiple injections on various chiral stationary phases to quantify the separated PCB atropisomers accurately.

Enantiomer enrichment of PCB atropisomers within environment samples is often expressed as an enantiomer fraction (EF) [70], defined as:

$$EF = \frac{E1}{E1+E2} \qquad \text{or} \qquad \frac{(+)}{(+)+(-)} \qquad (1a,b)$$

where E1 and E2 represent the concentration of the first and second eluting enantiomers, respectively, if the elution order is unknown on a given stationary phase. If the elution order is known, then EF is calculated as the concentration of the (+)-enantiomer over the summed concentrations of both enantiomers. If no enantiomer enrichment has occurred (i.e., racemic mixture), the enantiomer fraction will equal 0.5. Quantification of EFs greater or less then 0.5 suggests enantioselective processing has occurred within the sample or within the

underlying food web followed by bioaccumulation for biota samples. Earlier studies have used enantiomer ratios (ER = (+)/(-) or E1/E2) to describe enantiomer enrichment of chiral PCBs within environmental matrices [17, 37, 39, 44]. However, several drawbacks exist when using ERs to describe enantiomer enrichment. Ratios are a function of a multiplicative scale and produce skewed data resulting in biased ER values that can range from 0 to infinity. With no upper boundary, a unit change in ER in one direction is not equivalent to the same change in the opposite direction, causing biased graphical representations and statistical analysis [70, 71].

The ability of GC to be combined with sensitive and selective gas phase detectors is advantageous for determining the EFs of PCB atropisomers within environmental samples. Electron capture detection (ECD) is ideal for the detection of chiral PCBs due to its sensitivity towards halogenated compounds and has been used to investigate enantiomer enrichment within sediment [37], arctic fox and polar bears [48], sharks [18], and human milk [72]. The drawback of using this method for detection of chiral PCBs is its relatively poor selectivity and inability to distinguish PCBs from other electronegative components within the sample (including other PCB congeners), which could lead to errors in quantifying EFs. Studies have utilized MDGC techniques to help eliminate co-elution problems [17, 18, 36, 37, 48, 53, 69, 72] for ECD analysis. However, the use of selective detectors such as mass spectrometers has become the dominant method of detection for environmental analysis of PCBs.

Mass spectrometry (MS) combines both selectivity and sensitivity (ng to pg range) where PCB atropisomers are detected based on their mass to charge ratio (*m/z*), and thus reduces the chance of interferences from co-eluting chemicals. Although this method of

detection is mass selective, interferences can still occur with sample components that share the same *m/z* ratio or other PCB congeners that contain the same degree of chlorination (homologue group). Wong and Garrison showed the separation of several PCB atropisomers on various chiral stationary phases can be performed using direct chiral GC/MS analysis, without co-elution with other congeners from the same homologue group within PCB technical mixtures [42]. However, the retention behaviour of PCBs needs to be accessed for the individual columns using methods outlined by Frame [73].

Increases in sensitivity and selectivity for environmental analysis can be gained by using tandem mass spectrometry (MS/MS) where transition between parent and daughter ions can be measured using multiple reaction monitoring (MRM). Targeted analytes (i.e., PCB atropisomers) will have their own unique ion transition compared to other components within sample, dramatically increasing the selectivity of MS/MS detection compared to that obtained using single MS detection. Monitoring selective ion transitions by MRM also reduces the noise detected within samples, increasing the signal/noise ratio and producing a lower limit of detection. Differences in sensitivity and selectivity for PCB atropisomers between MS and MS/MS detection were studied by Bucheli et al. where EFs were quantified and compared in various environmental matrices (sediment, soil, compost, bird tissue and eggs, and human milk) [52]. Detection limits using MS/MS detection ranged from 0.18-0.69 pg for the individual enantiomers of the PCB atropisomers investigated (PCBs 95, 132, 149, and 174) and were lower than those obtained by single MS detection (0.3-3 pg). Analysis using single MS detection resulted in non-detects for PCB atropisomers in several of the environmental matrices studied, whereas all PCB atropisomers were detected when analyzed by MS/MS [52]. Within the same study, EFs quantified by GC/MS, GC/MS/MS,

MDGC/MS and MDGC/MS/MS detection were found to deviate drastically between the various methods. The largest deviations in EFs quantified were observed for GC/MS and GC/MS/MS compared to MDGC/MS/MS where EFs were found to deviate up to 100% for analyses using one-dimensional GC. The methods of MDGC/MS and MDGC/MS/MS detection showed the smallest deviations in EFs, indicating that MDGC contributes more to the selectivity; however, greater sensitivity was obtained using MS/MS detection. Certified reference materials (CRMs) can also be used to validate accurate quantification of EFs of chiral PCBs using GC/MS and MDGC/MS techniques [74, 75]. Knowledge of EFs within CRMs can access possible co-elution of PCB atropisomers with congeners of the same homologue group, which is useful in the development of chiral analytical methodology.

Environmental Fate of PCB Atropisomers

Sediment

The fate of PCB atropisomers within the aquatic environment is dictated by their hydrophobicity and partitioning from the water column to natural organic carbon in sediment due to favourable chemical interactions. This partitioning (i.e., absorption, adsorption) will affect both enantiomers equally because they have the same physical/chemical properties, thus partitioning will not contribute to enantiomer enrichment. The first study to investigate the fate of PCB atropisomers within sediment was conducted by Glausch et al., where the authors observed racemic proportions of PCBs 95, 132, and 149 within sediment samples from the River Elsenz in southern Germany [37]. However, subsequent studies observed enantiomer enrichment of PCB atropisomers within sediment [36, 42, 44, 56, 76], suggesting that some form of biological processing is occurring. Wong et al. found non-racemic EFs for several penta-, hexa-, and heptachlorinated PCB atropisomers within sediment from Lake

Hartwell (SC, USA), the Hudson River (NY, USA), and Housatonic River basins (MA, USA) [44]. Enantioselective degradation within sediment has been attributed to anaerobic microbial reductive dechlorination (Figure 4 and 5), where previous studies within Lake Hartwell have shown this to occur based on shifts in congener distributions with depth of sediment and accumulation of *ortho*-chlorinated congeners, the products of *meta*- and *para*-dechlorination [77]. Enantiomer enrichment of chiral PCBs varied between different sampling sites within Lake Hartwell, which could be attributed to the presence of different microbial populations within the sediment. Reductive dechlorination has been shown to be congener-specific among different sampling sites [78-81], suggesting that different microbial populations can catalyze reductive dechlorination of PCBs to varying degrees using enzymes that may be enantioselective. This was demonstrated in laboratory studies by Pakdeesusuk et al. where enantioselective reductive dechlorination was observed for PCB 91 and 95 by microorganisms present within Lake Hartwell sediment [76]. Microorganisms spiked with PCBs 132 and 149 showed that reductive dechlorination to PCB 91 and 95 was not enantioselective; however, further reductive dechlorination of PCB 91 and 95 was found to be enantioselective (Figure 6). Non-racemic EFs observed for PCB 132 (EF = 0.55) within Lake Hartwell sediment [44] contradict findings found in laboratory microcosm studies. Pakdeesusuk et al. proposed that the EF observed for PCB 132 within Lake Hartwell sediment may be due to enantioselective formation from reductive dechlorination of higher chlorinated congeners; however, this process has not yet been investigated [76]. The EF of PCB 132 measured within Lake Hartwell sediment may also be influenced by an influx of non-racemic material from other sources, which has been observed by Asher et al. for PCB

95 within the Hudson River Estuary [55]. Analysis of dated sediment cores from Lake Hartwell showed that enantiomer enrichment of PCBs 91, 132, and 176 reversed with depth,

Figure 4. Examples of possible meta- and para- reductive dechlorination pathways of PCBs 201, 200, and 197 leading to the formation and loss of PCB atropisomers (enclosed in boxes). Achiral congeners are shown in bold italics. Biphenyl chlorine substitution pattern shown in parentheses (ring 1- ring 2). Reprinted from [44] with permission © (2001, American Chemical Society)

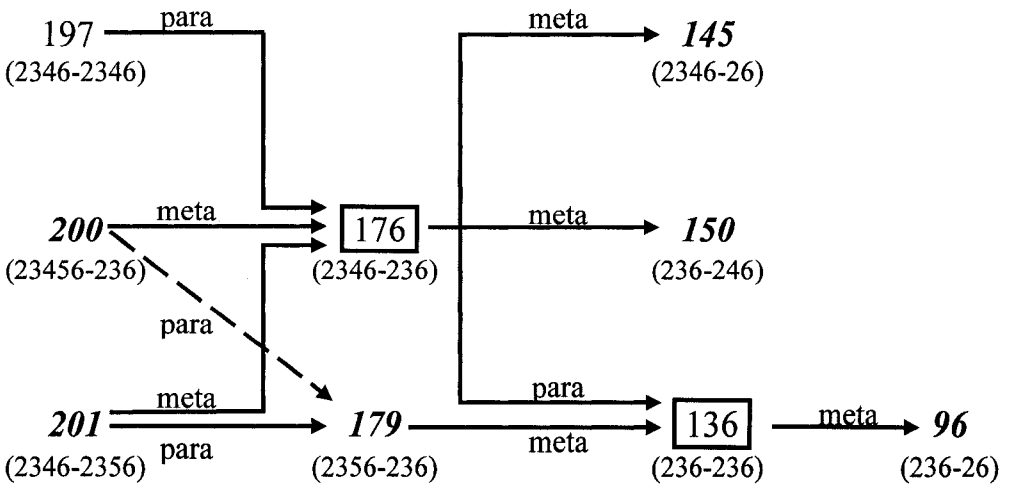

Figure 5. Examples of possible *meta-* and *para-* reductive dechlorination pathways of PCB 196 leading to the formation and loss of PCB atropisomers (enclosed in boxes). Achiral congeners are shown in bold italics. Biphenyl chlorine substitution pattern shown in parentheses (ring 1- ring 2). Reprinted from [44] with permission © (2001, American Chemical Society).

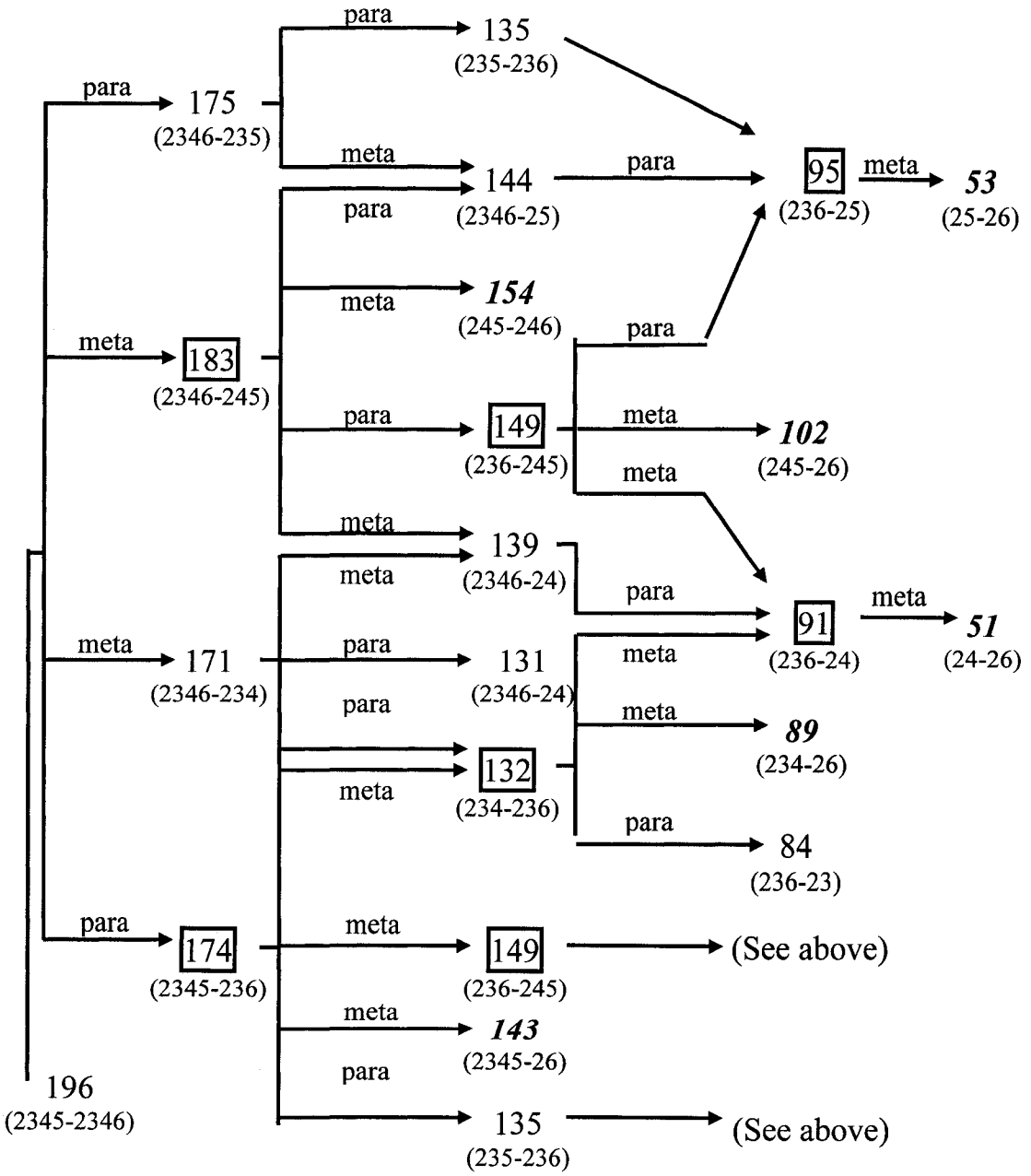

Figure 6. Concentratrion of PCB 132 and its major dechlorination products (A-C). Enantiomer fractions (EFs) for PCB 132 and 91 (D, E) in PCB 132 spiked microcosms vs. time. Autoclaved controls with PCB 132 (open circles, crosshatched bars), live treatments with PCB 132 (filled circles, filled bars), EF = 0.5 (---).Reprinted from [76] with permission © (2003, American Chemical Society).

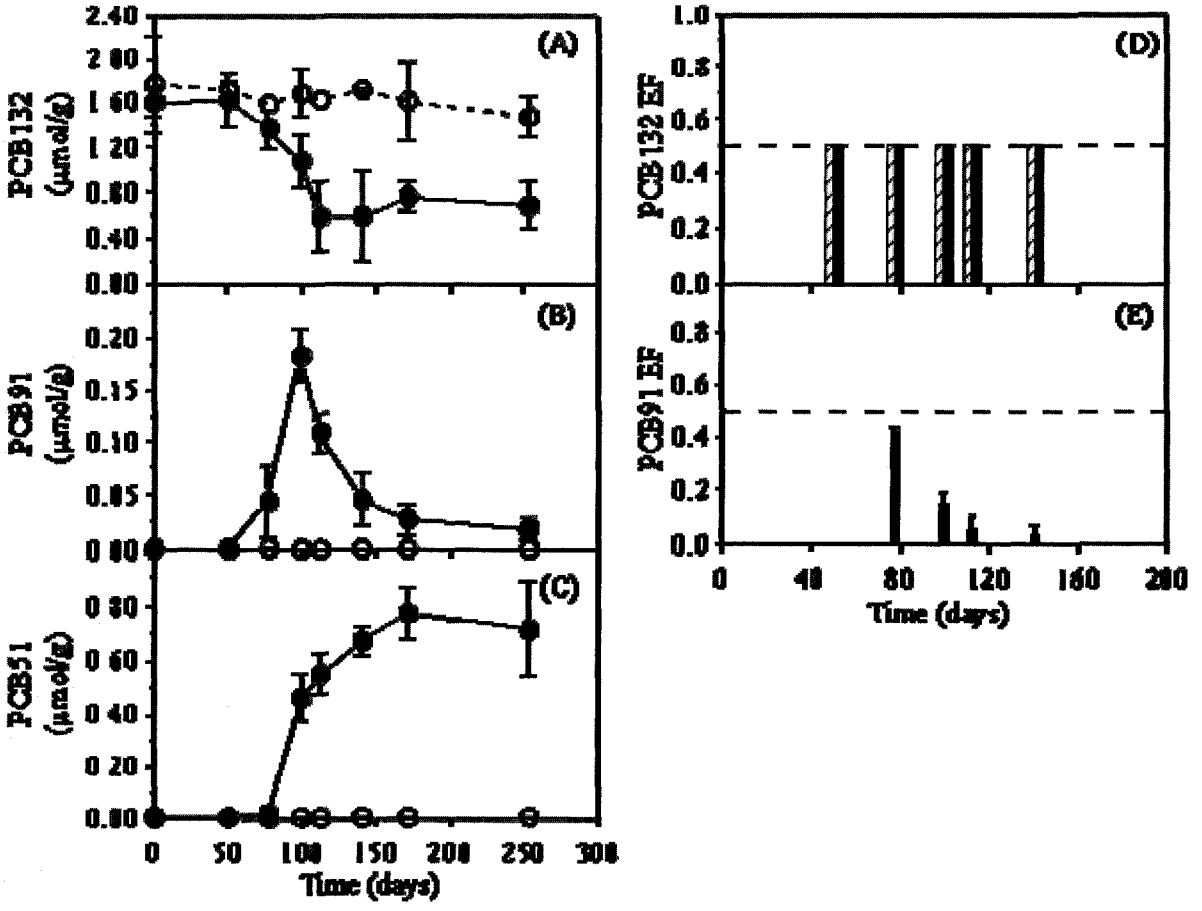

which supports the hypothesis that different microbial populations exist within a given sediment core, each having enzymes of different enantioselective specificity for reductive dechlorination [56].

Soil and air

Soil is the major sink to which PCB atropisomers partition within the terrestrial environment. Microbial degradation of PCB atropisomers under aerobic conditions may also be enantioselective based on results previously observed within sediment [36, 42, 44, 56, 76]. Garcia-Ruiz et al. observed no enantioselective degradation of PCBs 45, 88, 91, 95, 136, 144, 149 and 176 incubated with *Jonibacer* sp. strain MS3-O2 over a 10 day period [82]. The lack of enantioselective degradation observed could be attributed to a slow rate of degradation in that the incubation time allotted for degradation to occur was insufficient. This has been observed in lab studies investigating anaerobic reductive dechlorination in sediment for PCB atropisomers, where microbial reductive dechlorination was not observed for PCBs 132 and 149 until 50 days after initial exposure [76]. The enzymes responsible for enantioselective degradation will also be dependent upon the microbial population present within the soil. Singer et al. found enantioselective degradation of PCB atropisomers to vary between different bacteria strains under aerobic conditions [83], and is supported by similar findings within sediment [44, 56].

Since the production of PCBs ceased in the late 1970s within North America and Europe, current sources of PCBs to the atmosphere are believed to be predominantly from volatilization from contaminated environmental surfaces (i.e., soil, water) [84-87]. However, emission from PCB technical mixtures that have remained in use (i.e., capacitors, transformers, construction materials) may also contribute to atmospheric contamination [88,

89]. Partitioning processes between soil and the atmosphere (deposition, volatilization) are not enantioselective. Thus, comparing enantiomer enrichment signatures of chiral pollutants between soil and atmospheric compartments can help identify sources of pollutants to the atmosphere [90-92]. Robson and Harrad were the first to demonstrate this idea for PCB atropisomers, where non-racemic EFs for PCBs 95, 136, and 149 in U.K. soils were statistically different from racemic EFs (EF = 0.5) within the overlying air [49]. These results suggest that the source of atmospheric PCBs was not due to volatilization from the soil, but from emission of unweathered PCBs that have remained in use. Recent studies by Harrad et al. reported that concentrations of PCBs within indoor air in the West Midlands of the U.K. have not significantly changed over the past 10 years [93]. The EFs for PCB atropisomers detected within indoor and outdoor air were all racemic or near racemic; however, EFs within soil were found to be non-racemic in the rural regions outside of the city center of Birmingham [54, 94]. These results suggest that the source of atmospheric PCBs was through ventilation of indoor air from urban centers and not volatilization from contaminated soil. This is further supported by other studies within the literature where air concentrations of PCBs decreased with increased distance from urban centers [94-96]. Jamshidi et al. observed racemic EFs of chiral PCBs detected in soil in the city of Birmingham not to be statistically different from the EFs quantified in the overlying air, indicating that the city center may be a point source of atmospheric PCBs within this region [94]. Recent studies by Asher et al. found similar results where racemic EFs for PCB atropisomers detected in air overlying the Hudson River Estuary (HRE) suggested that the source of atmospheric PCBs is from unweathered sources in nearby urban and industrial centers [55]. Non-racemic EFs detected for PCB 95 within the water column of the HRE

were similar to those detected within sediment of the Upper Hudson River [44] and correlated to river discharge from the Upper Hudson, indicating that source of contamination of the HRE was from the Upper Hudson River.

Biota

Enantiomer enrichment of PCB atropisomers within biota indicates that some form of biological processing (i.e., metabolism) has occurred and has been investigated in various organisms (Table 2). Uptake would generally not be considered a mechanism for enantiomer enrichment since accumulation of PCBs is governed by passive diffusion and will affect both enantiomers of PCB atropisomers equally [97]. However, uptake of non-racemic signatures through predator-prey relationships or contact with environmental media containing enantiomer enriched signatures can contribute to enantiomer enrichment within biota, which can be transferred throughout the food web.

Only a few studies have investigated the fate of PCB atropisomers on a food web level. Wong et al. observed enantiomer enrichment of several PCB atropisomers to increase from lower to higher trophic levels within the Lake Superior aquatic food web [50]. This is supported by similar findings within an arctic food web outlined in Chapter 2 [51]. Racemic EFs detected for phytoplankton and zooplankton species comprising the lower trophic levels [45, 50, 51] suggests that these organisms have limited capacity to metabolize chiral PCBs, and do not contribute to enantiomer enriched signatures in biota present at higher trophic levels. However, non-racemic EFs have been observed within bivalves and invertebrates, *Mysis relicta* and *Diporeia* within freshwater ecosystems [35, 50]. These are sediment-dwelling organisms that feed on organisms closely associated with the sediment or rely on sediment and sedimentary particles within the water column as a food source [98-100].

Table 2. Biota investigated for enantiomer enrichment of PCB atropisomers

Organism	References
phytoplankton/zooplankton	[45], [50], [51]
invertebrates/bivalves	[35], [101] ,[50], [101]
fish	[41], [43], [58], [50], [51], [52], [102]
birds/bird eggs	[43], [51], [53], [52]
seals	[38], [103], [51]
dolphins/porpoises	[39], [40], [45], [46]
sharks	[41], [18]
whales	[40], [45]
wolverines	[48]
rodents	[104], [105], [106], [107]
humans	[17], [47], [54], [52], [57]

Microbial reductive dechlorination of PCB atropisomers within sediments has been shown to be enantioselective [56, 76], possibly contributing to the non-racemic burden within these organisms by uptake from the sediment. This is supported in findings by Wong et al. who found non-racemic EFs detected in bivalves to be not statistically different from EFs detected within sediment [43]. Another possible explanation is that these organisms have the capacity to metabolize chiral PCBs enantioselectively, although previous studies have concluded that these organisms have limited metabolic capabilities towards PCBs [108-111]. This hypothesis is supported in findings outlined in Chapter 3 where biological processing of chiral PCBs by *Mysis relicta* was found to be enantioselective in laboratory exposure studies [101]. Although analysis for PCB metabolites was not conducted in *Mysis relicta*, it strongly

suggests that enantioselective processing of chiral PCBs within these organisms is due to metabolism; however, uptake of chiral PCBs from non-racemic sources cannot be ruled out as a source of enantiomer enrichment observed within these organisms in the natural environment.

Fish are considered to have limited metabolic capabilities towards PCBs due to lower cytochrome P-450 activity (CYP) compared to mammals and birds [112-114]. However, non-racemic EFs of PCB atropisomers have been detected in fish within the natural environment [43, 50, 51], which suggests that fish may also metabolize chiral PCBs enantioselectively. Wong et al. observed enantiomer enrichment within largemouth bass (*Micropterus salmoides*) and bluegill sunfish (*Lepomis macrochirus*) for PCBs 91, 95, 136, and 149 [43]. Although the authors attributed enantiomer enrichment to metabolic activity, they could not rule out uptake of non-racemic EFs through diet since prey species were not determined. Non-racemic EFs detected in fish species within the Lake Superior aquatic food web were attributed to both uptake from enantiomer enriched sources as well as metabolism of chiral PCBs. For several PCB atropisomers, EFs were statistically different between fish species and their diet, indicating enantioselective metabolism, which is supported by laboratory exposure studies [58, 102] and detection of PCB metabolites in fish from the natural environment [115-117].

Species variability has been observed to have an effect on EFs detected within biota. Non-racemic EFs for PCBs 149 and 174 showed different enrichment patterns between grey seals (*Halichoerus grypus*) and ringed seals (*Phoca hispida*). EFs observed in grey seals were 0.39 and 0.45 for PCB 149 and 174, respectively. In ringed seals, EFs for PCB 174 were 0.59 and racemic for PCB 149 [51, 103]. Differences in enantiomer specificity between

the organisms could not be attributed to differences in enantiomer elution order since both studies utilized the same chiral stationary phase for their analysis. This suggests that enzymes responsible for metabolism possess different enantiomer selectivity between the two seal species. This is supported by similar findings within fish [43, 50, 51, 58], birds [51], dolphins and whales [45]. Diet may also influence the difference in EFs observed between different species as well as individuals within a given species, particularily in migratory species. Migration to areas with prey containing different enantiomer enriched signatures could contribute to the variability observed for EFs, where large variations have been observed within individual species of fish [43, 50] and birds [51].

Enantiomer enrichment within higher trophic level organisms (i.e., birds and mammals) is often attributed to metabolism due to greater CYP activity. Norström et al. observed enantioselective degradation of PCB 132 within rats followed by the enantioselective formation of the methyl sulfonyl-PCB 132 metabolite, indicating that enantiomer enrichment within those rats may have been due to enantioselective metabolism [106]. This finding supports earlier reports of non-racemic EFs of chiral PCB methyl sulfone metabolites within rats [118], seals [119-121], porpoises [122], birds [121], polar bears [119], and humans [121, 123]. However, recent studies have shown that other biological processes, besides metabolism, may affect enantiomer enrichment of chiral PCBs. Laboratory studies involving rats exposed to a commercial mixture of PCBs showed enantiomer enrichment for (+)-PCB 149 within skin, liver, and adipose tissues, but enrichment of (-)-PCB 149 within blood [105]. Enantiomer fractions detected within these compartments were statistically different from the EFs within the commercial mixture, which suggests that selective tissue distribution may affect enantiomer enrichment of PCB 149 within rats. This hypothesis is

supported by recent studies by Kania-Korwel et al. who observed changes in concentration and enrichment of (+)-PCB 136 within tissues of rats depending on the route of exposure (oral vs. intraperitoneal injection) [107]. Higher degrees of enantiomer enrichment as well as higher concentrations will have a significant impact on enantioselective toxicity. Thus studies using different routes of exposure could produce different toxicity endpoints. Gender may also need to be considered in the enrichment of PCB atropisomers. Hoekstra et al. observed enrichment of PCB 91 to be significantly correlated with body length in male bowhead whales (*Balaena mysticetus*), but was not observed in females [45]. The EFs for PCB 91 were correlated to concentration within males, but not in females. This may be attributed to females reducing their PCB burden through maternal transfer [124], and affecting the rate of metabolism. Similar findings have been observed in cod (*Gadus morhua*) for chlordane where enrichment of the (-)-enantiomer of *cis*- and *trans*-chlordane was found in females, whereas the opposite was observed in males [125]. These findings suggest that other factors besides metabolism may affect enantiomer enrichment within organisms and may be gender specific.

These results provide insights into enantioselective mechanisms that may occur within humans; however, due to the difficulty in obtaining human tissues, few studies on enantiomer enrichment of PCB atropiosmers within humans exist. Non-racemic EFs have been reported for PCBs 95, 132, and 149 within postmortem human liver tissues [47] and are comparable to EFs within human milk [17, 57] and feces [54]. Non-racemic sources of PCBs can be taken up through the diet but enantiomer enrichment of these congeners may also be due to metabolism, which is supported by findings of enantiomer enriched chiral PCB methyl sulfone metabolites within human liver tissue [123].

Metabolites of PCB atropisomers

The chlorine substitution pattern for many of the chiral PCBs places them in a class of congeners that are susceptible to metabolism due to the presence of vicinal hydrogen atoms at their *meta-para* positions [126, 127]. Generally, the process of metabolism aids in the elimination of xenobiotics from the body by increasing their polarity to aid in their secretion or excretion. However, metabolism may also produce metabolites that are of greater persistence and toxicity compared to the original compound. Although various metabolites of PCBs can be formed, the two major classes of research focus are the methyl sulfone ($MeSO_2$-PCBs) and the hydroxylated metabolites (OH-PCBs).

Metabolism of PCBs is mediated by reaction with the CYP enzyme system within biota and has been extensively reviewed by Letcher et al. [128]. Due to their non-planar conformation, PCB atropisomers are preferred substrates of CYP 2B, and possibly CYP 2C and 3A enzymes [127, 129]. Reaction with CYP enzymes results in the oxidation of PCBs to form an arene oxide intermediate through Phase I metabolism [128] (Figure 7). Subsequent opening of the epoxide ring can result in the formation of both *meta*- and *para*-OH-PCBs, although CYP 2B enzymes within rodents can catalyze the direct insertion of a hydroxyl group at the *meta*-position [130, 131]. The arene oxide can also undergo Phase II conjugation with glutathione which can be further processed through the mercapturic acid pathway (MAP) to form the $MeSO_2$-PCB metabolites (Figure 6) [132]. Although both $MeSO_2$-PCBs and OH-PCBs metabolites can be formed through the metabolism of PCB atropisomers, studies have primarily focused on the $MeSO_2$-PCBs due to their bioaccumulation potential [133]. The $MeSO_2$-PCBs have been detected within

Figure 7. Metabolism of PCBs to hydroxylated (OH-PCB) and methyl sulfone ($MeSO_2$-PCB) metabolites.

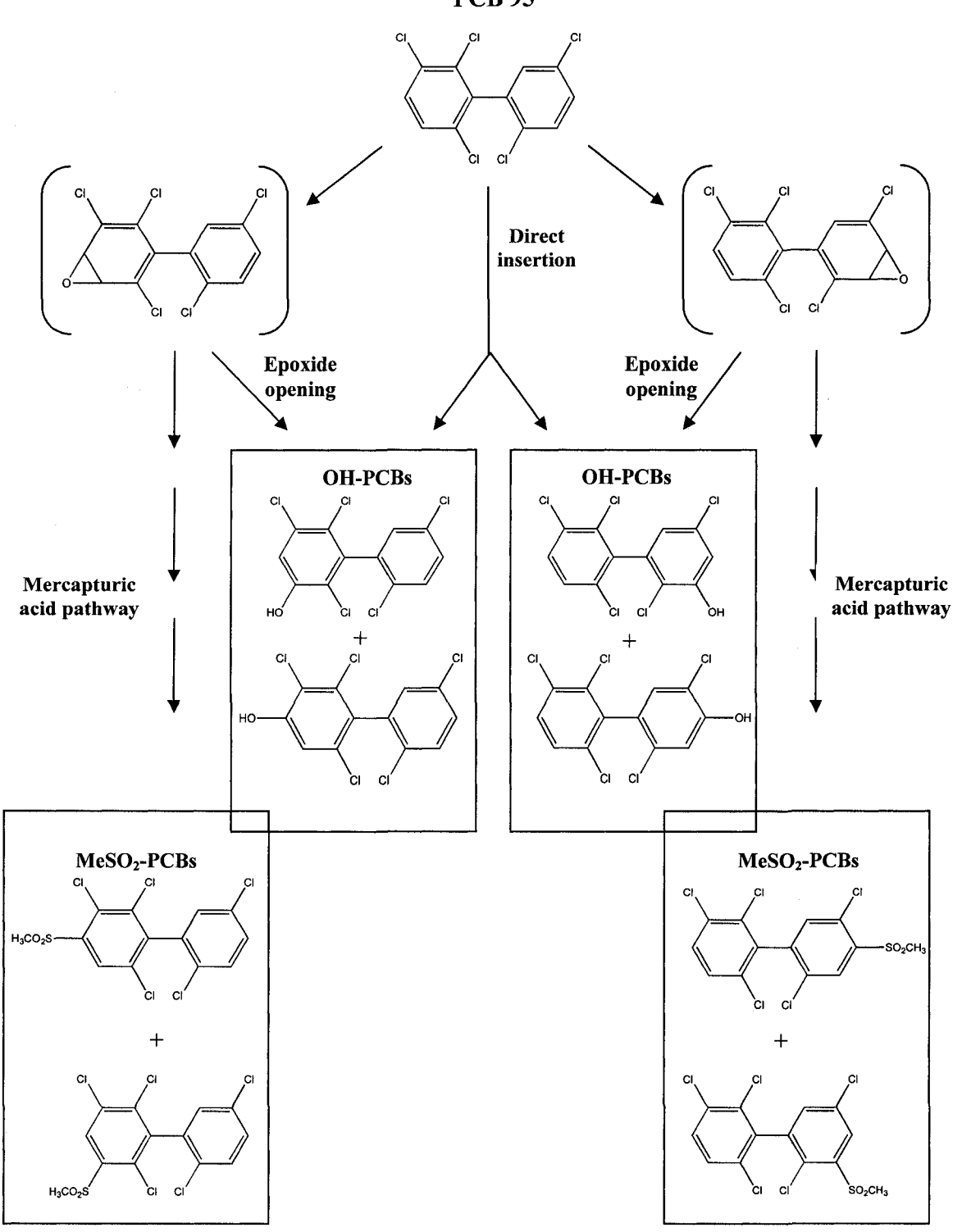

fish [117, 134], birds [121, 135, 136], and various tissues of marine [121, 133, 137-139] and terrestrial mammals [121, 134, 140-142].

As with PCBs, the $MeSO_2$-PCB metabolites of chiral congeners can exhibit axial chirality and can exist as stable enantiomers within the body, where enantiomer enrichment of these metabolites has been observed in various organisms [106, 118-123]. Chiral $MeSO_2$-PCBs can also be formed from an achiral (i.e., prochiral) parent PCB congener. Enantiomer enriched signatures of the chiral $MeSO_2$-PCB metabolites are most likely attributed to enantioselective metabolism of the parent chiral congener. However, other processes such selective protein binding, tissue transport, and continued metabolic degradation may also contribute to enantiomer enrichment of the chiral $MeSO_2$-PCB metabolites.

Studies have found that most $MeSO_2$-PCB accumulation is localized within the adipose, lung, and liver tissue within biota [128, 143]. Trends in selective tissue retention have been observed between the 4-$MeSO_2$-PCBs and 3-$MeSO_2$-PCBs with the 4-$MeSO_2$-PCBs generally dominating within lung and adipose tissue while the 3-$MeSO_2$-PCBs dominate within the liver [118-120, 133, 141, 144]. Selective protein binding has been attributed to selective tissue retention of 4-$MeSO_2$-PCBs where studies have shown that these metabolites bind specifically to lung tissues within rodents [145-147]. However, variations have been observed between different species. For example, the 3-$MeSO_2$-PCBs tend to dominate within adipose tissue of beluga whales and harbour porpoises compared to the 4-$MeSO_2$-PCBs [148, 149]. Greater retention of 4-$MeSO_2$-PCB 132 over 3-$MeSO_2$-PCB132 was observed in liver tissues of rats exposed to the racemate of PCB 132 [106] and is supported by earlier findings by Larsson et al. [118]. Enantiomer enrichment has been observed for several of the chiral $MeSO_2$-PCBs within both lung and liver tissue of seals,

rats, and humans [118, 120, 122, 123]. However, it is unclear whether enantiomer enrichment within these tissues is attributed to metabolic formation/degradation or selective tissue binding. Enantiomer enrichment within liver and lung tissues appears to be dependent upon the substitution position of the $MeSO_2$ group. Chiral methyl sulfone PCBs substituted at the *para*-position generally resulted in enrichment of the first eluting enantiomer within these organisms, whereas enrichment of second eluting enantiomer was observed for *meta*-substituted $MeSO_2$ PCBs. The chiral stationary phases used within these studies utilized the same modified cyclodextrin as a chiral selector (heptakis (2,3-di-*O*-methyl-6-*O*-tert-hexyldimethylsilyl)-β-cyclodextrin), so reversal of elution order for the enantiomers of these metabolites can be ruled out. Thus, the mechanism responsible for enantiomer enrichment within these tissues may be similar among these organisms. Norström et al. showed that enantioselective formation of the 3-$MeSO_2$-PCB 132 and 4-$MeSO_2$-PCB 132 was preceded by the enantioselective degradation of the PCB 132 racemate exposed to rats [106]. This indicates that the mechanism for enantiomer enrichment of these metabolites was due to enantioselective metabolism of the parent congeners. However, this study did not rule out that other processes that may affect enantiomer enrichment of the metabolite after its formation. Enantioselective metabolism of 3-$MeSO_2$-PCB 149 was observed when incubated with rat liver hepatocytes even though metabolism of the parent congener was not enantioselective [150]. This observation is supported by findings within ringed seals where no enantiomer enrichment for PCB 149 was observed [51] but non-racemic proportions of 3-$MeSO_2$-PCB 149 have been detected [119]. Thus, $MeSO_2$-PCBs may undergo further enantioselective processing (i.e., metabolism, selective protein binding or transport) after their formation. This possibility is an area of research in need of further study. It should also

be mentioned that another source of enantiomer enrichment of $MeSO_2$-PCBs may be through dietary accumulation, which has been observed in polar bears [133].

Along with the $MeSO_2$-PCBs, metabolism of the PCB atropisomers will also produce OH-PCBs. Most of these metabolites are expected to be readily excreted and have limited bioaccumulation potential [132]. However, within the last decade, studies investigating the fate of OH-PCBs have drastically increased based on findings of bio-persistent OH-PCB congeners within plasma and blood of various biota as well as other environmental matrices [102, 116, 151-159]. Persistence of OH-PCBs within plasma is attributed to their chlorine substitution pattern where congeners with a *para*-substituted hydroxyl group with adjacent substituted chlorine atoms are structurally similar to the thyroid hormone, thyroxine (T4) (Figure 8). This allows OH-PCBs to bind to the thyroid transport protein, transthyretin [152, 160] with a higher affinity, allowing them to persist within the blood, although their

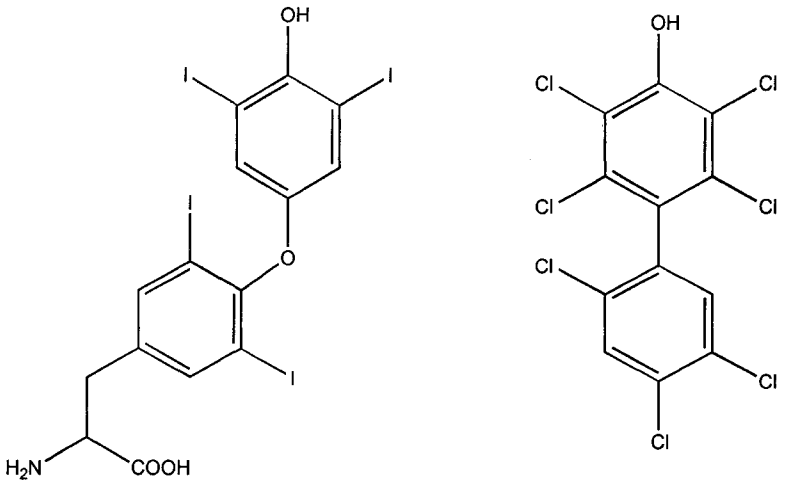

Thyroxine **4-OH-PCB 187**

Figure 8. Chemical structures of thyroxine and 4-OH-PCB 187.

prescence has also been detected within mammalian brain, liver, and adipose tissue [157, 159]. No investigations of the OH-PCBs of the PCB atropisomers have been conducted within environmental samples and can be attributed to a couple of reasons. Many of the chiral congeners are directed through the MAP due to their chlorine substitution pattern (2, 5 or 2, 3, 6 chlorine substitution on at least one phenyl ring) forming the persistent $MeSO_2$-PCBs [106, 118, 120-123] along with the OH-PCBs that do not bioaccumulate [128, 132]. The OH-PCBs of the chiral congeners do not share the same structural characteristics to OH-PCBs found to persist within blood and plasma; however, several studies have reported more than half of the OH-PCBs detected within environmental samples cannot be identified with authentic standards [102, 116, 151, 153, 156-158]. Haraguchi et al. showed the proportion of OH-PCBs to MAP derived metabolites to increase from the metabolism of 2, 5 chlorine substituted PCBs with increasing chlorination on the other phenyl ring; however, decreases in overall metabolism rate occurred also occured with increased chlorination [161]. Unidentified OH-PCBs found within environmental samples may consist of the OH-PCBs of the chiral congners, particularily those with higher degrees of chlorination (5 or more chlorines). Results reported within Chapter 4, show the formation of OH-PCBs from several PCB atropisomers following *in vitro* enantioselective metabolism within rat and human CYP enzymes. Enantioselective metabolism of the parent congeners suggests that the formation of the chiral OH-PCBs is also enantioselective and may be present within biota in non-racemic proportions. These findings stress the need for appropriate standards for identification of unknown OH-PCBs, and possible method development for the separation of chiral OH-PCBs if their presence is confirmed within biota.

Out of the identified OH-PCBs found to persist, 4-OH-PCB 187 is a major contributor to the total OH-PCB accumulation detected within biota [102, 116, 128, 151, 152, 154-157, 162]. The source of this metabolite is through the metabolism of its parent congener, PCB187; however, metabolism of PCB atropisomer 183 followed by a 1,2 shift of the hydroxyl group can also produce this metabolite [128, 152], although its overall contribution to the formation of 4-OH-PCB 187 has not been investigated. Studies have detected 3'-OH-PCB 183 at comparable levels to 4-OH-PCB 187 within cetacean brain tissue [157] and to a much lesser extent within human plasma [162]. However, this metabolite co-elutes with 3'-OH-PCB 182, and its contribution to overall OH-PCB contamination cannot be determined.

Enantioselective toxicity of PCB atropisomers

Various studies have reported the enantiomer enrichment of chiral PCBs within various biota, but few studies have investigated the enantioselective toxicity that may arise due to the enantiomer enrichment. Puttman et al. observed that both enantiomers of PCB 139 were phenobarbital-type inducers of CYP activity within rats. However, the (+)-PCB 139 showed significant increases in the production of aminopysine N-demethylase, aldrin epoxidase as well as total CYP content compared to the (-)-PCB 139 [10]. Enrichment of the (+)-PCB 139 within the liver could explain this difference in potency, where elimination of the (-)-PCB 139 through metabolic or transport pathways would reduce its concentration thus affecting its potency. Recent studies have observed enantiomer enrichment of (+)-PCB 136 to be more pronounced within organ tissues of mice dosed orally compared to intraperitoneal injection [107]. This observation would suggest that the potency of (+)-PCB 139 would increase within rats if oral dosage was used as the route of administration. To avoid

pharmokinetic influences on the individual enantiomers, *in vitro* studies using chick embryo liver cells were utilized by Rodman et al. [11]. The authors observed the (+)-PCB 139 to be a more potent inducer of ethoxyresorufin-O-deethylase (EROD), benzphetamine N-demethylase (BPDM) and total CYP activity. In contrast, the (-)-enantiomers of PCBs 88 and 197 were more potent inducers of EROD and BPDM activity within this study. Though these studies provide useful insight into the toxicity of PCB atropisomers, a majority of the chiral congeners detected in non-racemic proportions within biota have never been investigated for their enantioselective toxicity and demonstrates that further research within this area is needed.

The exposure to the $MeSO_2$-PCBs has been implicated in several biological and toxicological effects within mammals [128]. Specific tissue retention of these metabolites within lung and liver tissues [128, 143] has been linked to pulmonary distress [163] induction of hepatic CYP enzymes [164], cell communication and endocrine disruption [164, 165], and reproductive toxicity [166]. However, no studies have investigated the enantioselective toxicity of the chiral $MeSO_2$-PCBs that are enantiomerically enriched within biota.

Studies investigating the toxicity of the OH-PCBs have primarily focused on their thyroidogenic effects [160, 167]. As mentioned earlier, the high binding affinity of OH-PCBs to the thyroid transport protein, transthyretin, reduces thyroid hormone levels within plasma and may negatively impact fetal brain development [167, 168] due to maternal transfer of OH-PCBs [169, 170]. Maternal transfer may also increase mortality rates within offspring. For example, survival rate of Japanese quail egg embryos was drastically reduced upon exposure to OH-PCB 107 and OH-PCB 187 [171]. Estrogenic activity for the OH-PCBs varies between congeners and appears to be dependent upon their chlorine substitution

pattern [172-174]. Hydroxylated PCBs have also been shown to inhibit glucuronidation, limiting detoxification of other persistent organic pollutants and increasing the toxicity by producing biologically reactive intermediates [175]. Since none of the chiral OH-PCBs have yet to be identified within the surrounding environment, toxicological studies for these particular metabolites do not exist nor have methods been developed to separate their individual enantiomers.

Chapter 2: Using enantiomer fractions of chiral polychlorinated biphenyls to gain insight on biotransformation within arctic biota[2]

Introduction

The bioaccumulation potential of PCBs has been extensively studied. Uptake of these compounds from the surrounding environment results in accumulation in organisms as the PCBs are transferred throughout food webs [6, 7, 27, 28]. Since the production of PCBs in North America ceased in 1977, concentrations of PCBs in areas near where they were used have decreased over the years. However, with their resistance to environmental degradation and semi-volatile nature, PCBs are still found in remote ecosystems around the world [5].

The Northwater Polynya (NOW) is a highly productive open-water region in northern Baffin Bay of the Canadian Arctic. The NOW food web consists of a variety of zooplankton and invertebrate communities, arctic cod consuming invertebrates, seabirds (dovekie, thick-billed murre, black guillemot, northern fulmar, ivory gull, black-legged kittiwake, glaucous gull) feeding mainly upon invertebrates and forage fish (primarily arctic cod), and marine mammals (ringed seals) eating mostly arctic cod [176]. Reduced diversity of species, long food webs that are similar across the region, and limited impact of pollution point sources makes arctic food webs ideal for studying food web accumulation of persistent organochlorine compounds [177-180], including PCBs [177, 181, 182]. Previous studies by Fisk et al. have reported the fate of PCBs (including the chiral congeners) within the NOW

[2] A version of this chapter has been published. Warner, N. A. et al. Environmental Toxicology and Chemistry. 2005. 24: 2763-2767.

food web. [177]. Using trophic magnification (TMFs) and biomagnification factors (BMFs), these studies observed bioaccumulation of PCBs, particularly in seabirds and ringed seals,

Figure 9. Geographical location of the Northwater Polynya

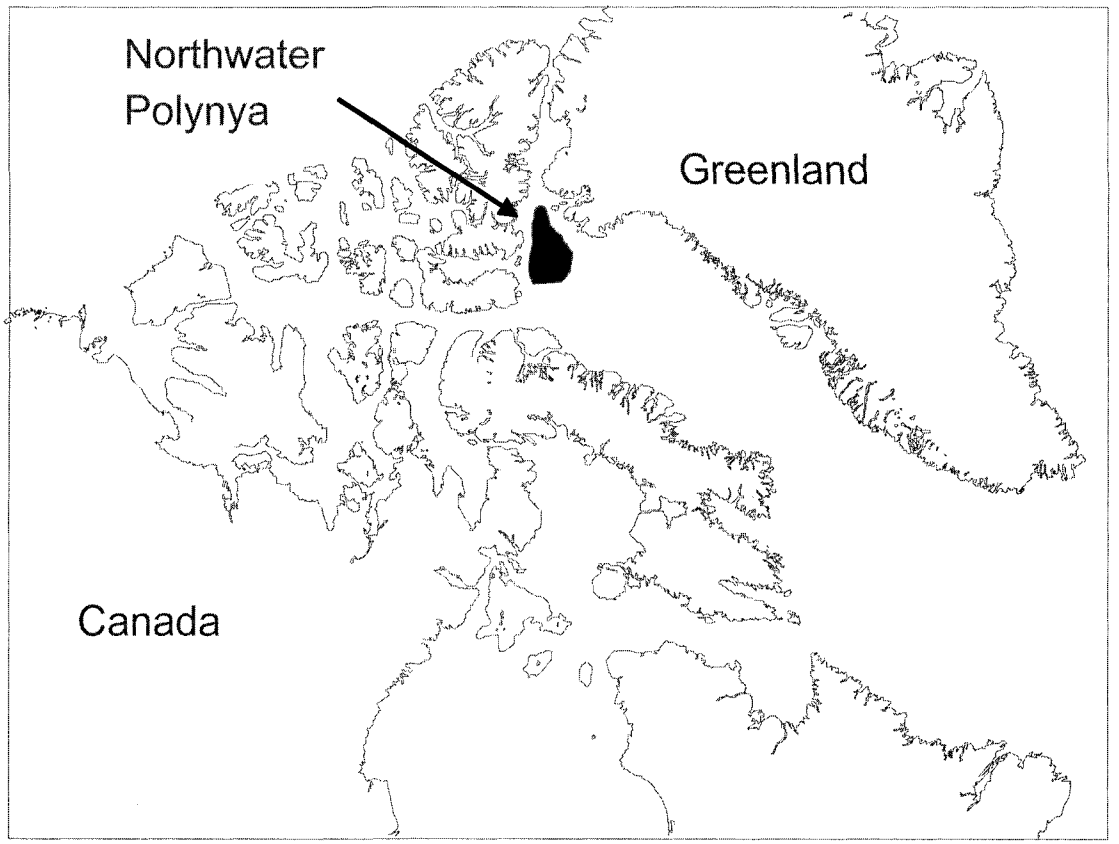

with little evidence of biotransformation. Studies using TMFs and/or BMFs can determine biotransformation of PCBs indirectly, but if the rate of accumulation is greater than the rate of metabolism, the ability of these methods to determine biotransformation is greatly reduced.

Chiral analysis is an area of study offering enhanced insight into biological processes affecting chemical pollutants. Nineteen of the 209 PCB congeners are asymmetrically substituted and are axially chiral (atropisomerism) due to restricted rotation around the C-C ring connecting bond [8]. Enantiomers have the same physical and chemical properties such

as hydrophobicity, vapor pressure, and polarity, which are important for determining their behavior in the environment, but they may exhibit different biological [12, 13] and toxicological properties [10, 11]. Selective biotransformation of one enantiomer over the other can result in enrichment of the other enantiomer in an organism. Thus, chiral analysis may be useful for detecting and elucidating biological fate processes, particularly biotransformation (metabolism), within organisms [13, 39, 45, 178, 179, 181, 183-185].

The objective of this study was to investigate the fate of chiral PCBs within the NOW and to provide insight on biotransformation of PCBs among organisms occupying different trophic levels. This is of particular significance, since the enantiomer composition of chiral PCBs at lower trophic levels within arctic marine food webs has received little attention. Enantiomer composition of chiral PCBs in higher trophic level organisms (i.e., seals and seabirds) is of particular significance since they have greater metabolic capabilities compared to zooplankton and fish, and can provide insight into possible detoxification mechanisms in warm-blooded organisms. To date, chiral analysis of PCBs in seals is limited to a few studies [38, 103] and in birds is limited to analysis of eggs [53]. To the best of our knowledge, this is the first report of direct chiral analysis of enantiomer composition of PCBs in zooplankton, fish, and seabirds in an ecosystem.

Methods and Materials

Sample collection

Sample collection was carried out by collaborators Aaron Fisk, Ross Norstrom, and colleagues during the 1998 April to July voyage of the *CCGV Pierre Radisson*, and consisted of zooplankton (*Calanus hyperboreus*), Arctic cod (*Boreogadus saida*), ringed seal (*Phoca hispida*), and seabirds including dovekie (*Alle alle*), thick-billed murre (*Uria lomvia*), black

guillemot (*Cepphus grille*), northern fulmar (*Fulmaris glacialis*), ivory gull (*Pagophila eburnea*), black legged kittiwake (*Rissa tridactyla*), and glaucous gull (*Larus hyperboreus*). Details of sample collection have been published previously [177, 178]. Briefly, zooplankton samples were collected from vertical tows of the water column using 1m × $1m^2$ zooplankton nets (520 μm mesh). Hand held nets were used for the opportunistic collection of Arctic cod near the water surface. Seabirds were collected with the use of a shotgun and seal tissues were obtained from Inuit hunters from the Grise Fiord, Canada and Qânâq, Greenland. A summary of samples collected is outlined in Appendix 1.

Sample extraction and data analysis

Sample extraction and cleanup were performed by collaborator Aaron Fisk and colleagues, and described in detail elsewhere [140, 181, 182]. Briefly, sample tissues (whole organism for zooplankton and fish, liver tissues for birds, and blubber from ringed seals) were ground with anhydrous sodium sulfate, and extracted by Soxhlet extraction using dichloromethane/hexane (1:1). Concentrations of PCB congeners detected can be found in Appendix 2. Trophic level position for individual organisms was previously determined by Fisk et al. [177] using stable nitrogen isotope analysis and are reported in Appendix 1. A relatively constant enrichment of ^{15}N occurs (3-4 ‰) with increasing trophic level, thus a relative trophic position can be obtained for organisms using stable nitrogen isotopes [186]. Abundances of stable nitrogen isotopes reported in Appendix 1 were calculated based on the deviation from standards ($\delta^{15}N$ ‰) according to the following equation:

$$\delta^{15}N \text{ ‰} = [(^{15}N/^{14}N\text{sample}/^{15}N/^{14}N\text{standard}) - 1] \times 1000 \quad (2)$$

where $^{15}N/^{14}N$ standard values were based on atmospheric nitrogen. Trophic levels ($TL_{consumer}$) were determined relative to the copepod *Calanus hyperboreus* (primary herbivore), which was assumed to be representative of the base of the food web occupying a trophic level of 2. Trophic levels were determined according to the following relationship:

$$TL_{consumer} = 2 + (\delta^{15}N_{\ consumer} - \delta^{15}N_{C.\ hyperboreus})/3.8 \quad (3)$$

where $\delta^{15}N_{C.\ hyperboreus}$ is equal to 7.7 and 3.8 representing the isotopic enrichment factor between trophic levels. Due to differences in diet-tissue isotopic fractionation, Fisk et al. [177] modified equation 3 for trophic level calculation for seabirds to:

$$TL_{bird} = 3 + (\delta^{15}N_{consumer} - 10.1)/3.8 \quad (4)$$

Chiral analysis of PCBs 91, 95, 149, 174, 176, and 183 on a subset of the collected samples [177, 178] of the species mentioned above were carried out by gas chromatography mass spectrometry using various stationary phases: Cyclosil-B (J&W Scientific, Folsom, CA, USA), Chirasil-Dex (Varian, Palo Alto, CA, USA), and BGB-172 (BGB Analytik, Adiswil, Switzerland). Details of analysis have been described elsewhere [75]. Briefly, for Cyclosil-B and Chiralsil-Dex, 2 µl aliquots were injected in splitless mode (injector temperature, 250°C) with He as a carrier gas at a constant flow of 1 ml/min. Initial oven temperature of 60°C held for 2 min, temperature ramp of 10°C/min to 150°C, followed by 1°C/min up to 250°C and held for 20 min. For the BGB-172, injection and carrier gas conditions are identical to those described for the Cyclosil-B and Chirasil-Dex stationary phases. Initial oven temperature of

60°C held for 2 min, temperature ramp of 15°C/min to 150°C, followed by 1°C/min up to 225°C and held for 15 min. The GC/MS transfer line temperature was held at 280°C, with the ion source (70 eV electron energy) and quadrupole temperatures of 230°C and 150°C, respectively. Chiral PCB compositions were expressed as enantiomer fractions (EFs) [70]:

$$\mathrm{EF} = \frac{E_1}{E_1 + E_2} \tag{1a}$$

where E_1 and E_2 represent the concentrations of the first and second eluting enantiomers, respectively, when the enantiomer elution order was unknown: PCB 91 and 95 on Chirasil-Dex, and PCB 183 on BGB-172 [75]. For PCB 149, the (-)-enantiomer elutes first while for PCB 174 and 176, the (+)-enantiomer elutes first on Chirasil-Dex [75]. For these congeners enantiomer fractions were calculated as:

$$\mathrm{EF} = \frac{(+)}{(+) + (-)} \tag{1b}$$

Average and standard deviation of EFs for racemic standards ranged from 0.496 ± 0.004 to 0.505 ± 0.008 [50]. A 95% confidence interval (± 0.032) was used as a conservative measure of EF precision for the racemic standards (EF = 0.5) [50] based on variation observed in EFs for racemic standards analyzed on several stationary phases. Calculated EFs falling outside the 95% confidence interval (0.5 ± 0.032) were considered non-racemic. Enantiomer fraction distributions among different species were compared using a one-way analysis of variance with Tukey honestly-significant-difference tests run on all significantly different groups (overall $p < 0.05$). All enantiomer fractions for PCBs detected in the subset of biota investigated are reported in Appendix 3.

Results and Discussion

Zooplankton and arctic cod

Chiral analysis of the omnivorous copepod *Calanus hyperboreus* showed racemic EF values 0.507, 0.490, and 0.493 for PCBs 91, 95, and 149 respectively. Other chiral PCBs investigated were not detected (Table 3). Enantiomer composition was also observed to be racemic for chiral organochlorine pesticides within zooplankton and fish inhabiting the NOW and chiral PCBs within other Arctic regions [45, 178, 183], which supports our findings at lower trophic levels (except PCB 95 in Arctic cod). Unfortunately, other invertebrate species could not be investigated in this study. Non-racemic EFs have been observed in mysids and amphipods in freshwater food webs for chiral PCBs [50]. In that case it was unclear whether stereoselective degradation had occurred or whether the non-racemic EFs observed were from uptake from primary producers or the surrounding environment (sediment). Borgå et al. recently reported non-racemic EFs for chiral organochlorine pesticides in arctic marine ice fauna, zooplankton, and benthos [187]. Enantiomer fractions within these organisms was not statistically different from EFs within the water column, indicating non-racemic EFs is most likely due to accumulation from the water column and sediments; however, the authors could not rule out that biotransformation had occurred.

Enantiomer fractions in Arctic cod for PCB 91 and 149 were 0.524 and 0.509 respectively, suggesting no biotransformation and/or no selective elimination of the enantiomers. However, a non-racemic average EF value of 0.463 was observed for PCB 95. One possible explanation for this non-racemic EF value is stereoselective biotransformation, although fish are not considered efficient at metabolizing PCBs with exception of sculpin [115, 117]. Wong et al. found a mean PCB 95 EF of 0.286 for sculpin in Lake Superior,

Table 1. Average enantiomer fractions (EFs) for polychlorinated biphenyls (PCB) ± standard deviation for Northwater Polynya (Canada) biota. Sample sizes for analysis are given in parentheses for each organism. Asterisks (*) represent EF values based a single measurement. Boldface represents non-racemic EF values (EF values falling outside the racemic confidence interval (0.5 ± 0.032). ND represents non-detect (correlates to concentrations less than 0.1 ng/g wet weight per analyte).

Organism	Enantiomeric Fractions					
	PCB 91	PCB 95	PCB 149	PCB 174	PCB 176	PCB 183
Calanus hyperboreus	0.507 ± 0.012 (n = 3)	0.490 ± 0.001 (n = 3)	0.493 ± 0.006 (n = 3)	ND	ND	ND
Arctic cod	0.524 ± 0.001 (n = 2)	**0.463 ± 0.001 (n = 3)**	0.509 ± 0.036 (n = 3)	ND	ND	ND
Dovekie	ND	0.503 ± 0.007 (n = 2)	**0.111***	ND	ND	ND
Thick-billed murre	**0.676***	**0.742 ± 0.078 (n = 5)**	**0.151 ± 0.071 (n = 5)**	ND	ND	ND
Black guillemot	**0.191***	**0.586 ± 0.037 (n = 2)**	**0.200 ± 0.032 (n = 5)**	ND	ND	ND
Northern fulmar	**0.623 ± 0.009 (n = 3)**	**0.762 ± 0.041 (n = 3)**	**0.418 ± 0.045 (n = 5)**	ND	ND	**0.294***
Ivory gull	**0.497***	**0.840 ± 0.015 (n = 2)**	**0.262 ± 0.089 (n = 5)**	ND	ND	ND
Black-legged kittiwake	**0.542 ± 0.162 (n = 4)**	**0.694 ± 0.179 (n = 4)**	**0.403 ± 0.008 (n = 5)**	ND	ND	ND
Glaucous gull	**0.137 ± 0.024 (n = 5)**	**0.609 ± 0.177 (n = 5)**	**0.277 ± 0.052 (n = 5)**	**0.828***	ND	**0.443***
Ringed seal	**0.063 ± 0.034 (n = 12)**	**0.849 ± 0.072 (n = 12)**	0.478 ± 0.045 (n = 13)	**0.590 ±0.055 (n = 12)**	**0.435 ± 0.049 (n = 3)**	**0.461 ± 0.042 (n = 12)**

USA, a value that was significantly different from the EFs observed in their prey [50]. It is unclear why PCB 95 was susceptible to enantioselective processing in Arctic cod compared to PCB 91 and 149. All three congeners have vicinal hydrogen atoms in meta-para positions, making them susceptible to cytochrome P-450 metabolism [126, 127]. Wong et al. observed similar differences for EF distributions between PCBs 95 and 136 in rainbow trout [58]. Both congeners have similar chlorine substitution patterns (PCB 95: 2,3,6-2,5 on the two phenyl rings; PCB 136: 2,3,6-2,3,6) and have vicinal hydrogen atoms in both of their *meta-para* positions. However, PCB 95 remained racemic in trout throughout uptake/depuration experiments, while PCB 136 was degraded enantioselectively. This suggests that enantioselective degradation of chiral PCBs is regioselective and species dependent, due to the differences observed in enantiomer enrichment for PCB 95 between trout and Arctic cod.

Seabirds

A comparison of EF values in prey and predators within the NOW suggests stereoselective biotransformation of chiral PCBs within higher trophic level organisms (i.e., seabirds and ringed seals). Enantiomer enrichment observed within biota with respect to trophic postion is represented in Figure 10. The two primary food sources for NOW seabirds are Arctic cod and zooplankton [188], which racemic EF values were found for PCB 91, 95 (except Arctic cod) and 149 (Table 3, Figure 10). Most seabirds exhibited non-racemic EFs for PCB 91, 95, and 149. Extensive E2-PCB 91 enrichment was observed in glaucous gulls with a mean PCB 91 EF value of 0.137 for PCB 91. All seabirds, with exception of dovekie, exhibited mean EF values of 0.586 or greater for PCB 95. For PCB 149, all seabirds exhibited EFs of 0.403 and lower, with the alcids (dovekie, thick-billed murre, black guillemot) having the lowest EFs. Non-racemic EF values were also found for PCBs 176 and

Figure 10. Enantiomer fraction (EF) distributions for PCBs 91, 95, and 149 within Northwater Polynya biota. Boxplots are defined as follows: Center line, median; boxplot edges, 25th and 75th percentile; whiskers, smallest and largest value within the distribution. Dotted line represents racemic enantiomer fractions of 0.5. Distributions not significantly different from one another share the same letter designation. Asterisks (*) represent enantiomer fraction value based on a single measurement

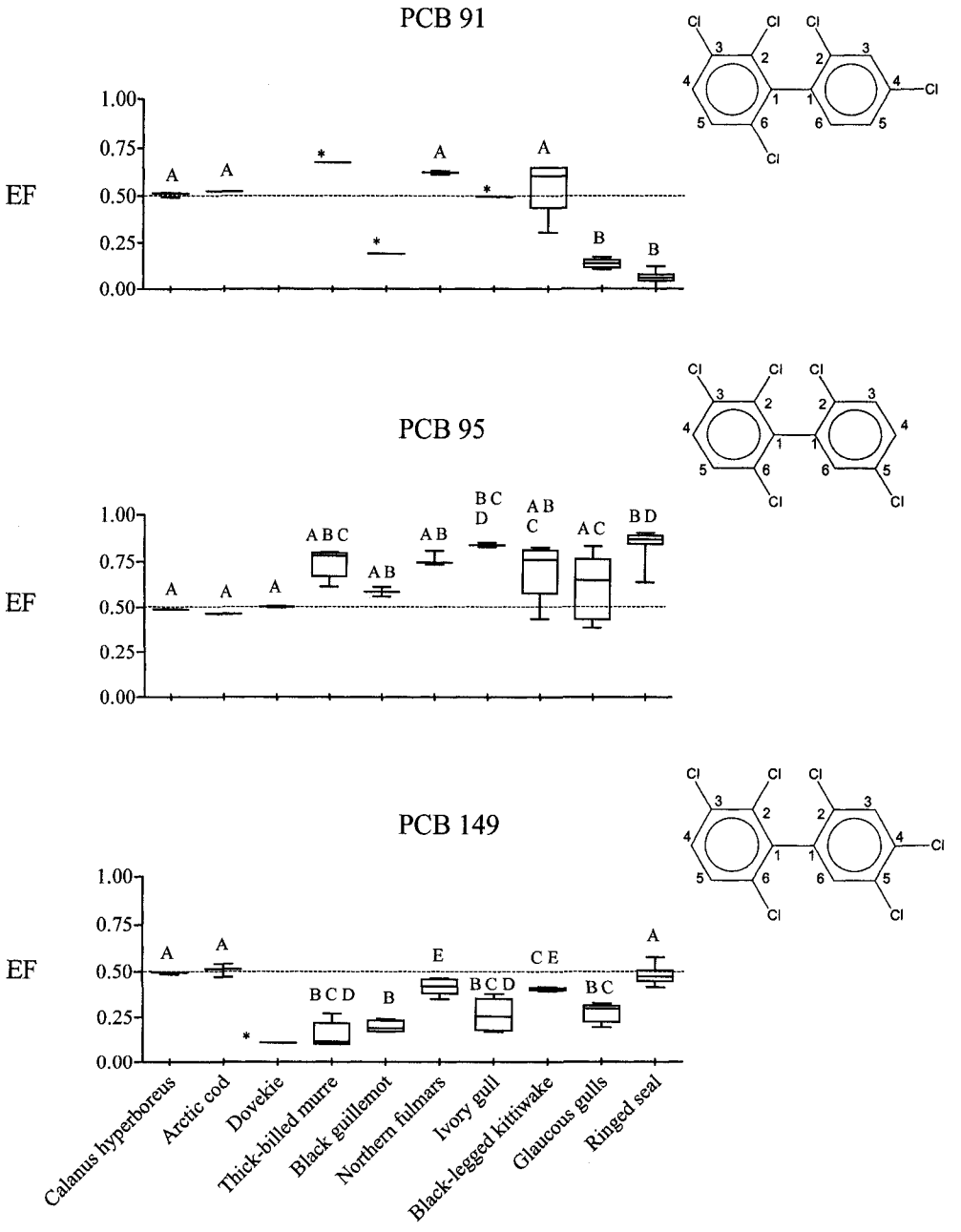

183 in northern fulmars and in glaucous gulls (Table 3), but these values are based on only a single measurement.

Seabirds may feed on a variety of different zooplankton species throughout the year [188]. Although only one species was examined in this study, previous reports have found that EFs of other organochlorine pollutants in zooplankton were similar to those in the water column within the NOW and other Arctic regions [178, 179, 187]. Thus, the EFs observed in *Calanus hyperboreus* would likely be representative of EFs present in the water column and other plankton. Based on our results, it is unlikely that EFs observed in seabirds is solely due to accumulation from invertebrates. Enantiomer fractions present in invertebrates would need to be on the magnitude of those observed in seabirds, which was not observed and is unlikely due to the low biotransformation ability of marine invertebrates [178, 179, 187]. Also, apart from dovekies, the seabird diet consists primarily of Arctic cod, which had racemic EFs for PCBs 91 and 149. Although Arctic cod had an average non-racemic EF for PCB 95, the average EFs observed in seabirds for PCB 95 were higher than the EFs in the prey species, indicating that stereoselective biotransformation had occurred.

Enantiomer fractions for PCB 95 and 149 were non-racemic in the same direction for all seabird species (except dovekie for PCB 95) (Figure 10) with the E1-PCB 95 and (-)-PCB 149 being enriched. Vicinal hydrogen atoms present in the *meta-para* positions make these particular congeners more susceptible to CYP 2B-like enzyme attack [126, 127] compared to recalcitrant congeners, which have no vicinal hydrogen atoms. Drouillard et al. found that PCB congeners having vicinal hydrogen atoms in one or both *meta-para* positions had lower biomagnification factors, relative to recalcitrant PCB 180, and higher elimination rates in American kestrels (*Falco sparverius)* compared to congeners with no vicinal *meta-para*

hydrogen atoms [189]. The most important mechanism contributing to high elimination rates of these readily cleared congeners in birds is biotransformation [190, 191]. Fisk et al. observed enantioselective metabolism of chiral chlordane components within the same seabird species of the NOW food web [184], with enrichment of (+)-oxychlordane and (+)-heptachlor epoxide in all seabirds. These results suggest that seabirds may possess similar stereoselective biotransformation processes for chiral PCBs 95, 149, and chlordane compounds. The EF profile observed for PCB 91 (2,3,6-2,4 substitution) appears to be species dependent among seabirds compared to the profiles observed for PCB 95 (2,3,6-2,5 substitution) and 149 (2,3,6-2,4,5) (Figure 10). Chlorine substitution pattern appears to have an effect on the enantiomer enrichment processes occurring within seabirds. The presence of the *meta*-substituted chlorine (position 5') is a structural characteristic shared by PCB 95 and 149, but not PCB 91. As with the observations made in arctic cod, it is likely that regioselective metabolic processes are affecting the EF distribution of PCB 91 among seabird species.

The range of EF values for PCB 95 in glaucous gulls and PCB 91 and 95 in black-legged kittiwakes was substantially larger then those compared to distributions observed in other seabirds (Figure 10). These wide distributions may be attributed to the wide range of organisms consumed in their diets. For example, glaucous gulls are opportunistic feeders. They consume arctic cod, seabird chicks, and scavenge marine mammal carcasses [188]. Scavenging behavior has also been observed in ivory gulls and northern fulmars [188], which could be another source for the observed non-racemic EF distributions. The distributions of EFs for scavenging seabirds (i.e., ivory gulls and northern fulmars) and ringed seals (Figure 9) were not statistically different ($p > 0.05$) for PCB 95, supporting this hypothesis.

Although most of these seabirds breed within the Arctic, migration to other regions during the winter may also attribute to the wide range of EF values observed. Glaucous gulls and black-legged kittiwakes are migratory birds. As these birds migrate, they will feed upon other organisms that may contain enantiomer enriched signatures of chiral PCBs, causing enantiomer enrichment within their tissues through the accumulation from other sources of prey.

Ringed seals

Nonracemic EF values were observed in ringed seals for PCB 91 and 95 (Figure 10), but racemic EF values were observed in the primary prey species (arctic cod), except for PCB 95. Although seals have limited CYP2B-type biotransformation compared to other mammals [126, 180], results from our study suggest that stereoselective biotransformation of chiral PCBs may be occurring in ringed seals. This is further supported by work done by Wolkers et al., where the presence of a CYP2B-like enzyme was found in ringed seals, although its functional significance is still unknown [192]. Nonracemic EFs were also detected for PCBs 174, 176, and 183 (Table 3) in ringed seals for this study.

Enantiomer fraction distributions among PCB 91, 95, and 149 were different in ringed seals. Though all have vicinal hydrogen atoms present in one or both *meta-para* positions, non-racemic EFs were observed for PCB 91 (E2 enriched) and PCB 95 (E1 enriched), but not for PCB 149. The 3- and 4-$MeSO_2$ metabolites of PCB 149 have been found within ringed seals [36], showing that they are capable of biotransforming PCB 149. Thus, our results indicate that enantiomers of PCB 149 are metabolized at equal rates (non-stereoselective) in ringed seals. What is also interesting to note is that Wiberg et al. found non-racemic distributions of 3-$MeSO_2$-PCB 149 in ringed seals, suggesting that the

production or elimination of this metabolite is stereoselective [119]. However, Letcher et al. found the abundance of 3-$MeSO_2$-PCB 149 in ringed seals to be 3 times less than that observed for 4-$MeSO_2$-PCB 149, which suggests enantiomer enrichment of 3-$MeSO_2$-PCB 149 may be due to further metabolic degradation. In addition, E2-PCB 91 and E1-PCB 95 were enriched in ringed seals. As mentioned earlier for birds, PCB 95 has two sets of vicinal *meta-para* hydrogen atoms, while PCB 91 only has one (Figure 10), and both are susceptible to CYP 2B-like metabolism. Why different enantiomers are enriched between the two congeners if they are being degraded by the same mechanism is unclear. Stereoselective biological processes that alter EFs in ringed seals and other Arctic species appear also to be regioselective. Though exact pathways of PCB accumulation in arctic biota are unknown, it is clear that they are stereoselective.

Conclusions

Chiral PCBs measured in the NOW food web indicated that arctic biota can potentially biotransform chiral PCB atropisomers. Previous studies using achiral methods (e.g., BMFs) have shown that chiral PCB congeners biomagnified in the NOW food web, but provided little information about biotransformation of PCBs except in extreme cases where congeners were readily metabolized. In this study, highly nonracemic enantiomeric fractions (EFs) were observed in several seabird species and ringed seals, but racemic EFs were found in prey (zooplankton and fish). This suggests that stereoselective and species-specific biotransformation of individual PCB stereoisomers by birds and mammals, although uptake of non-racemic sources cannot be ruled out. These results are consistent with previously reported biotransformation activity of chiral organochlorine pesticides α-HCH and chlordane

within these organisms. This study demonstrates the utility of using chiral analysis of PCBs to investigate biotransformation within biota of arctic food webs.

Chapter 3: Enantioselective processing of chiral organochlorine contaminants by freshwater invertebrates[3]

Introduction

Organochlorine (OC) compounds, such as PCBs and pesticides (e.g., HCH, chlordane and nonachlor) were extensively used in the past. Although these 'legacy' chemicals are currently present at low concentrations within most environmental compartments, their lipophilicity allows them to accumulate and magnify in organisms within food webs [6, 7, 27, 28] and they are still a topic of environmental concern.

The fact that some of these OC compounds are chiral can provide enhanced insight into biological processes affecting these chemicals within food webs. Enantiomer enrichment of chiral OC pollutants has been found in a variety of organisms such as fish, birds, seals, polar bears, and whales, in ecosystems ranging from mid-latitude regions to the Arctic [45, 50, 51, 178, 179, 183, 187]. Enantiomer enrichment of chiral OC contaminants is most likely attributed to metabolism, as metabolites of both PCBs and OC pesticides have been found in higher trophic level organisms (i.e., mammals and birds) [119, 135, 140]. Racemic proportions of chiral OC contaminants are commonly found in lower trophic level organisms (i.e., zooplankton) and any enantiomer enrichment observed has been found not to be statistically different from the surrounding environment (i.e., water) [45, 51, 178, 179, 187]. This observation suggests that plankton generally have limited biotransformation capabilities, and that accumulation of OCs is not stereospecific within these organisms;

[3] A version of this chapter has been published. Warner, N.A. and Wong, C. S. Environmental Science & Technology. 2006. 40: 4158-4164.

however, recent studies have shown enantiomer enrichment of chiral OC contaminants by macrozooplankton species [50, 187]. Enantiomer enrichment observed within these organisms is most likely attributed to accumulation from surrounding habitat (i.e., seawater, sediment); however, biotransformation or other enantioselective processing could not be ruled out.

Enantiomer distribution of chiral contaminants at the lower trophic levels has received little attention. Given the recent findings of enantiomer enrichment of chiral OCs in some zooplankton, the focus of this study is to determine whether the opossum shrimp *Mysis relicta* is capable of processing chiral OC contaminants stereoselectively. Mysids are an important component of freshwater aquatic food webs, comprising a major part of diets for many freshwater fish species. Playing the role as both a predator and prey, mysids act as an important vector in the transport and recycling of pollutants through aquatic food webs [193]. Understanding the toxicokinetics of mysids will help provide insight into contaminant fate at lower trophic levels and into trophodynamics of bioaccumulative pollutants. To the best of our knowledge, this is the first laboratory study of stereoselective processing of chiral OCs by invertebrates.

Methods and Materials

Sample collection and experimental design

Mysis relicta were collected from Kootenay Lake, British Columbia, Canada in December of 2004. Specimens were obtained from vertical and horizontal tows using zooplankton nets (1 m × 1 m^2, 520 μm mesh) and stored in chilled water filled coolers (5°C). Samples were transported back to the University of Alberta and transferred to holding tanks contained within an environmental chamber set at 5°C. Animal care and water qualitity

conditions throughout the experiment are outlined in Appendix 3. Surficial sediment was collected from Lac la Biche, Alberta, using an Eckman sampler, placed in 4 L jars, and sieved through a 500 μm sieve. Sediment was homogenized in a polypropylene carboy with the use of a Teflon stirbar, and 12 L of homogenized sediment were transferred to a glass carboy and spiked with several chiral and achiral OCs (purity > 99%): PCBs (chiral congeners 91, 95, 136, 149, 183, and achiral 153), α-HCH, β-HCH, γ-HCH, *trans*-chlordane, and *trans*- and *cis*-nonachlor (Accustandard, West Haven, CT). All test chemicals were dissolved in approximately 10 ml of methanol, added to the slurry and mixed for 24 hours. Once spiked, sediment was then transferred to 4 L jars and refrigerated (5°C) until use, at which point 1.5 L of unspiked (control) or spiked (experiment) wet sediment was added to individual 19 L aquaria followed by 15 L of non-chlorinated water. The slurry was allowed to settle before mysids were introduced.

Approximately 60 – 100 mysids were transferred to individual aquaria containing control or spiked sediment. All aquaria were aerated and pH, ammonia, nitrate and nitrite levels were monitored in each tank through the duration of the experiment. Water changes (10%) were carried out weekly to help maintain water quality. Mysids were fed krill flakes once a week throughout the experiment as a supplementary food source. After a 10-day exposure to the spiked sediment, mysids were transferred to aquaria containing clean sediment to allow for a depuration phase. Control and experimental mysids were collected on days 7, 10, 23, 35, and 55 with an aquarium net, and placed into 4 L beakers filled with clean water at 5° C to purge their guts for 24 hours. Mysids were then collected and placed in precombusted (450°C for 4 hours) glass jars and frozen (-20°C) until extraction.

Sample Extraction

Collected mysids were weighed and extracted using previously reported methods in the literature [140]. Briefly, samples were homogenized with Na_2SO_4 (precombusted at 450°C for 4 hours) by mortar and pestle, surrogate standards, PCB 30 and 204 (purity > 99%) (Accustandard, West Haven, CT) were added, and OCs extracted via Soxhlet extraction with dichloromethane. Extracts were concentrated and an aliquot (ca. 10%) was used to determine lipid abundance gravimetrically. Lipids were removed by gel-permeation chromatography (GPC) (1:1 hexane: dichloromethane). Extracts were solvent exchanged into hexane, and fractionated by alumna/silica chromatography [194]. Internal standards (PCB 166 and tetrachloro-*m*-xylene) were added as a volume corrector while PCB 30 and 204 served as recovery standards. Krill flakes and sediment were extracted in a similar manner. Sediment extracts required no GPC and activated copper was added to remove sulfur.

Data analysis

Extracts were analyzed by gas chromatography mass spectrometry using two different chiral stationary phases: Chirasil-Dex (Varian, Palo Alto, CA, USA), and BGB-172 (BGB Analytik, Adliswil, Switzerland), as previously outlined in Chapter 2. Chiral compositions were expressed as EFs [70] using equations previously defined in Chapter 2:

$$EF = \frac{E1}{E1+E2} \tag{1a}$$

where E1 and E2 represent the concentration of the first and second eluting enantiomer when elution order is unknown (i.e., PCB 91 and 95 on Chirasil-Dex). When the elution order is known, EFs are expressed as the concentrations of the (+) and (-) enantiomers:

$$EF = \frac{(+)}{(+)+(-)} \quad (1b)$$

A standard deviation of ± 0.032 (95% confidence) was used a conservative measure of EF precision for racemic standards (EF = 0.5) [50]. Average EFs for racemic standards ranged between 0.461-0.523 for all analytes investigated. Recoveries for PCB 30 and 204 ranged between 142 ± 13% and 110 ± 8%, respectively for contaminated mysids. Recoveries of the targeted analytes from certified reference material EC-5 (sediment) ranged from 35-88% (n = 2) for analytes investigated.

Results and Discussion

Concentrations and EFs in sediment and krill flakes

The fraction of organic carbon present in the spiked sediments was 32.6 ± 5.6 % by weight determined by loss on ignition and assuming that half the loss was organic carbon. This value is consistent with the hypereutrophic conditions present at Lac la Biche. Analyte concentrations in spiked sediment ranged from 13,100 ng/g for PCB 136 to 37.5 ng/g for PCB 183 (Table 4). For the control sediment, PCBs 95, 136, 149, 153 and the HCH isomers were detected at low concentrations (<0.1% of the spiked sediment concentrations) just above detection limits. Thus the contribution of natively-contaminated OCs to the spiked sediments was negligible.

Racemic EFs were observed for all chiral analytes in the spiked sediment (Table 4). Previous lab studies have documented the change of enantiomer composition for chiral PCBs within sediment [44, 76] as a result of microbial reductive dechlorination. Racemic EFs in the spiked sediment indicate that enantioselective microbial degradation did not occur over

Table 4. Concentration and enantiomer fraction (EF) of targeted analytes for control mysids, control sediment, and spiked sediment. Concentrations are given in ng/g dry weight for sediment and ng/g wet weight for control mysids. Sample size (n): control and spiked sediment, n =4; control mysids, n = 5. Non-detects represented as ND.

Congener	Control Sediment	Spiked Sediment	Control Mysids
PCB 91			
ng/g	ND	1390 ± 279	0.73 ± 0.91
EF	-	0.506 ± 0.002	0.48 ± 0.07
PCB 95			
ng/g	0.32 ± 0.32	1250 ± 253	2.14 ± 2.08
EF	0.50 ± 0.02	0.503 ± 0.001	0.498 ± 0.005
PCB 136			
ng/g	0.49 ± 0.45	13100 ± 2510	1.42 ± 2.08
EF	0.537 ± 0.076	0.497 ± 0.012	0.497 ± 0.026
PCB 149			
ng/g	0.89 ± 0.79	1270 ± 254	6.96 ± 8.45
EF	0.49 ± 0.02	0.501 ± 0.001	0.496 ± 0.001
PCB 183			
ng/g	ND	38 ± 4	ND
EF	-	0.48 ± 0.01	-
PCB 153			
ng/g	0.58 ± 0.52	2480 ± 496	4.86 ± 5.53
α-HCH			
ng/g	4.66 ± 4.38	752 ± 449	41 ± 40
EF	0.502 ± 0.014	0.510 ± 0.004	0.50 ± 0.02
β-HCH			
ng/g	1.70 ± 0.95	1370 ± 900	5.91 ± 6.83
γ-HCH			
ng/g	1.05 ± 1.22	70 ± 36	0.68 ± 1.2
trans-Chlordane			
ng/g	ND	1380 ± 757	ND
EF	-	0.512 ± 0.003	-
trans-Nonachlor			
ng/g	ND	1690 ± 986	1.33 ± 1.51
cis-Nonachlor			
ng/g	ND	1560 ± 931	ND

the time period of the experiment. Analytes were not detected in krill flakes (< 0.02 ng/g), therefore contaminant burden in mysids is solely due to spiked sediment exposure.

Mysid achiral chemical composition

The lipid abundance in mysids ranged from 1.5–2.0 % by weight. Lipid abundance was found to be smaller than reported values with the literature [50, 99, 195], thus concentrations were reported in wet weight. No difference in mysid concentration trends over time was observed between concentrations reported in wet weight basis compared to concentrations reported in lipid weight basis. Concentrations for control mysids were reported as the average of analytes detected in all control samples (n=5), and ranged from 0.73-6.96 ng/g wet weight for detected PCB congeners (Table 4). Pesticide concentrations were similar to the PCB concentrations in control mysids except for α-HCH, which had the highest concentration (41 ng/g wet weight) of all the targeted analytes. This is probably due to the higher concentration of α-HCH in the control sediment, compared to other OC contaminants investigated (Table 4). Concentrations in mysids exposed to spiked sediment were at least one order of magnitude higher then concentrations observed within the control mysids (Figure 9). Mysid concentrations for spiked treatments at each time point were a composite of all organisms within a given tank (n = 1) to avoid pseudoreplication. Concentrations for day 7 and 10 ranged from 13 – 972 and 14.6 – 1450 ng/g for all PCB congeners, respectively, and 44.3 – 188 and 53.9 - 454 ng/g for HCH isomers and OC pesticides respectively.

Mysid concentrations declined for some but not all analytes during the depuration phase (Figure 11). Concentrations within exposed mysids for PCB 183, β-HCH and *cis*-

nonachlor showed no appreciable decrease in concentrations during the depuration phase. The difference in analyte concentrations for days 23, 35 and 55 was within the average %RSD observed for PCBs (23.4%) and HCH isomers and OC pesticides (59.3%) within the

Figure 11. Concentrations (ng/g wet weight) and EFs for OC contaminants in mysids as a function of time. Dashed line represents concentration; solid line represents EFs; dotted lines around racemic EF of 0.500 represent 95% confidence measure of racemic EF precision (EF = 0.500 ± 0.032). Vertical solid line at 10 day represents the end of the uptake phase of the experiment. Only concentration profiles are shown for achiral compounds.

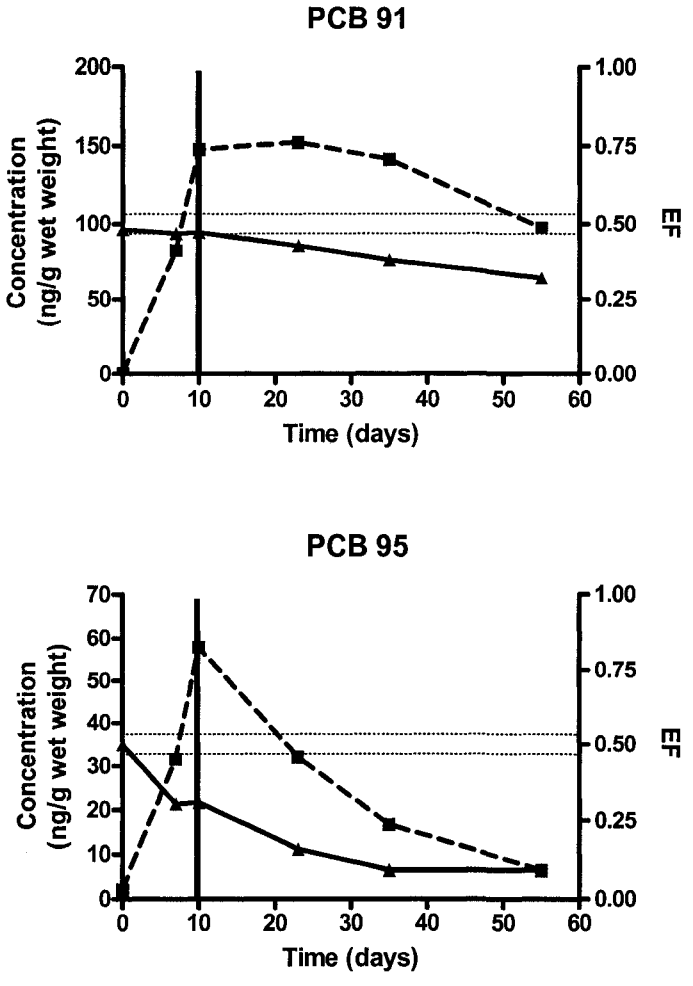

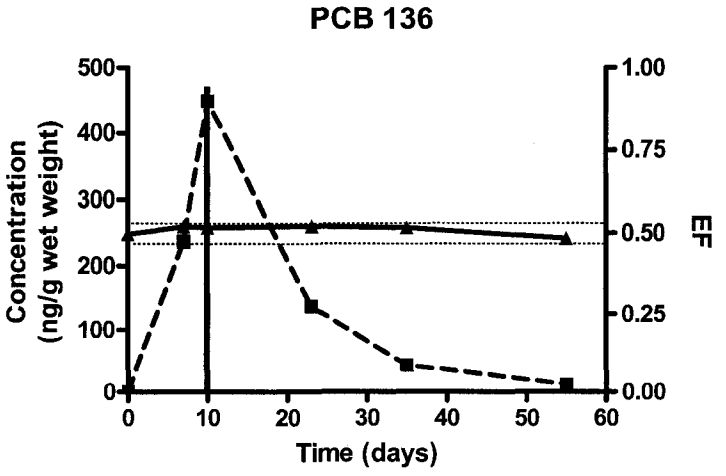
PCB 136
Concentration (ng/g wet weight)
EF
Time (days)
0
100
200
300
400
500
0.00
0.25
0.50
0.75
1.00
0
10
20
30
40
50
60

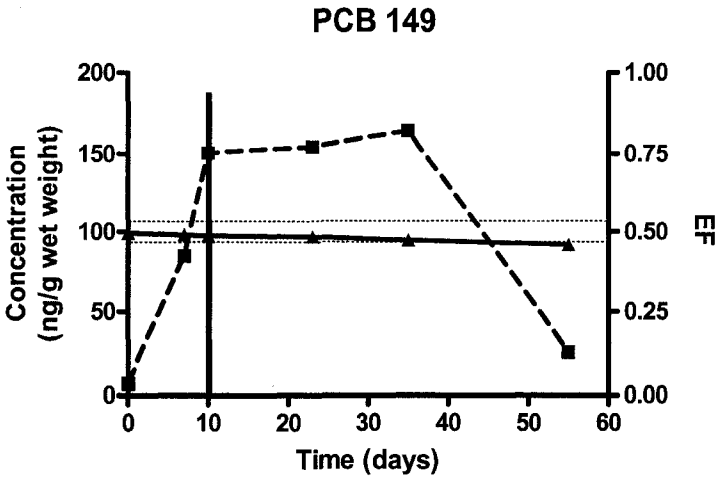
PCB 149
Concentration (ng/g wet weight)
EF
Time (days)
0
50
100
150
200
0.00
0.25
0.50
0.75
1.00
0
10
20
30
40
50
60

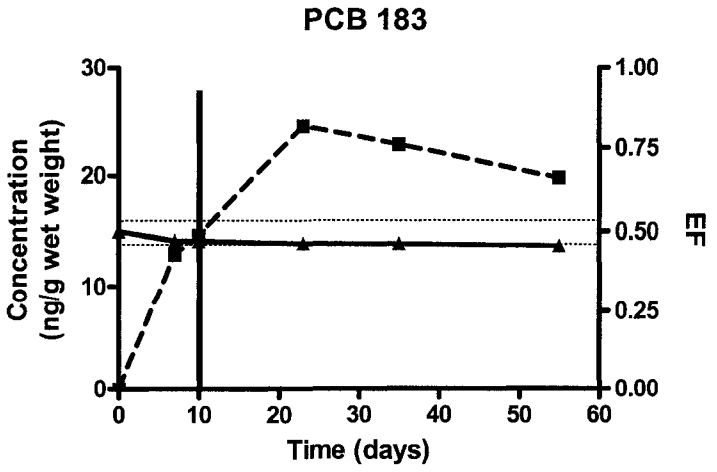
PCB 183
Concentration (ng/g wet weight)
EF
Time (days)
0
10
20
30
0.00
0.25
0.50
0.75
1.00
0
10
20
30
40
50
60

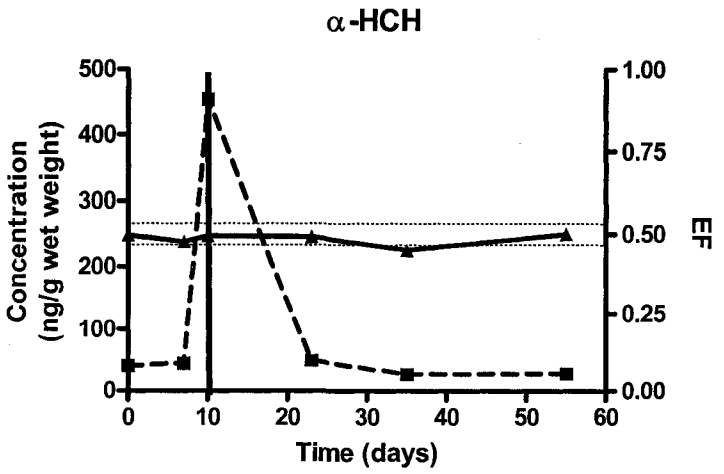
α-HCH
Concentration (ng/g wet weight)
EF
Time (days)
0
100
200
300
400
500
0.00
0.25
0.50
0.75
1.00
0
10
20
30
40
50
60

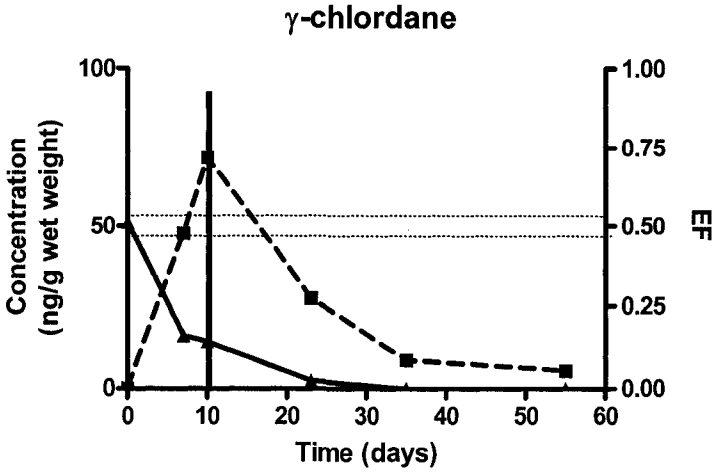
γ-chlordane
Concentration (ng/g wet weight)
EF
Time (days)
0
50
100
0.00
0.25
0.50
0.75
1.00
0
10
20
30
40
50
60

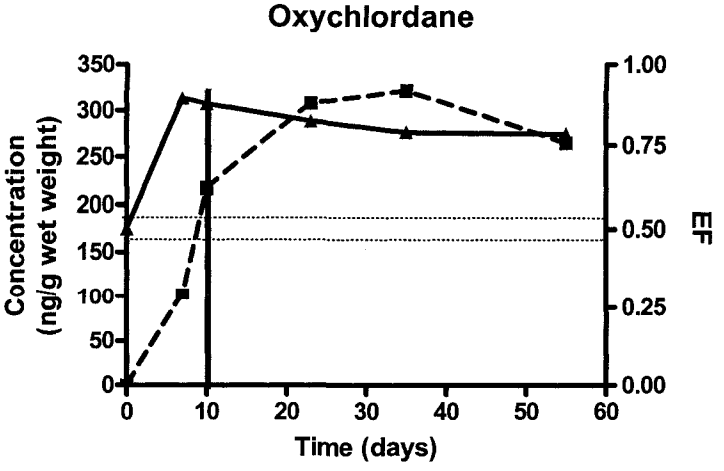
Oxychlordane
Concentration (ng/g wet weight)
EF
Time (days)
0
50
100
150
200
250
300
350
0.00
0.25
0.50
0.75
1.00
0
10
20
30
40
50
60

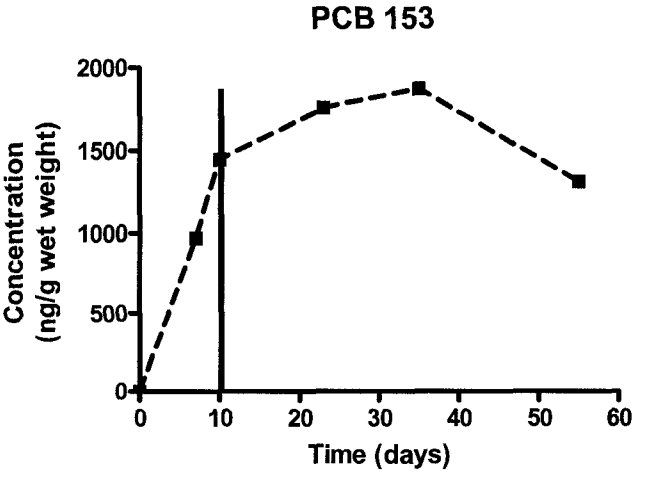
PCB 153
Concentration (ng/g wet weight)
2000
1500
1000
500
0
0
10
20
30
40
50
60
Time (days)

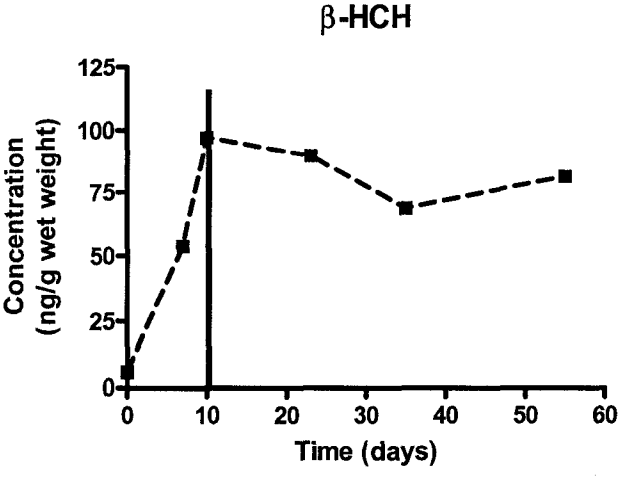
β-HCH
Concentration (ng/g wet weight)
125
100
75
50
25
0
0
10
20
30
40
50
60
Time (days)

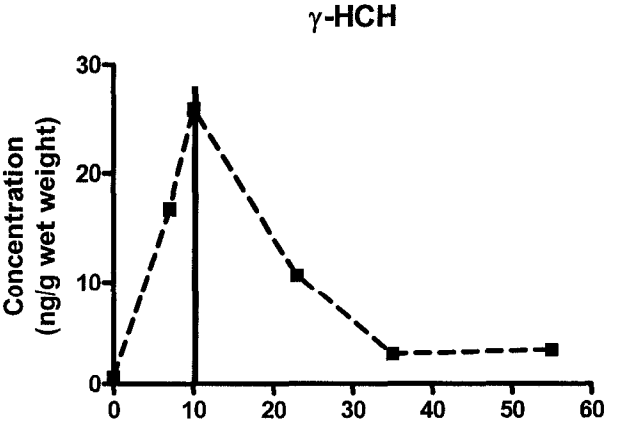
γ-HCH
Concentration (ng/g wet weight)
30
20
10
0
0
10
20
30
40
50
60

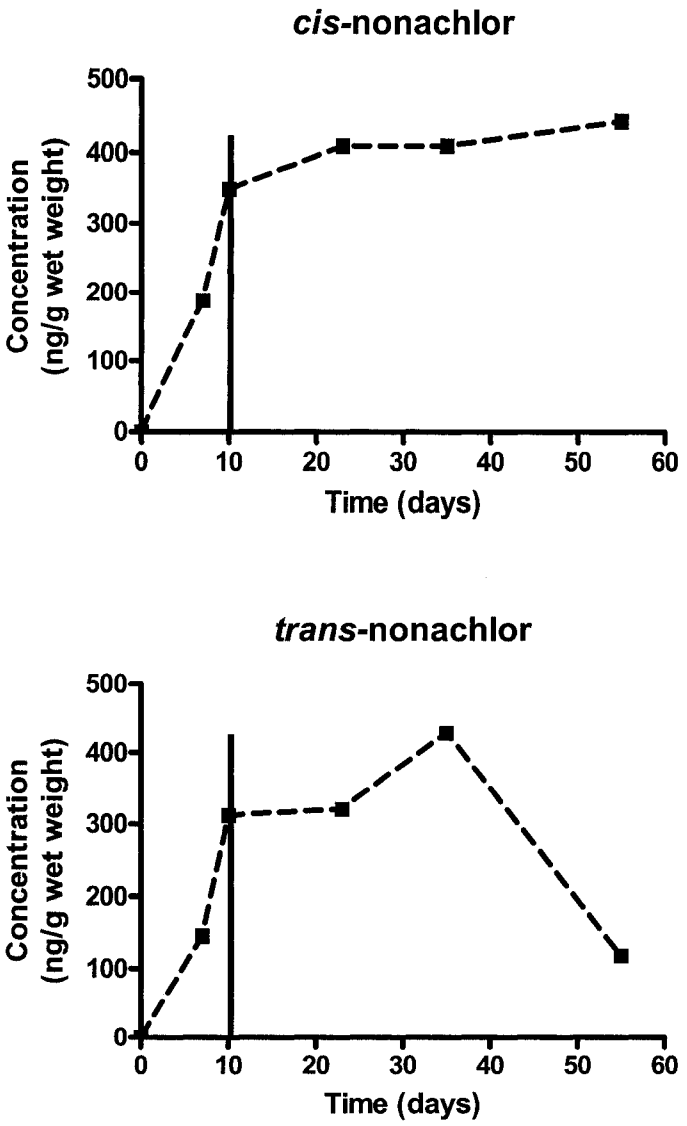

spiked sediment. This observation could be due to a combination of factors. The resistance to biological/chemical degradation of these chemicals has been well documented in the literature. Higher chlorinated biphenyls have been shown to exhibit greater resistance to biological processing [196, 197] and would explain why no appreciable decrease in concentration for PCB 183 was observed. This was also observed for PCB 153 up to day 35, which is also extremely resistant to biological degradation. In comparing the persistence of

the HCH isomers within the environment, β-HCH has been reported to be the most recalcitrant and having a high bioaccumulation potential [198, 199]. This is supported by our results, as β-HCH was the most persistent of all the HCH isomers within the exposed mysids. Another factor contributing to the concentration trends observed is the mysids' feeding behaviour. Mysids are known raptorial feeders and scavengers [98, 99] and will feed upon other mysids [200] as well as scavenge carcass of deceased organisms [201]. No appreciable decrease in concentration during the depuration phase may be attributed to mysids maintaining their contaminant burden from the consumption and scavenging of other mysids. This argument is also supported by observation, where the population of mysids within both control and experimental tanks decreased over time (average loss of 15% over the course of the experiment) and could not be accounted. Rates of elimination for PCBs were highest for PCB 136 and 95. PCB 149 showed no appreciable decline in concentration up to day 35 of the depuration phase suggesting that elimination, if any, was occurring slowly up to this point. *Trans*-Chlordane, α- and γ-HCH showed declines in their concentration during the depuration phase, whereas no appreciable decline was observed for trans-nonachlor until much later in the depuration phase. Physical uptake or abiotic processes could not explain differences in elimination rates for OC contaminants. For example, the log K_{ow} values for the HCH isomers is fairly similar and should be eliminated a similar rate if partiontioning is the mechanism responsible for elimination; however, very different elimination rates are between these isomers is observed. These finding argues that metabolism for α- and γ-HCH is occurring, or that β-HCH is being retained by some unknown mechanism. Similar results were also observed for the PCBs. For example, the log K_{ow} for PCB 91 and 95 is 6.13 [202]. If elimination within the mysids was solely due to physical-chemical processes (i.e.,

partitioning), one would expect the concentration profiles to be similar for the two congeners; however, this is not observed. The concentration of PCB 91 declines at a much slower rate then PCB 95 (Figure 11). Both congeners contain 5 substituted chlorines, and chlorine substitution pattern around the biphenyl core differs by the position of one chlorine between PCB 91 (2,3,6 - 2',4') and PCB 95 (2,3,6- 2',5'). Chlorine substitution pattern of PCB congeners is important in determining the ease of metabolism. It has been shown that chlorine substitution will dictate which of the many cytochrome P-450 (CYP) enzymes will metabolize particular congeners [126]. For example, PCB congeners possessing vicinal hydrogen atoms in their *meta, para* positions are susceptible to CYP 2B metabolism in mammals. One possibility for the difference is that the elimination process is regioselective, which is supported by similar findings within the literature. Wong *et al.* observed differences in EFs between PCB 95 and 136 in rainbow trout [58]. Both congeners have similar chlorine substitution patterns, each possessing vicinal hydrogen atoms in their *meta, para* positions on both rings; however, throughout uptake/depuration experiments, PCB 95 remained racemic whereas PCB 136 was degraded enantioselectively. Differences in EFs have also been observed for PCB 91, 95 and 149 within ringed seals presented in Chapter 2 [51]. These congeners also possess vicinal hydrogen atoms in their *meta, para* positions on one (PCB 91 and 149) or both rings (PCB 95), however, enantiomer enrichment was only found for PCB 91 and 95, whereas PCB 149 was found in racemic proportions, suggesting that stereoselective metabolism may also be regioselective for these congeners.

Mysid enantiomer composition

Chiral PCBs and OC pesticides in control mysids were found to be racemic (Table 4). A significant increase ($p < 0.05$) in non-racemic EFs for *trans*-chlordane and PCBs 91, 95,

and 149 was observed over time in mysids exposed to spiked sediment (Figure 11). A depletion of the (+)-*trans*-chlordane and E1-PCB 95 was observed within 7 days after initial exposure. The EFs at day 10 were similar to that observed at day 7 for *trans*-chlordane and PCB 95, probably due to continual influx of racemic exposure from the sediment. The presence of oxychlordane in exposed mysids showed that *trans*-chlordane was undergoing stereoselective biotransformation (Figure 11). It is unlikely that the source of oxychlordane was nonachlor biotransformation, as nonachlors are recalcitrant and would have to lose a chlorine atom to form the epoxide, oxychlordane. Enantioselective analysis of oxychlordane shows enrichment of the (+)-enantiomer, indicating that the formation of oxychlordane is occurring from the enantioselective biotransformation of *trans*-chlordane. Non-racemic EFs were observed within 23 and 55 days after initial exposure for PCB 91 and 149, respectively. For PCB 149, EFs remained racemic until 55 days after initial exposure, wherein a non-racemic EF (0.459) as well as a significant decline in concentration was observed. This suggests that stereoselective mechanisms acting upon (+)-PCB 149 were occurring more slowly compared to those acting upon *trans*-chlordane, PCBs 91 and 95. Non-racemic EFs were also observed for PCB 183 (Figure 11) near the end of the experiment. However, the slope of EF vs. time was not significantly different from zero ($p > 0.05$), indicating that no stereoselective degradation had occurred for PCB 183. Our results agree with field observations for PCB 91 and 95, where enrichment of the first eluting enantiomers were observed in mysids in Lake Superior [50]; however, EFs for PCB 149 differed between this study and the observations made in Lake Superior [50]. This difference could be attributed to uptake of non-racemic EFs from the surrounding environment in Lake Superior, as non-racemic EFs have been observed in environmental compartments (i.e., sediment, water) for

chiral OC contaminants [43, 50, 76]. It should be noted that EFs measured for PCB 91 and 95 in mysids from Lake Superior could also be attributed to uptake of non-racemic EFs from the surrounding environment; however, from the findings presented in this study, the EFs observed in mysids from Lake Superior is most likely due to metabolism. For *trans*-chlordane, depletion of the (+)-enantiomer has also been observed in amphipods in the Arctic [187].

The most likely explanation for the non-racemic compositions observed for PCBs 91, 95, 149, and *trans*-chlordane is stereoselective biotransformation (metabolism). For the PCB congeners, all have *meta-para* vicinal hydrogen atoms that are amenable to CYP 2B biotransformation, suggesting that mysids may have CYP 2B-like detoxification activity. *Trans*-chlordane is known to be more labile than most other chlordane compounds [58] and is consistent with our hypothesis. The rapid decrease in concentrations for α-HCH and PCB 136 are consistent with non-stereoselective biotransformation. To our knowledge, this is the first evidence for stereoselective biotransformation of OC pollutants by invertebrates, and suggests that field observations of non-racemic compositions of chiral OC contaminants in zooplankton [50, 187] may be due to biotransformation.

Low trophic level organisms are considered to have limited biotransformation capabilities for OC contaminants [45, 51, 178, 179, 187]. Previous laboratory studies have shown mysids are capable of metabolizing benzo(*a*)pyrene, but have no metabolic activity towards PCBs [110, 203]. However, these studies used PCB 153 for their investigation, which is well known for its recalcitrance. Non-racemic EFs observed may also be due to other enantioselective processes such as selective protein binding. This is unlikely to affect the enantiomer composition observed for Soxhlet solvent extraction is an exhaustive

technique, and any analyte that may be selectively bound to proteins will be removed. Opportunistic feeding behaviour and flexible diets (zoo- and phytoplankton, amphipods, sediment and detritus, dead organisms, other mysids and fish larvae [98, 99, 200, 201, 204, 205]) may allow mysids to have a more enhanced metabolic system compared to other zooplankton to process chemicals accumulated from a such a variety of food sources. Because spiked sediment had racemic amounts of chiral OC contaminants throughout the experiment, the EFs observed within the mysids was not due to uptake from the surrounding environment but via metabolic degradation. Our results do not prove that biotransformation was occurring for PCBs since metabolite products such as methylsulfonyl- and hydroxylated PCBs were not studied; however, the presence of oxychlordane in non-racemic proportions does show stereoselective biotransformation of *trans*-chlordane.

Minimum elimination rates for chiral OC contaminants within mysids

Estimates of minimum biotransformation rates can be calculated, using nonlinear least squares regression of the changes in EF over time [50, 58] from the following expression:

$$EF = \frac{1}{1 + \frac{(-)_o}{(+)_o} e^{((k+)-(k-))t}} \quad (5)$$

where t is the mysids' age, $k+$ and $k-$ are the elimination rate constants (metabolic and non-metabolic) for the (+) and (-) enantiomers respectively, and $(+)_o$ and $(-)_o$ are the initial concentrations of the (+) and (-) enantiomers respectively in the mysids. Although neither $k+$

nor *k*- are known, a minimum biotransformation rate constant (k_{min}) can be calculated assuming that stereoselective metabolism is acting upon only one of the enantiomers, and the rate for non-metabolic elimination is the same both enantiomers and is not stereoselective. Taking this into account, we can rearrange equations 5 and yield:

$$EF = \frac{1}{1 + \frac{1 - EF_{mysid}}{EF_{mysid}} e^{-k\min t}} \quad (6)$$

It should be noted that calculated rates are conservative measures of elimination and are only used to compare the elimination of the analytes investigated in this study. Half-lives of PCB 95 and *trans*-chlordane elimination were approximately 3 and 9 days, respectively (Table 5). Longer half-lives of 51 and 231 days were observed for PCB 91 and 149, respectively.

Table 5. Minimum elimination rate (k_{min}) (± stanard error) and half-life for PCB 91, PCB 95, PCB 149, and *trans*-chlordane. Rates are calculated as per equation 6. All rates are given in reciprocal days (d^{-1}) and half-life is reported in days (d).

	PCB 91	PCB 95	PCB 149	*trans*-chlordane
k_{min} (d^{-1})	$(0.01 \pm 6.5) \times 10^{-4}$	0.074 ± 0.010	$(0.003 \pm 1.80) \times 10^{-4}$	0.207 ± 0.014
Half-life (d)	51	9.37	231	3.35

It is likely that the rapid elimination rates calculated for mysids in this study are due to the exposure concentrations, which were higher than that in field studies (ΣPCB_{mysids} = 280 ng/g lipid) [50], and are not likely to reflect those for mysids in open waters exposed to lower contaminant concentrations. Higher elimination rates at higher concentrations suggest

possible enzyme induction and that the detoxification mechanism within mysids may be CYP mediated.

Conclusions

Elimination of chiral polychlorinated biphenyls (PCBs) and organochlorine (OC) pesticides by the opossum shrimp, *Mysis relicta,* was found to occur stereoselectively under laboratory conditions. Rapid accumulation occurred within mysids exposed to sediment contaminated with chiral OC compounds. Enantiomer enrichment was observed within mysids for the first eluting enantiomer and the (-)-enantiomer of PCB 95 and *trans*-chlordane, respectively, after 7 days of exposure to spiked sediment, and for PCBs 91, 149 and 183 over longer time periods. Enantiomer fractions decreased with concentration during the depuration phase of the experiment for PCBs 91, 95 and *trans*-chlordane, showing that elimination of these chemicals is stereoselective. Oxychlordane was detected after exposure, indicating that mysids metabolize *trans*-chlordane enantioselectively. Minimum elimination rates calculated were higher than biotransformation rates calculated for fish in previous studies. This study is the first to show stereoselective processing of chiral OC contaminants by aquatic invertebrates.

Chapter 4: Enantioselective biotransformation of chiral polychlorinated biphenyls *in vitro* and formation of hydroxylated metabolites (OH-PCBs)

Introduction

Environmental concentrations of polychlorinated biphenyls (PCBs) have slowly declined over the years as a result of international regulations on their production and use. However, PCBs are still among the most abundant organohalogen contaminants present in the environment because of their inherent environmental persistence [26]. Food web biomagnification of PCBs [28, 206-209] presents an increased toxicological risk to higher trophic level organisms. Despite that higher trophic level organisms may have greater metabolic capacity to eliminate accumulated PCBs through biotransformation, this is not necessarily a detoxifiction step considering that PCBs may be transformed to bioactivated and persistent metabolites [128].

Phase I metabolism of PCBs is known to include reaction with the cytochrome P-450 (CYP) enzyme system [128] to yield hydroxylated PCBs (OH-PCBs). These may be conjugated and excreted in either the urine or feces due their increased polarity; however, some OH-PCBs can persist in the blood and plasma of various organisms [135, 151, 152, 154-156]. The mechanism responsible for OH-PCB persistence in blood and plasma is attributed to structural similarities to the thyroid hormones, particularly thyroxine (T4). This allows OH-PCBs to bind to the thyroid transport protein, transthyretin [167, 180], with much higher affinity compared to thyroxine, and thereby potentially causing hormone disruption, or cytotoxic and thyroidogenic effects.

In recent years, enantiospecific analysis has been used to provide insight into the biotransformation capacity of organisms towards chiral PCBs (i.e., atropisomers) [8] that otherwise could not be determined by routine monitoring of food webs using achiral techniques and parameters (e.g., BMFs) [18, 43, 45, 50, 51, 101]. Biological processes that favor processing of one enantiomer over the other will cause enantiomer enrichment, and may influence toxicological risks if one enantiomer is inherently more toxic [10, 11]. Enantiomer enrichment in organisms has mainly been attributed to metabolism; however, we are unaware of any studies that have directly compared the biotransformation rates of the individual chiral PCB enantiomers. This is a critical data gap because other biological processes, including selective protein binding [12, 118] and tissue transport [13] can also influence enantiomer compositions in certain tissues or fluids. Thus the mechanism(s) for controlling PCB enantiomer enrichment are poorly understood.

Many chiral PCBs are directed through the mercapturic acid pathway during metabolism to form persistent methylsulfonyl PCB metabolites ($MeSO_2$-PCBs) [106, 118, 120-123]; however, little data is available for OH-PCBs of the chiral congeners. Many of the OH-PCBs detected within environmental samples remain unidentified due to the lack of appropriate standards. Given laboratory and field observations of non-racemic chiral PCBs in invertebrates [101], fish [50, 58], birds [51, 53], and mammals [17, 18, 38, 45, 46, 51, 105, 106], it is possible that many of the unidentified OH-PCBs in samples are from degradation of the chiral congeners. This hypothesis has not been yet been tested to date, thus the objective of this study was to investigate enantioselective metabolism of chiral PCBs and the formation of OH-PCBs *in vitro* using purified mammalian CYP isozymes. An understanding of the factors controlling stereo-specific kinetics of chiral PCBs and formation of their

hydroxylated metabolites in a simple *in vitro* system will aid in understanding the biological fate of chiral PCBs *in vivo* and may also help to identify OH-PCBs detected in the surrounding environment.

Methods and Materials

Chemicals and reagents

Rat CYP 2B1 and 3A2 isozymes, and human CYP 2B6 and CYP 3A5 isozymes, insect cell control supersomes (P450 reductase and cytochrome b_5) and NADPH regeneration solutions (solution A: 26.1 mM NADP+, 66 mM glucose-6-phosphate, 66 mM $MgCl_2$; solution B: 40 U/ml glucose-6-phosphate dehydrogenase, 5 mM sodium citrate) were purchased from BD Biosciences (San Jose, CA). These particular enzymes were chosen because the chlorine substitution pattern of chiral PCBs makes them preferred substrates for CYP 2B and 3A, respectively, in rodents and humans [127, 129]. Racemic chiral PCBs 45, 84, 91, 95, 132, 136, 149, 183 and recovery standards PCB 30 and 204 (>99% purity) were obtained from Accustandard (West Haven, CT). Acetone solutions of chiral PCBs (5 µg/ml) were prepared as single congeners or mixtures. Mass-labelled hydroxylated PCBs (4-hydroxy-[$^{13}C_{12}$] PCB 29; 4-hydroxy-[$^{13}C_{12}$] PCB 61; 4-hydroxy-[$^{13}C_{12}$] PCB 120; 4-hydroxy-[$^{13}C_{12}$]PCB 159; 4-hydroxy-[$^{13}C_{12}$]PCB 172; 4-hydroxy-[$^{13}C_{12}$]PCB 189) were obtained from Wellington Laboratories (Guelph, ON, Canada) as recovery standards for metabolite extraction (chemical purity > 98%, isotopic purity > 99%).

In vitro biotransformation assays

In vitro assays contained 25 pmol of CYP isozyme, 50 µl of solution A and 10 µl of solution B (NADPH regeneration system) and 915 µl of potassium phosphate buffer (110 mM, pH 7.4). The amount of CYP isozyme used was determined through *in vitro* assay

incubations with all the chiral PCB congeners at varying CYP dosages of 10, 20, and 40 pmol and incubation periods ranging from 10-60 minutes. These preliminary screens determined that 25 pmol of enzyme and a 30 min incubation period were appropriate for our individual congener assays. Assays were spiked with either a mixture of racemic chiral PCBs or individual racemic chiral PCB congeners (25 ng of each congener in all cases) and incubated for 30 minutes at 37.5°C. Incubations were terminated with 1 ml of ice-cold methanol and immediately extracted. Control assays were run under the same conditions, except 75 pmol of insect control supersomes, which contained no CYP, were used to equal the protein content of the rat and human CYP isozyme incubations.

Extraction procedure

Extraction of PCBs and their hydroxylated metabolites has been previously described in the literature [151] and are outlined in detail in Appendix 5. Briefly, 20 ng of each PCBs 30 and 204, and the mass-labelled OH-PCBs were added as internal standards to the incubation vial after biotransformation reactions were terminated. The incubations were acidified with HCl and extracted with 6 ml of 1:1 methyl-*t*-butyl ether (MTBE)/hexane. The organic phase was collected, solvent exchanged to hexane, and partitioned with 6 ml of 1 M KOH to separate the weakly acidic OH-PCBs from the neutral organic phase. The aqueous fraction, containing OH-PCBs, was then acidified and back-extracted into MTBE/hexane (1:1). The organic phase was collected, solvent exchanged to hexane, and derivatized with diazomethane to convert the OH-PCBs into their respective methoxy-PCBs (MeO-PCBs) derivatives for instrumental analysis.

The neutral fraction, containing the chiral PCBs, was purified using an acidified silica gel column (3 g, 22% H_2SO_4) and elution with 20 ml of 15% (v/v) dichloromethane

(DCM)/hexane. The MeO-PCB fraction was purified using a 5 g column of the acidified silica gel and elution with 50 ml of 1:1 DCM/hexane. Both PCB and MeO-PCB fractions were finally solvent exchanged to hexane, reduced to a final volume of approximately 200 µl and fortified with 50 ng of PCB 159 (Accustandard, West Haven, CT) as a volume corrector.

Instrumental analysis

Chiral PCBs and MeO-PCBs were quantified using an Agilent 5890 (Mississauga, ON, Canada) gas chromatograph equipped with an electron capture detector (GC/ECD). Separation of PCBs was performed on a DB-XLB column (30 m × 0.25 mm × 0.5 µm, J & W Scientific, Folsom CA, USA) as previously reported [73]. Briefly, 2 µl samples were injected in splitless mode at 250°C with helium as carrier gas and at a constant head pressure of 27.5 psi. Initial oven temperature was held at 100°C for 1 min, then ramped at 2.5°C /min to 293 °C, and then held for a further 2 min. The detector temperature was 320°C, and nitrogen was used as a make-up gas. The MeO-PCB fraction was also separated using the DB-XLB column but under slightly different conditions: a constant head pressure of 15 psi helium was used and initial oven temperature was held at 100°C initial temperature for 2 min, ramped at 20°C/min to 240°C, held for 25 minutes, ramped at 10°C/min to 275°C followed by a 14 min hold.

Authentic OH-PCB standards for the chiral PCBs are not commercially available and therefore any detected OH-PCBs could not be accurately quantified. Peaks detected by GC/ECD analysis were then analyzed by GC/high resolution mass spectrometry (GC/HRMS) using an Agilent 6890 GC interfaced to a Kratos M-50 magnetic sector high resolution mass spectrometer (Manchester, United Kingdom). The same GC conditions were used, except helium carrier gas had a flow rate of 34 cm/s. Single ion monitoring in electron impact (EI)

mode (70 eV) with a mass resolution of 10,000 was used to scan unknown peaks for theotretical mass to charge ratios (*m/z*) of the molecular ions of the derivatized OH-PCBs outlined in Table 6.

Table 6. Calculated and obtained masses of methoxy-PCBs (MeO-PCBs) from individual chiral PCB congener assays by GC/HRMS.

	Relative retention time[a]	Mass obtained	Integrated mass range
MeO-PCB 45	0.6797	319.93293 321.92998 323.92703	319.93343 - 319.93243 321.93048 - 321.92948 323.92753 - 323.92653
MeO-PCB 84	0.9298	353.89395 355.89100 357.88805	353.89445 - 353.89345 355.89150 - 355.89050 357.88855 - 357.88755
MeO PCB 91	0.8886	353.89395 355.89100 357.88805	
MeO-PCB 95 (1)[b]	0.8477	353.89395 355.89100 357.88805	
MeO-PCB 95 (2)[b]	0.8627	353.89395 355.89100 357.88805	
MeO-PCB 132	1.3555	387.85498 389.85203 391.84908	387.85548 - 387.85448 389.85253 - 389.85153 391.84958 - 391.84858
MeO-PCB 136	1.0448	387.85498 389.85203 391.84908	

[a] Relative retention time was calculated using MeO-PCB 120 as a reference standard.
[b] MeO-PCB 95 (1) and (2) refer to first eluting and second eluting peaks corresponding to the mass of a pentachlorinated MeO-PCB detected for PCB 95 rat CYP 2B1 assay.

Enantiospecific analysis of chiral PCB congeners was performed GC/MS, using several chiral stationary phases: Cyclosil-B (30 m × 0.25 mm × 0.25 μm, J&W Scientific, Folsom, CA, USA), Chirasil-Dex (30 m × 0.25 mm × 0.25 μm, Varian, Palo Alto, CA, USA) and

BGB-172 (30 m × 0.25 mm × 0.18 μm, BGB Analytik, Adliswil, Switzerland). Details on chromatographic conditions have been previously reported [75] and are outlined in Chapter 2. Enantiomer enrichment of chiral PCB congeners was reported as enantiomer fractions (EFs) as shown in equation 1[70]:

$$EF = \frac{E1}{E1+E2} \qquad \text{or} \qquad \frac{(+)}{(+)+(-)} \qquad (1a,b)$$

where E1 and E2 represent the concentration of the first and second eluting enantiomers, respectively, when the elution order is unknown on a given stationary phase (i.e., PCBs 45, 91 and 95 on Chirasil-Dex/Cyclosil-B, and PCB 183 on BGB-172). When the elution order was known (i.e., (−/+) for PCB 84, 132 and 136 on Chirasil-Dex), then EF was calculated as the concentration of the (+)-enantiomer over the summed concentrations of both enantiomers. Enantiomer fractions for racemic standards ranged from 0.485 to 0.506. A 95% confidence interval of 0.5 ± 0.032 for racemic EF values was used to determine if enantiomer enrichment had occurred within the *in vitro* assays [50]. Calculated EFs falling outside this range were considered non-racemic.

Average percent recovery and standard deviation was reported for all internal standards. Recoveries of PCB 30s and 204 were 80 ± 20% and 93 ± 14%, respectively. Concentrations of chiral PCB congeners were recovery corrected based on the recoveries obtained for PCB 204. Recoveries of mass-labelled derivatized OH-PCB standards were found as follows: 52 ± 27% (MeO-PCB 29), 48 ± 19% (MeO-PCB 61), 78 ± 13% (MeO-PCB 120), 81 ± 18% (MeO-PCB 159), 84 ± 16% (MeO-PCB 172), and 79 ± 16% (MeO-PCB 189). Extraction efficiency of OH-PCBs was dependent upon the degree of

chlorination, with lower recoveries obtained for the lower chlorinated OH-PCBs. Our recoveries here were consistent with OH-PCB extraction efficiencies of other studies using this extraction technique [151, 156, 158].

Results and Discussion

Preliminary assays with mixtures of chiral PCB congeners

Rat CYP 2B1 and 3A2

As previously discussed, incubation screens were conducted with a mixture of all the chiral congeners at various isozyme dosages and incubation periods to determine if enantioselective degradation was occurring, and to find an appropriate amount of isozyme and incubation period for the individual assays. In these mixture studies, enantiomer enrichment by rat CYP 2B1 was observed for PCBs 45, 84, 91, 95, 132 and 136 at all isozyme concentrations and incubation times investigated (Figure 12). Similar assay screens were performed with rat CYP 3A2 but showed no evidence of enantiomer enrichment for any of the chiral PCBs, thus these isozymes were not further investigated. Enantiomer enrichment for chiral PCBs was also reported *in vivo* in rats [105, 106], where enrichment of E1-PCB 95 and (+)-PCB 132 was observed in adipose, skin, liver, and lung tissue. The same enrichment pattern for PCB 95 and 132 was observed in our incubations and suggests that the mechanism responsible for enantiomer enrichment of these congeners *in vivo* could be the selective biotransformation by CYP 2B1. We observed no enantiomer enrichment of PCB 183 by rat CYP 2B1, which may be attributed to overall biotransformation recalcitrance due to the higher degree of chlorination [196] and lack of vicinal *meta, para* hydrogen atoms, which make other PCBs amenable to CYP 2B and 3A activity [127, 129].

Figure 12. GC/MS chromatograms of *in vitro* biotransformation screens of chiral PCBs separated on Cyclosil-B stationary phase for control and rat CYP 2B1 assays. Rat CYP 2B1 assay was incubated for 30 minutes with 20 pmol of enzyme. Enantiomers of PCB 84 and 149 could not be resolved on this stationary phase.

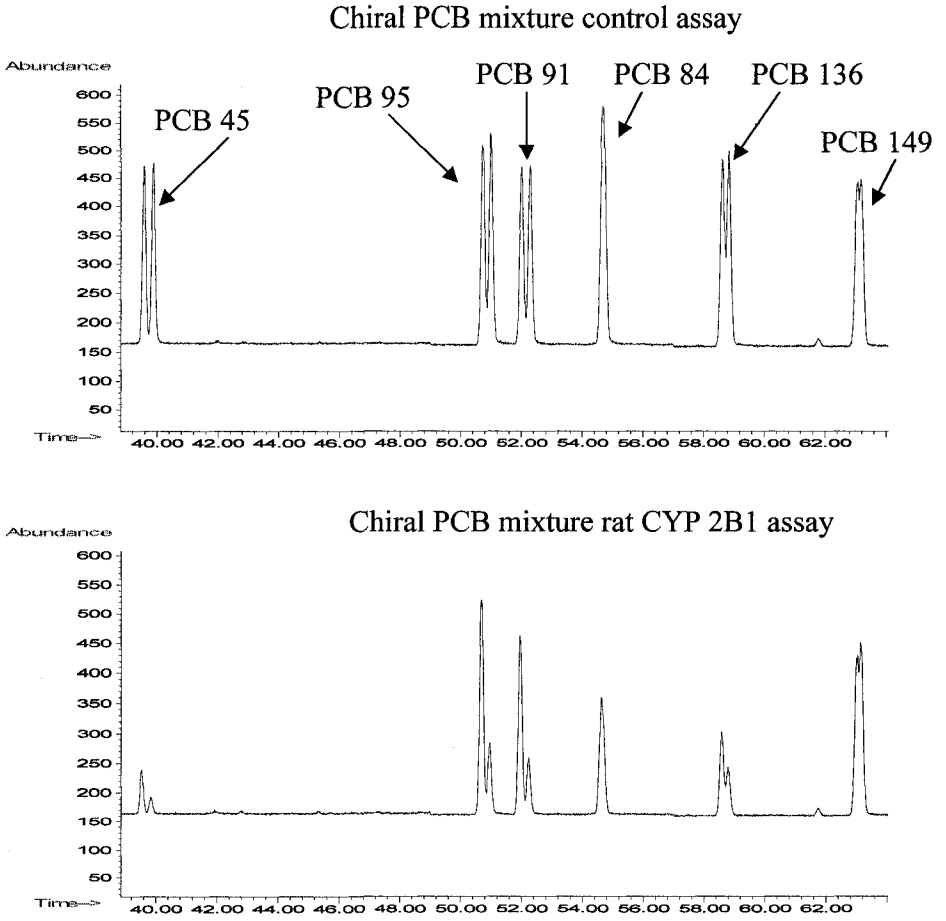

No significant enantiomer enrichment was observed for PCB 149 in any of the rat CYP 2B1 assay screens except at 40 pmol enzyme dosage incubated for 40 minutes (EF = 0.464). The slope of PCB 149 concentration vs. time for was found to be statistically different from zero ($\rho < 0.05$) over the 60 minute in period indicating biotransformation of PCB 149, but at a much slower rate compared to the other congeners. Larsson et al. [118]

reported enantiomeric enrichment of 4-$MeSO_2$-PCB 149 metabolite in rats exposed to a technical PCB mixture and postulated that enantioselective metabolism or selective transport across cell membranes may be responsible. Enantiomer enrichment of 4-$MeSO_2$-PCB 149 differed between tissues (liver EF = 0.82 vs. lung EF = 0.24) [118] which may suggest that other processes (i.e., selective protein binding or transport) besides enantioselective metabolism are responsible for the enantiomer enrichment of this metabolite in rats. In our experimental system, enantioselective biotransformation is the only possible mechanism explaining the enantiomer enrichment because there are no transport processes, and lack of enantiomer enrichment in the control assays rules out selective protein binding as a possible mechanism *in vitro*. Non-racemic EFs of chiral $MeSO_2$ PCBs detected in rats exposed to technical mixtures of PCBs *in vivo* suggests these metabolites may be formed enantioselectively through the metabolism of the parent congener [118]. Enantiomer enrichment for PCB 149 in the current work did not occur to the same extent observered for 4-$MeSO_2$ PCB 149 in rats [118], but this is not surprising. This can be attributed to the longer incubation times used for *in vivo* experiments in rats as well as the induction of enzymes by higher dose concentrations administered, which were 1000-fold greater then concentration levels used within our experiments. Another possible explanation is that enantiomer enrichment of 4-$MeSO_2$ PCB 149 is not due to enantioselective metabolism of PCB 149, but other Phase II enzymatic processes that are involved in its formation and/or metabolism. This is supported by the findings of Huhnerfuss et al. [150] who observed enantioselective metabolism of 3-$MeSO_2$-PCB 149 by rat liver hepatocytes even though metabolism of PCB 149 was not enantioselective. Competition for the enzyme active site by

other congeners present may also have affected the enantiomer enrichment of PCB 149 in these particular assays.

Human CYP 2B6 and 3A5

Enantiomer enrichment was observed for PCB 45 within 30 minutes when the PCB mixture was incubated with 20 pmol of human CYP 2B6, and no enrichment was observed in control assays. Enantiomer enrichment was not observed for any of the remaining congeners but a decrease in concentration was observed for PCBs 91 and 132 in the longer incubations. This indicates that biotrnsformation of chiral PCB congenrs does not necessarily proceed enantioselectively. This is an important consideration when interpreting EFs from human and environmental samples, in that a racemic signature does not indicate that no biotransformation has occurred. As with our rat CYP 2B1 assay screens, the limited amount of CYP isozyme used in our incubations may affect enantiomer selective processes (i.e., metabolism) by competition at the isozyme active site by other congeners with higher affinity. *In vitro* assay screens involving CYP 3A5 showed no enantiomer enrichment for any of the chiral PCBs and was not further investigated in this study.

Individual congener incubations

Individual congener assays were conducted to determine if OH-PCBs were produced during the enantioselective metabolism of chiral PCBs. Incubations involving one congener simplified the experimental system by eliminating potential competition effects, and also by eliminating ambiguity of which parent congener yielded which OH-PCBs. Focus was placed on chiral congeners that demonstrated enantiomer enrichment in our earlier assay screens (i.e., PCBs 45, 84, 91, 95, 132, and 136) with rat and human isozymes (rat CYP 2B1, human CYP 2B6). Based on the extent of enantiomer enrichment observed in the assays, 25 pmol of

CYP isozyme and a 30 minute incubation period was deemed appropriate to observe enantiomer enrichment within our individual congeners.

Rat CYP 2B1

Enantioselective degradation was observed for PCBs 45, 84, 91, 95, 132, and 136 when individual PCB standards were incubated with rat CYP 2B1 (Table 7).

Table 7. Enantiomer fractions (EFs) of chiral PCB congeners for standards, control assay, and individual PCB congener rat CYP 2B1 assays. Racemic EF confidence interval of 0.500 ± 0.032 used to determine enantiomer enrichment.

	PCB 45	PCB 84	PCB 91	PCB 95	PCB 132	PCB 136
Standard (n = 3)[a]	0.497 ± 0.005	0.503 ± 0.003	0.498 ± 0.001	0.497 ± 0.001	0.503 ± 0.004	0.503 ± 0.002
Control (n = 1)	0.498	0.494	0.501	0.497	0.495	0.497
CYP 2B1 assay (n = 1)	0.822	0.551	0.353	0.616	0.619	0.415

[a] Number of replicates (n). Enantiomer fractions presented are based on separation obtained using Chirasil Dex stationary phase.

Enantiomer enrichment was observed for E1 of PCBs 45 and 95, and E2 of PCB 91. Enantiomer enrichment of the (+)-enantiomer was observed for PCBs 84 and 132, while the (-)-enantiomer of PCB 136 was enriched. The enantiomer enrichment pattern for PCBs 84, 95, and 132 observed here has also been observed *in vivo* for mice [104] and rodents [105, 106], indicating that enantioselective metabolism could be responsible for the enantiomer enrichment of these congeners within rodents. Enantiomer enrichment patterns in our incubations of PCBs 91, 95 and 132 are also observed in sharks [18], porpoises [46] and seals [38, 51, 103], again suggesting that the mechanism of enantiomer enrichment within these organisms could be due to is similar to CYP 2B-like metabolism. For example, a CYP 2B-

like enzyme has been identified in ringed seals [192] and CYP 2B-like activity has been measured in other seal species [210].

Human CYP 2B6

Enantioselective metabolism in the human CYP 2B6 individual congener assays was not as extensive as observed in the individual rat CYP 2B1 assays. Only enantiomer enrichment of E2-PCB 45 and (+)-PCB 132 was observed, while all other congeners remained racemic for human CYP 2B6 incubations (Table 8).

Table 8. Enantiomer fractions (EFs) of chiral PCB congeners for standards, control assay, and individual PCB congener human CYP 2B6 assays. Racemic EF confidence interval of 0.500 ± 0.032 used to determine enantiomer enrichment.

	PCB 45	PCB 91	PCB 132
Standard (n = 3)[a]	0.499 ± 0.006	0.496 ± 0.002	0.500 ± 0.003
Control (n = 1)	0.501	0.501	0.511
Individual CYP 2B6 assay (n = 1)	0.437	0.492	0.537

[a] Number of replicates (n). Enantiomer fractions presented are based on separation obtained using Chirasil-Dex stationary phase.

Our results are consistent with other findings where enrichment of (+)-PCB 132 has been observed in human liver tissue and breast milk [17, 47], suggesting that enantioselective CYP metabolism could be the mechanism. Enantiomer enrichment of E1-PCB 95 and (-)-PCB 149 was also been observed in human liver tissues [47], but was not observed in our incubations. Enantiomer enrichment of PCB 95 and 149 in human liver tissues may be attributable to other CYP 2B or 3A isozymes not investigated in this study. Although no

enantiomer enrichment was observed for PCB 91, decreases in concentration were observed over time indicating that metabolism had occurred, but not enantioselectively.

Enrichment of PCB 45 differed between rat CYP 2B1 and human CYP 2B6. The former showed enrichment of the first-eluting enantiomer (EF > 0.5), whereas the opposite (EF < 0.5) occurred for the latter, suggesting that a different enantiomer preference exists for these two isozymes. This result is not unexpected since differences in enantiomer enrichment have previously been reported to be species dependent, even among closely related species. For example, enrichment of (-)-PCB 149 was observed in harbour and gray seals, while (+)-PCB 149 was found to be enriched in Baikal seals, and no enrichment was observed in Caspian seals [38]. This has also been observed in seabirds in the Northwater Polynya presented in Chapter 2 where enantiomer enrichment of PCB 91 was also species dependent [51] and is further supported by finding different EFs for chiral chlordane components in northern fulmars and black-legged kittiwakes in the same region [184]. Enrichment of PCB 45 was more pronounced in incubations of rat CYP 2B1 compared to incubations with human CYP 2B6. Rat CYP 2B1 can catalyze the direct insertion of a hydroxyl group at the *meta*-position of the biphenyl core of PCBs [131], and our results suggest this process is enantioselective. This mechanism may also be occurring for human CYP 2B6 isozyme but at a much slower rate. Enantiomer enrichment of PCB 132 in our individual congener assay was unexpected. As previously discussed, no enantiomer enrichment was observed for PCB 132 in the human CYP 2B6 assays incubated with the mixture of chiral PCBs. This is strongly suggests that competition for the enzyme active site by other congeners may affect enantiomer enrichment of the individual PCB congeners in our in vitro system, and warrants further investigations.

Identification of OH-PCBs

Metabolite fractions recovered from individual congener incubations with rat CYP 2B1, human CYP 2B6, and control assays were analyzed by GC/ECD to investigate the formation of OH-PCBs. Electron capture detection was chosen due to its sensitivity towards halogenated compounds and with no commercial standards available for most OH-PCBs of the chiral congeners, the sensitivity of this technique towards OH-PCBs was required. Detection of peaks, not present within our control assays, were observed in the rat CYP 2B1 MeO-PCB fraction extracts from the individual congener incubations of PCBs 91 and 95 (Figure 13). This suggested that these peaks were due to formation of PCB metabolites and were not artifacts of the matrix used in the incubations. The identity of these metabolites was confirmed by GC/HRMS to correspond to the expected mass of the primary and secondary ions of petachlorinated MeO-PCBs (i.e., derivatized OH-PCBs) (Table 6). For PCB 95 incubated with rat CYP 2B1, two metabolite peaks were detected with the same mass as a pentachlorinated MeO-PCB (Figure 13), indicating the formation of two hydroxylated metabolites from the metabolism of this one congener. This may be explained by the multiple unsubstituted *meta-para* sites available on this congener. PCBs having vicinal hydrogen atoms at the *meta-para* positions makes them more susceptible to oxidation by CYP 2B [126, 127]. The chlorine substitution pattern for PCB 95 (2, 3, 6 substitution on one phenyl ring, 2, 5 on the other) allows it to have two open *meta-para* sites available for oxidation, possibly resulting in the formation of two different pentachlorinated OH-PCBs. This alos explains why we only observe one PCB metabolite from PCB 91, for it contains only one open *meta-para* site. Based on this explanation, we should also expect to see the

Figure 13. Metabolite fractions of control and rat 2B1 assays for chiral PCBs analyzed by GC-ECD. Mass-labelled derivatized standards: MeO-PCB 29 (1); MeO-PCB 61 (2); MeO-PCB 120 (3); MeO-PCB 187 (5); MeO-PCB 159 (6); MeO-PCB 172 (7). PCB 159 (volume corrector) (4); pentachlorinated MeO-PCB (circled peaks)(8).

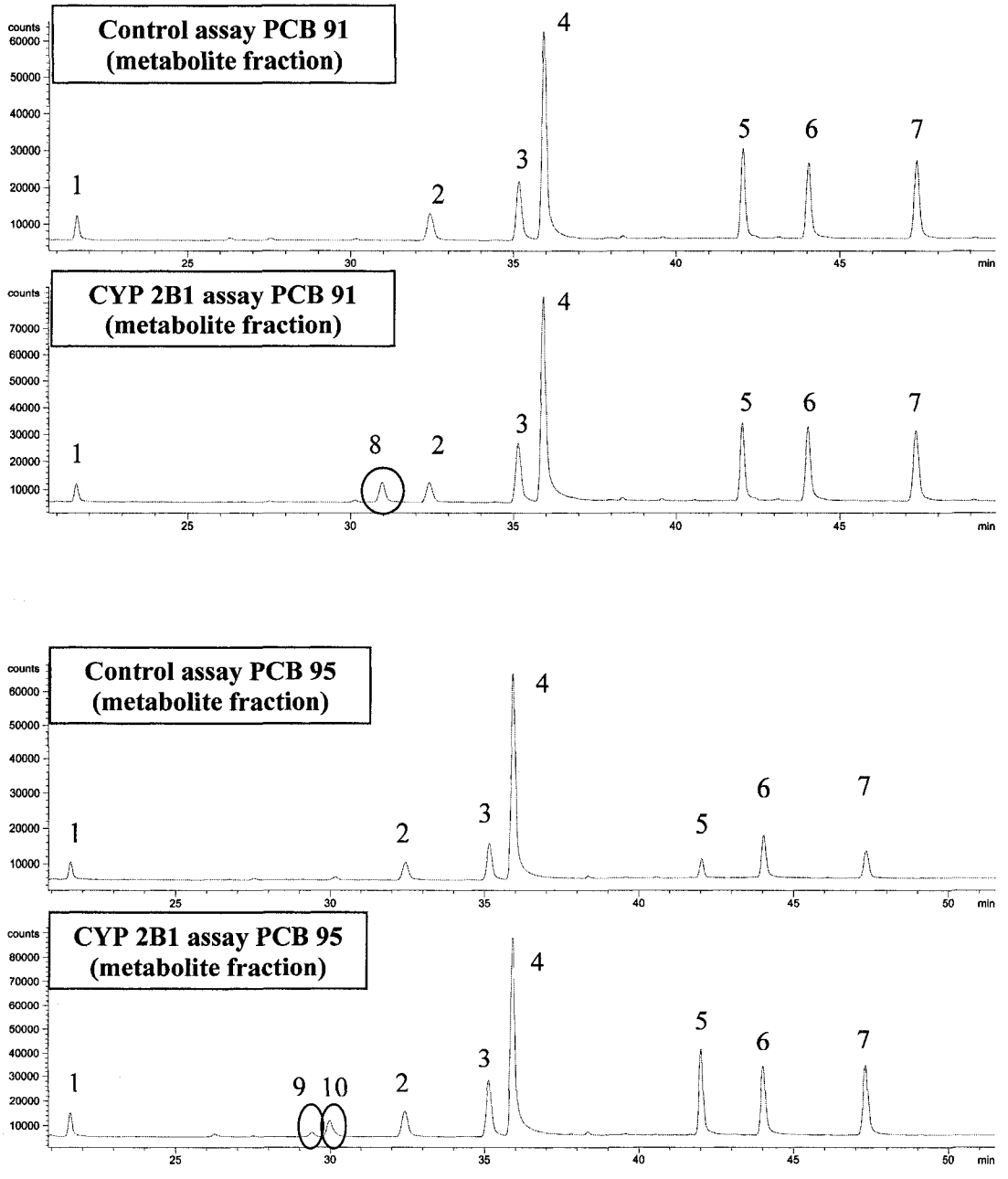

formation of two OH-PCBs for PCB 84, which also contains two open *meta-para* sites, but only one pentachlorinated MeO-PCB was detected for this congener. This suggests that the positioning of chlorine atoms around the biphenyl core along with vicinal hydrogen atoms in the *meta-para* positions has an effect on metabolism by rat CYP 2B1. The formation of OH-PCB metabolites was also detected for the remaining chiral congeners.

Rat CYP 2B1 has been shown to catalyze the direct insertion of a hydroxy group in PCB metabolism [130, 131], and results here suggest that this process is enantioselective in rats. We cannot state categorically that this is true because as a result of not having authentic OH-PCB standards, we lack mass-balance data to demonstrate that production of OH-PCBs was a major metabolic fate in our system. For example, PCBs may also undergo epoxidation by the CYP enzymes, rather than direct OH insertion. However, we performed a semi-quantitation by using the response factor of the closest eluting OH-PCB to the metabolite of interest. These OH-PCB concentrations corresponded to 64-96% of the decrease in concentration observed for the corresponding parent PCB congeners, indicating that a substantical proportion of the parent PCBs were degraded by CYP-mediated metabolism. This percentage may not reflect the amount of hydroxylated metabolites produced *in vivo* since conjugation by Phase II metabolic processes may also direct the formation of other metabolites.

For human CYP 2B6, unknown peaks detected in the MeO-PCB fractions of PCB 45, 91 and 132 corresponded to the same retention times and masses expected for tetra-, penta-, and hexachlorinated MeO-PCBs (Table 6), thus confirming the formation of the OH-PCB metabolites. The peak area of metabolites detected in human CYP 2B6 assays by GC-ECD was 5-10 times less abundant than OH-PCBs in the rat CYP 2B1 study. Decrease in PCB

concentration in human CYP 2B6 incubations was comparable to those in the rat CYP 2B1 incubations. The lower concentration of OH-PCBs formed by human CYP 2B6 may be attributed to a different biotransformation mechanism compared to rat CYP 2B1, which is supported by the lack of enantiospecific metabolism observed for human CYP 2B6.

A large portion of the OH-PCBs detected within studies investigating the fate of PCBs in biotic and abiotic environment cannot be identified due to the lack of available standards [102, 116, 151, 153, 156-158]. Unidentified di- to hexachlorinated OH-PCBs were predominant in bottlenose dolphins [156], which were consistent with the findings of Kunisue et al. who found unidentified penta- and hexachlorinated OH-PCBs to be predominant within the brain tissue of cetaceans [157]. Our results show the formation of tetra-, penta-, and hexachlorinated OH-PCBs, likely via the enantioselective metabolism of chiral PCBs.

Chiral PCB enantiomer biotransformation kinetics

Four general mechanistic routes have been proposed for chiral specific metabolism by organisms [211]. First, two enantioselective enzymes are available, each converting one of the enantiomers at different rates. Second, both enantiomers are simultaneously metabolized by one enzyme but at different rates. Third, one enantiomer is preferentially metabolized followed by the other enantiomer, but only when the first enantiomer has been completely metabolized. Finally, one enantiomer is enantioselectively metabolized by one enzyme and racimization of the other enantiomer by an isomerase. The first and fourth scenario could be ruled out as mechanisms in the current *in vitro* system as all incubations only utilized a single enzyme, none of which are considered isomerases and, furthermore, the detection of a large fraction of metabolites seems to minimize the potential importance of racemization. This

leaves only the second and third scenarios as possible routes of enantioselective metabolism in our incubations.

The labile individual chiral PCBs showed an increase in enantiomer enrichment with a decrease in concentration over longer incubation times (Figure 14). The enantiomers of PCB 45 were metabolized by rat CYP 2B1 at the fastest rate among all the chiral PCB enantiomers with E1-PCB 45 and E2-PCB 45 metabolized at a rate of 3.8×10^{-2} and 6.9×10^{-2} min^{-1}, respectively (Table 7). This is consistent with literature observations, in which elimination rates for PCBs decreased with higher degrees of chlorination in rats [196, 197]. For all enantiomers investigated, the slopes of first order-decay plots (not shown) were statistically different from zero except for (+)-PCB 132, suggesting that metabolism of PCB 132 only affected the (-)-enantiomer. Norström *et al.* found formation of both *meta* and *para* substituted $MeSO_2$-PCB 132 metabolites in rats exposed to (+)-PCB 132, but at much lower concentrations compared to rats expose to (-)-PCB 132 [106]. This suggests that employing longer incubation periods *in vitro* may reveal a significant decrease in the concentration of (+)-PCB 132, but was beyond the scope of our study. Rate constants among individual enantiomers of chiral PCB congeners were not statistically different, except for PCBs 95 and 132 (Table 9), indicating that the individual enantiomers for these congeners were metabolized at different rates. These results suggest that the route by which enantiomer enrichment occurs within our incubations was due to different rates of metabolism of the individual enantiomers, which is supported by other findings of enantioselective metabolism within rats [106]. To the best of our knowledge, this is the first study to investigate the rates of metabolism for the individual enantiomers of chiral PCBs and the first time that it has been shown that both enantiomers are degraded by a single isozyme.

Hydroxylated PCBs of chiral congeners could make up a portion of the unidentified OH-PCBs that have been detected in the surrounding environment, which could be confirmed if more authentic standards become available. It would be advantageous to have more authentic standards available.

Conclusions

Enantiomer enrichment of chiral polychlorinated biphenyls (PCBs) and the formation of OH-PCBs demonstrated that rat CYP 2B1 and human CYP 2B6 isozymes can enantioselectively metabolize chiral PCBs *in vitro*. Enantiomer enrichment was observed for PCBs 45, 84, 91, 95, 132, and 136, with EFs ranging from 0.353 to 0.822, when incubated individually with rat CYP 2B1. Enantioselective metabolism was also observed for PCBs 45 (EF = 0.437) and 132 (EF = 0.537) when incubated with human CYP 2B6. Hydroxylated PCBs were unambiguously identified for all individual chiral PCBs enantioselectively degraded by rat CYP 2B1 and human CYP 2B6 by GC/HRMS. Semiquantitative analysis indicated that OH-PCBs formed accounted for more than half of the total congener metabolized by rat CYP 2B1. These OH-PCB congeners did not correspond to any available authentic standards, suggesting that some of the many unidentified OH-PCBs detected in wildlife may have arise from *in vivo* biotransformation of the chiral PCB congeners. Both enantiomers of chiral PCBs were metabolized simultaneously by the rat CYP 2B1 isozyme (except for (+)-PCB 132), but at different rates, resulting in enantiomer enrichment. This is the first study to show that both enantiomers can be transformed simultaneously by a single isozyme. Different metabolic rates between chiral PCB enantiomers, and similar enrichment patterns compared to field observations, supports that metabolism is a prime mechanism responsible for enantioselective processing of chiral PCBs in mammals. Formation of OH-

PCBs via an enantioselective OH insertion mechanism was suggested, and this may represent a source of the unidentified OH-PCBs currently found within the environment.

Table 9. Pseudo-first order biotransformation rate constants for individual enantiomers of chiral PCB congeners.

	Chlorine substitution pattern[a]	Pseudo-first order rate constant (10^{-2}, min^{-1})	Correlation coefficient	ρ value[b]
PCB 45	2,3 - 3,6			
E1		3.8	0.77	0.02
E2		6.9	0.68	0.04
PCB 84	2,3,6 - 2,3			
(+)		2.2	0.87	0.01
(-)		1.6	0.88	0.01
PCB 91	2,3,6 - 2,4			
E1		1.9	0.75	0.03
E2		0.8	0.75	0.02
PCB 95	2,3,6 - 2,5			
E1		0.8	0.94	< 0.01
E2		2.3	0.97	< 0.01
PCB 132	2,3,4 - 2,3,6			
(+)		0.08	0.11	0.59
(-)		0.9	0.83	0.03
PCB 136	2,3,6 - 2,3,6			
(+)		2.6	0.80	0.02
(-)		1.6	0.86	0.01

[a] Chlorine substitution pattern is presented as substitution of ring 1 - substitution of ring 2 format, e.g., PCB 95 (2,2',3,5',6) is presented as 2,3,6 - 2,5.

[b] Probability threshold was set at 0.05, thus $\rho < 0.05$ indicates slope of ln(concentration) vs. time trends are statistically different from zero.

Figure 14. Concentration (ng/ml) (■) and enantiomer fractions (EFs) (▲) vs. time (minutes) for individual chiral PCB congeners incubated with 25 pmol of rat CYP 2B1 enzyme. Dotted lines around racemic EF of 0.500 represent the 95% confidence interval of racemic EF precision (± 0.032). Enantiomer fractions reported for PCB 91 were based on separation using Cyclosil-B stationary phase. All concentrations have been recovery corrected.

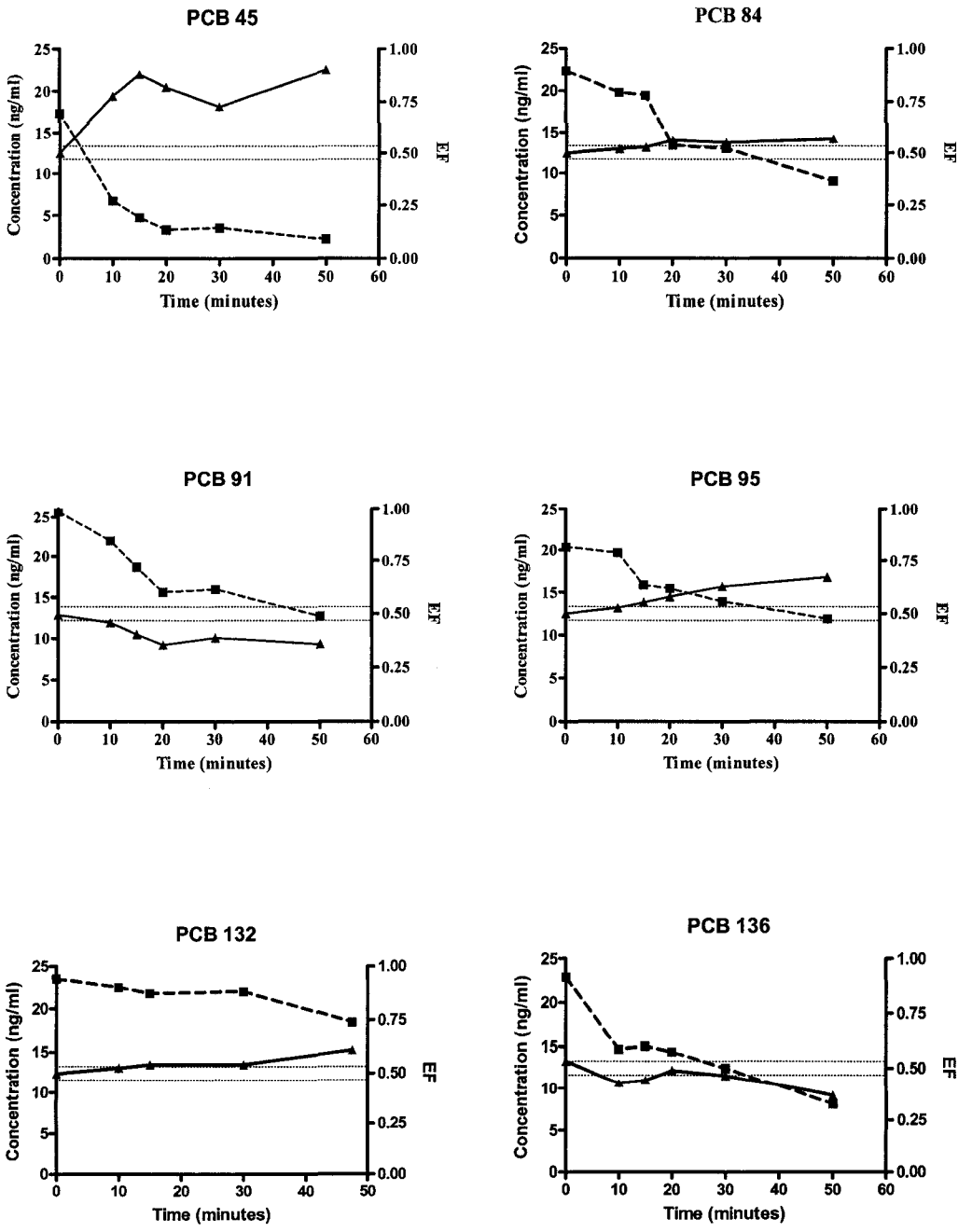

Chapter 5: Conclusions and Future Directions

Findings presented within this dissertation have shown that metabolism is the major process responsible for enantiomer enrichment of PCB atropisomers within *in vivo*, *in vitro* and field based studies. Comparison of EFs detected within seabirds and marine mammals to organisms that comprise their diet within the NOW food web indicate that enantioselective metabolism is occurring in these higher trophic level organisms. Several studies, including the work presented in Chapter 3, have documented the fate of persistent chiral organochlorine (OC) pollutants within the NOW food web. Future work on addressing the importance of migration of seabirds in relation to uptake of enantiomer enriched pollutants may help explain broad distributions of EFs observed within some seabird species. Future food web alterations caused by climate variations may also drastically affect the uptake and enrichment of chiral OCs within arctic ecosystems, which supports the need for continuous monitoring of these fragile ecosystems.

Uptake of non-racemic EFs from prey organisms can also contribute to enantiomer enrichment in organisms comprising the higher levels of the food web. *In vivo* laboratory studies presented have shown that the freshwater invertebrate, *Mysis relicta*, can metabolize persistent organochlorine contaminants enantioselectively. Enantiomer-enriched signatures of chiral OCs produce within these invertebrates can propagate up the food web, causing and/or contributing to enantiomer enrichment in biota at higher trophic levels. Future research into the enzymes responsible for enantioselective metabolism in *Mysis relicta* could indicate if these invertebrates metabolize chiral OCs in a similar manner as observed in mammals. No enantiomer enrichment within zooplankton in the NOW food web suggests that enantioselective degradation within invertebrates is species specific, and further

investigations are needed to assess if other invertebrates possess enantioselective metabolic capabilities.

Identification of OH-PCBs from enantioselective metabolism of chiral PCBs *in vitro* suggests these metabolites may be present in organisms containing non-racemic proportions of chiral PCBs. Although OH-PCBs of the chiral congeners have not been detected within biota, no commercial available standards exist for these metabolites making their identification in biota difficult. Due to the lack of authentic standards, a large portion of the OH-PCBs detected within biota cannot be identified (50-80%). Hydroxylated PCBs of the chiral congeners may make up a portion of the unidentified OH-PCBs within biota and stresses the need for authentic standards of these metabolites.

Though many studies have reported enantiomer enrichment of chiral PCBs within organisms, few have investigated the enantioselective toxicity that may arise and further research within this area is needed. Enantioselective metabolism of PCB atropisomers suggests that the formation of their metabolites will also be enantioselective; however, no studies have investigated enantioselective toxicity of chiral PCB metabolites. This is particularly significant for the chiral methyl sulfone PCBs, which have been shown to be enriched within tissues of biota and have similar accumulation potential to the parent PCB congeners. Upon identification of the OH-PCBs of the chiral congeners within biota, analytical methodology will need to be developed to separate the individual enantiomers and assess their enantioselective toxicity as well.

Appendix 1

Sample identification, stable nitrogen isotope abundance ($\delta^{15}N‰$), and trophic level for biota in the Northwater Polynya

Appendix 1: Sample identification, stable nitrogen isotope abundance ($\delta^{15}N‰$), and trophic level for biota in the Northwater Polynya. Data not available is represented by na. Data courtesy Aaron Fisk and Ross Norstrom.

File name	Latin name	Common name	Species code	Sex/ age	$\delta^{15}N$ ‰	Trophic level
npz 305	*Calanus hyperboreus*	None	HB	na	7.63	1.97
npz 345	*Calanus hyperboreus*	None	HB	na	6.82	1.76
npz 417	*Calanus hyperboreus*	None	HB	na	7.47	1.93
NWF005	*Boreogadus saida*	arctic cod	NWF	F/na	14.8	3.86
NWF006	*Boreogadus saida*	arctic cod	NWF	F/na	13.7	3.56
NWF008	*Boreogadus saida*	arctic cod	NWF	M/na	13.7	3.57
BLGU180	*Cepphus grylle*	black guillemot	BLGU	M/na	14.6	4.18
BLGU181	*Cepphus grylle*	black guillemot	BLGU	M/na	15.0	4.28
BLGU183	*Cepphus grylle*	black guillemot	BLGU	F/na	14.2	4.08
BLGU184	*Cepphus grylle*	black guillemot	BLGU	M/na	15.8	4.49
BLGU185	*Cepphus grylle*	black guillemot	BLGU	M/na	15.2	4.36
BLGU189	*Cepphus grylle*	black guillemot	BLGU	F/na	14.3	4.11
BLGU190	*Cepphus grylle*	black guillemot	BLGU	M	15.1	4.31
BLGU202	*Cepphus grylle*	black guillemot	BLGU	M	15.3	4.37
BLGU204	*Cepphus grylle*	black guillemot	BLGU	M	15.0	4.30
NOFU112	*Fulmaris glacialis*	northern fulmar	NOFU	M	13.9	4.01
NOFU130	*Fulmaris glacialis*	northern fulmar	NOFU	F	13.8	3.97
NOFU136	*Fulmaris glacialis*	northern fulmar	NOFU	F	13.3	3.83
NOFU140	*Fulmaris glacialis*	northern fulmar	NOFU	M	14.5	4.16
NOFU141	*Fulmaris glacialis*	northern fulmar	NOFU	F	14.1	4.05
NOFU159	*Fulmaris glacialis*	northern fulmar	NOFU	M	13.5	3.90
NOFU160	*Fulmaris glacialis*	northern fulmar	NOFU	F	14.1	4.06
NOFU177	*Fulmaris glacialis*	northern fulmar	NOFU	F	14.1	4.05
NOFU316	*Fulmaris glacialis*	northern fulmar	NOFU	M	14.4	4.14
GLGU008	*Larus hyperboreus*	glaucous gull	GLGU	F	15.3	4.38
GLGU009	*Larus hyperboreus*	glaucous gull	GLGU	F	15.5	4.41

File name	Latin name	Common name	Species code	Sex/ age(years)	$\delta^{15}N$ ‰	Trophic level
GLGU037	*Larus hyperboreus*	glaucous gull	GLGU	M/na	16.4	4.67
GLGU088	*Larus hyperboreus*	glaucous gull	GLGU	M/na	17.6	4.97
GLGU101	*Larus hyperboreus*	glaucous gull	GLGU	M/na	Na	Na
GLGU192	*Larus hyperboreus*	glaucous gull	GLGU	F/na	16.9	4.78
GLGU193	*Larus hyperboreus*	glaucous gull	GLGU	M/na	17.1	4.84
GLGU254	*Larus hyperboreus*	glaucous gull	GLGU	F/na	16.6	4.71
GLGU265	*Larus hyperboreus*	glaucous gull	GLGU	F/na	16.1	4.57
IVGU080	*Pagophila eburnea*	ivory gull	IVGU	F/na	14.2	4.09
IVGU081	*Pagophila eburnea*	ivory gull	IVGU	F/na	14.0	4.01
IVGU182	*Pagophila eburnea*	ivory gull	IVGU	M/na	13.5	3.90
IVGU191	*Pagophila eburnea*	ivory gull	IVGU	M/na	15.1	4.31
IVGU210	*Pagophila eburnea*	ivory gull	IVGU	M/na	13.6	3.91
BLKI113	*Rissa tridactyla*	black-legged kittiwake	BLKI	F/na	12.6	3.64
BLKI144	*Rissa tridactyla*	black-legged kittiwake	BLKI	M/na	13.0	3.75
BLKI145	*Rissa tridactyla*	black-legged kittiwake	BLKI	F/na	13.5	3.90
BLKI148	*Rissa tridactyla*	black-legged kittiwake	BLKI	M/na	13.0	3.77
BLKI149	*Rissa tridactyla*	black-legged kittiwake	BLKI	F/na	13.1	3.79
TBMU120	*Uria lomvia*	thick-billed murre	TBMU	M/na	na	na
TBMU128	*Uria lomvia*	thick-billed murre	TBMU	F/na	13.7	3.94
TBMU129	*Uria lomvia*	thick-billed murre	TBMU	F/na	14.0	4.04
TBMU135	*Uria lomvia*	thick-billed murre	TBMU	M/na	13.6	3.93

File name	Latin name	Common name	Species code	Sex/ age(years)	$\delta^{15}N$ ‰	Trophic level
TBMU142	*Uria lomvia*	thick-billed murre	TBMU	F/na	13.7	3.94
NORS002	*Phoca hispida*	ringed seal	NORS	M/40	16.9	4.40
NORS007	*Phoca hispida*	ringed seal	NORS	F/38	17.4	4.54
NORS010	*Phoca hispida*	ringed seal	NORS	M/23	16.9	4.40
NORS014	*Phoca hispida*	ringed seal	NORS	F/5	17.5	4.58
NORS019	*Phoca hispida*	ringed seal	NORS	M/23	17.7	4.62
NORS020	*Phoca hispida*	ringed seal	NORS	F/30	17.1	4.46
NORS026	*Phoca hispida*	ringed seal	NORS	F/17	17.3	4.52
NORS029	*Phoca hispida*	ringed seal	NORS	F/7	17.5	4.57
NORS033	*Phoca hispida*	ringed seal	NORS	F/22	17.6	4.60
NORS035	*Phoca hispida*	ringed seal	NORS	M/32	17.4	4.53
NORS045	*Phoca hispida*	ringed seal	NORS	F/43	17.5	4.56
NORS048	*Phoca hispida*	ringed seal	NORS	M/na	na	na
NORS055	*Phoca hispida*	ringed seal	NORS	F/4	16.6	4.33

Appendix 2

Concentration of PCB congeners detected within biota of the Northwater Polynya

Appendix 2. Concentration data was analyzed and provide by Dr. Aaron T. Fisk. PCB congeners with no concentration data presented were below the limit of detection (0.02 ng/g).

File name	Common name	PCB concentration (ng/g wet weight)											
		18	16/32	31	28	33/20	52	49	47/48	44	64	74	70/76
npz 305	None	0.15	0.03	0.61	0.21	0.07	0.19	0.10	0.08	0.08		0.07	0.18
npz 345	None	0.18	0.07	1.05	0.23	0.14	0.30	0.15	0.12	0.14	0.07		
npz 417	None	0.22	0.06	1.05	0.25	0.13	0.52	0.26	0.21	0.15	0.06	0.06	0.21
NWF005	Arctic cod	0.06		0.05	0.46		0.19	0.04	0.02		0.06	0.35	0.06
NWF006	Arctic cod	0.12		0.09	1.18		0.35	0.06	0.02		0.06	0.83	0.09
NWF008	Arctic cod	0.01		0.02	0.20		0.05	0.02	0.02		0.04	0.11	0.05
BLGU180	Black guillemot				0.59			0.06	0.17		0.29	3.16	0.90
BLGU181	Black guillemot				0.70			0.06	0.24		0.34	3.78	2.16
BLGU183	Black guillemot				1.66			0.07	0.55		0.55	6.51	0.85
BLGU184	Black guillemot				1.22			0.08	0.70		0.47	5.95	1.75
BLGU185	Black guillemot				0.69			0.07	0.25		0.27	3.97	0.54
BLGU189	Black guillemot				1.05			0.07	0.13		0.51	5.57	1.08
BLGU190	black guillemot				1.26			0.09	0.40		0.57	6.08	1.01
BLGU202	black guillemot				0.78			0.14	0.40		0.69	7.10	6.18
BLGU204	black guillemot				0.47			0.06	0.15		0.18	2.36	0.42
NOFU112	northern fulmar				1.86				0.76		0.34	4.51	0.55
NOFU130	northern fulmar				1.90				0.64		0.38	3.60	1.13
NOFU136	northern fulmar				1.18				0.35		0.25	2.49	0.20
NOFU140	northern fulmar				3.06				1.30		0.58	6.42	3.53
NOFU141	northern fulmar				2.55				0.90		0.46	6.64	0.40
NOFU159	northern fulmar				2.34				0.87		0.67	4.50	6.43
NOFU160	northern fulmar				1.53				0.51		0.33	4.32	0.42
NOFU177	northern fulmar				1.22				0.43		0.24	2.50	0.19
NOFU316	northern fulmar				2.41				1.46		0.61	6.71	6.88
GLGU008	glaucous gull			0.31	3.69		2.11		2.39		1.74	17.9	1.99
GLGU009	glaucous gull			0.12	2.93		2.80		2.60		1.44	16.3	1.12
GLGU037	glaucous gull			0.25	3.56		2.34		3.07		2.52	21.9	2.07

File name	Common name	PCB concentration (ng/g wet weight)												
		95/66	56/60	101/90	99	97	87	110	151	149	118	153	105	141
npz 305	None	0.20	0.15	0.22	0.07	0.06	0.06	0.10	0.09	0.07	0.22	0.11		0.02
npz 345	None	0.47		0.25	0.08	0.09	0.09	0.13	0.08	0.15	0.33	0.14	0.02	0.03
npz 417	None	0.41		0.24	0.20	0.08	0.08	0.12	0.07	0.14	0.33	0.15	0.02	0.03
NWF005	Arctic cod	0.15	0.04	0.22	0.14			0.11	0.13	0.08	0.37	0.71	0.06	
NWF006	Arctic cod	0.24	0.03	0.26	0.11			0.14	0.13	0.08	0.38	0.39		
NWF008	Arctic cod	0.09	0.04	0.08	0.07			0.08	0.19		0.20	0.20		
BLGU180	Black guillemot	0.71	0.20	1.88	1.07	0.22		0.53		0.43	3.48	5.14	0.93	0.16
BLGU181	Black guillemot	0.89	0.23	1.69	0.92	0.09		0.66		0.47	3.27	4.46	0.94	0.15
BLGU183	Black guillemot	1.69	0.41	3.20	2.34	0.30		1.24		0.86	6.91	9.67	1.91	0.29
BLGU184	Black guillemot	1.70	0.52	4.12	4.74	0.24		1.25		0.95	11.48	26.8	2.52	0.38
BLGU185	Black guillemot	0.90	0.25	1.70	1.50	0.24		0.67		0.64	3.93	6.14	1.03	0.16
BLGU189	Black guillemot	1.17	0.35	3.15	1.55	0.39		0.83		0.56	5.17	7.26	1.57	0.27
BLGU190	black guillemot	1.34	0.42	3.05	1.87	0.21		1.53		0.87	5.93	10.1	1.64	0.26
BLGU202	black guillemot	1.90	0.58	5.03	2.33	0.29		1.23		1.23	8.49	11.9	2.40	0.47
BLGU204	black guillemot	0.50	0.11	1.04	0.64	0.08		0.39		2.42	3.15	2.91	0.56	0.09
NOFU112	northern fulmar	2.54	0.47	0.38	4.54	0.17		0.30		0.44	14.1	27.3	5.28	0.13
NOFU130	northern fulmar	2.09	0.39	0.38	4.66	0.19		0.35		0.39	12.6	25.2	4.18	0.00
NOFU136	northern fulmar	1.19	0.24	0.21	3.09	0.09		0.23		0.27	8.69	21.2	2.61	0.09
NOFU140	northern fulmar	3.32	0.73	0.37	6.85	0.24		0.37		0.46	20.2	41.4	7.16	0.14
NOFU141	northern fulmar	3.67	0.60	0.57	8.12	0.40		0.52		0.32	23.2	46.4	7.29	0.17
NOFU159	northern fulmar	2.72	0.62	0.58	5.58	0.22		0.35		0.61	18.7	43.0	5.85	0.16
NOFU160	northern fulmar	1.93	0.38	0.38	4.31	0.17		0.36		0.39	13.0	24.8	4.14	0.00
NOFU177	northern fulmar	1.30	0.29	0.31	2.90	0.11		0.31		0.23	8.72	23.0	2.44	0.13
NOFU316	northern fulmar	4.79	1.09	0.34	9.89	0.33		0.53		0.48	29.3	54.4	10.8	0.00
GLGU008	glaucous gull	4.39	2.19	7.07	15.9	0.59		4.66		2.66	27.8	63.3	7.66	0.78
GLGU009	glaucous gull	4.02	1.70	6.82	16.4	0.45		4.08		2.07	31.8	73.6	6.92	0.42
GLGU037	glaucous gull	4.74	2.26	8.57	24.5	0.47		3.92		3.50	39.0	94.4	10.8	0.57

File name	Common name	PCB concentration (ng/g wet weight)												
		130/176	137	138	158	178	187	183	128	174	156	200/157	172	180
npz 305	None			0.11		0.03				0.03				0.03
npz 345	None			0.14	0.02	0.02	0.04	0.06						0.04
npz 417	None			0.14	0.02	0.00	0.04	0.03						0.04
NWF005	Arctic cod		0.02	0.48	0.06	0.02	0.12	0.07	0.06	0.02				0.22
NWF006	Arctic cod			0.33	0.05	0.02	0.08	0.04	0.05	0.02				0.09
NWF008	Arctic cod			0.24	0.07		0.06	0.03	0.06					0.11
BLGU180	Black guillemot	0.36	0.26	3.61	0.34	0.42	1.47	0.76	0.68	0.17	0.60	0.10	0.23	1.91
BLGU181	Black guillemot	0.42	0.19	3.29	0.27	0.44	1.28	0.49	0.57	0.11	0.45	0.05	0.20	1.37
BLGU183	Black guillemot	0.94	0.40	7.26	0.64	1.02	3.06	1.23	1.19	0.30	1.04	0.12	0.25	3.21
BLGU184	Black guillemot	2.10	1.27	17.4	1.29	1.61	5.35	3.79	3.02	0.42	2.82	0.34	1.25	12.5
BLGU185	Black guillemot	0.57	0.29	4.50	0.33	0.52	1.52	0.72	0.71	0.13	0.56	0.08	0.16	2.20
BLGU189	Black guillemot	0.89	0.36	5.18	0.57	0.98	1.86	0.72	0.83	0.13	0.85	0.08	0.24	2.01
BLGU190	black guillemot	0.88	0.52	7.78	0.54	1.09	2.88	1.37	1.38	0.19	1.21	0.11	0.30	4.31
BLGU202	black guillemot	1.03	0.51	8.50	0.72	1.41	3.28	1.38	1.58	0.51	1.42	0.15	0.27	3.68
BLGU204	black guillemot	0.33	0.11	2.26	0.18	0.28	0.88	0.35	0.35	0.08	0.39	0.04	0.07	0.95
NOFU112	northern fulmar	1.39	1.06	17.1	0.96	0.20	0.55	4.00	4.73		3.92	0.52	2.14	15.3
NOFU130	northern fulmar	0.65	0.91	15.0	0.80	0.13	0.47	3.70	3.73		3.34	0.46	1.90	15.5
NOFU136	northern fulmar	0.47	0.66	11.2	0.65	0.08	0.66	3.20	2.61		2.34	0.35	1.44	12.1
NOFU140	northern fulmar	0.83	1.54	24.5	1.29	0.28	1.05	6.39	6.83		6.23	0.79	3.28	25.5
NOFU141	northern fulmar	1.57	1.50	27.4	1.24	0.25	0.50	6.58	6.91		6.42	0.86	3.56	26.4
NOFU159	northern fulmar	1.34	1.30	22.7	1.27	0.26	1.03	6.69	6.26		5.66	0.75	3.11	28.7
NOFU160	northern fulmar	0.37	0.79	15.5	0.68	0.15	0.66	3.44	4.09		3.52	0.47	1.96	12.8
NOFU177	northern fulmar	0.46	0.46	10.6	0.43	0.11	0.56	2.92	2.54		2.20	0.31	1.28	12.6
NOFU316	northern fulmar	1.62	2.57	34.8	2.39	0.37	0.58	8.97	9.76		8.71	1.15	4.79	34.7
GLGU008	glaucous gull	3.30	3.46	51.8	3.14	2.91	13.4	9.68	6.46		7.36	0.63	2.15	28.9
GLGU009	glaucous gull	3.60	3.87	56.6	3.56	3.15	18.8	12.2	9.20		9.93	0.86	3.12	38.8
GLGU037	glaucous gull	6.03	5.22	80.6	5.54	7.79	29.6	15.6	13.4		12.8	1.46	3.83	48.2

File name	Common name	PCB concentration (ng/g wet weight)						
		170/190	196/203	208	195	207	194	206
npz 305	*Calanus hyperboreus*							
npz 345	*Calanus hyperboreus*	0.02						
npz 417	*Calanus hyperboreus*							
NWF005	Arctic cod	0.15	0.06		0.06		0.08	0.04
NWF006	Arctic cod	0.10	0.03		0.05		0.05	0.03
NWF008	Arctic cod	0.14	0.04		0.08		0.06	0.04
BLGU180	Black guillemot	0.76	0.39	0.05	0.16	0.08	0.31	0.18
BLGU181	Black guillemot	0.60	0.26	0.02	0.08	0.02	0.20	0.06
BLGU183	Black guillemot	1.28	0.71	0.05	0.16	0.07	0.51	0.20
BLGU184	Black guillemot	4.76	2.57	0.18	0.67	0.28	2.25	0.82
BLGU185	Black guillemot	0.87	0.39	0.04	0.15	0.05	0.33	0.13
BLGU189	Black guillemot	0.87	0.45	0.03	0.18	0.05	0.32	0.13
BLGU190	black guillemot	1.81	1.02	0.08	0.19	0.07	0.77	0.24
BLGU202	black guillemot	1.63	0.81	0.06	0.31	0.10	0.64	0.29
BLGU204	black guillemot	0.42	0.17		0.05	0.02	0.13	0.06
NOFU112	northern fulmar	6.71	3.11		0.66	0.19	2.37	0.95
NOFU130	northern fulmar	6.25	3.50		0.67	0.22	2.80	1.36
NOFU136	northern fulmar	5.36	2.58		0.51	0.21	1.92	0.79
NOFU140	northern fulmar	11.2	5.23		1.14	0.31	4.00	1.45
NOFU141	northern fulmar	11.2	5.80		1.32	0.49	4.12	1.79
NOFU159	northern fulmar	12.9	5.95		1.20	0.35	4.68	1.51
NOFU160	northern fulmar	5.89	2.54		0.64	0.24	1.90	0.87
NOFU177	northern fulmar	5.17	3.01		0.77	0.29	2.31	1.09
NOFU316	northern fulmar	14.9	8.14		1.62	0.54	6.28	2.81
GLGU008	glaucous gull	11.6	6.18	0.30	1.10	0.45	5.04	1.25
GLGU009	glaucous gull	14.4	8.38	0.46	1.45	0.76	7.26	1.91
GLGU037	glaucous gull	19.6	12.6	1.25	2.50	0.95	9.92	3.16

File name	Common name	PCB concentration (ng/g wet weight)												
		31	28	52	49	47/48	44	42	64	74	70/76	95/66	56/60	92
GLGU088	glaucous gull	0.28	8.07	4.57		4.67			4.80	28.8	10.8	8.70	4.11	
GLGU101	glaucous gull	0.31	3.31	1.61		1.99			2.33	14.1	6.94	3.93	2.01	
GLGU192	glaucous gull	0.08	3.62	2.49		1.91			1.43	12.0	0.89	3.41	1.70	
GLGU193	glaucous gull	0.15	6.88	5.60		3.53			2.94	18.4	0.80	5.38	3.37	
GLGU254	glaucous gull	0.33	5.02	2.29		3.08			1.60	16.4	1.48	4.37	2.04	
GLGU265	glaucous gull	0.00	8.24	0.97		4.08			3.67	23.1	1.01	5.13	1.53	
IVGU080	ivory gull		2.85			2.89			2.11	12.7	1.12	3.05	0.76	
IVGU081	ivory gull		3.46			2.40			1.56	14.4	0.37	3.33	0.90	
IVGU182	ivory gull		2.56			2.31			1.02	13.9	0.84	3.43	1.00	
IVGU191	ivory gull		3.45			3.15			1.32	13.9	0.84	4.34	1.90	
IVGU210	ivory gull		1.03			0.42			0.37	6.23	0.86	1.03	0.35	
BLKI113	black-legged kittiwake		2.23			0.68			0.24	4.92	0.43	2.64	1.01	
BLKI144	black-legged kittiwake		1.78			0.51			0.45	4.90	0.71	2.34	0.95	
BLKI145	black-legged kittiwake		3.95			0.93			0.69	7.97	0.65	3.57	1.14	
BLKI148	black-legged kittiwake		2.76			0.87			0.70	3.01	10.4	3.37	1.34	
BLKI149	black-legged kittiwake		1.80			0.46			0.27	3.47	0.24	1.54	0.48	
TBMU120	thick-billed murre		1.09			0.15			0.08	3.94	0.05	0.79	0.37	
TBMU128	thick-billed murre	0.02	1.83			0.45			0.13	3.41	0.18	1.40	0.42	
TBMU129	thick-billed murre		0.71			0.19			0.05	1.29	0.09	0.64	0.25	
TBMU135	thick-billed murre	0.02	0.99			0.12			0.09	1.83	0.10	0.65	0.25	
TBMU142	thick-billed murre	0.02	2.09			0.64			0.14	4.43	0.15	1.90	0.58	

File name	Common name	PCB concentration (ng/g wet weight)											
		101/90	99	97	110	149	118	153	105	141	130/176	137	138
GLGU088	glaucous gull	15.4	35.8	0.88	6.40	3.92	57.4	156	13.8	0.94	5.96	6.55	94.7
GLGU101	glaucous gull	6.94	15.1	0.44	2.60	2.43	26.7	71.8	6.84	0.57	3.33	3.51	52.3
GLGU192	glaucous gull	6.07	11.4	0.54	3.43	1.87	16.8	41.7	4.57	0.68	1.75	2.38	30.0
GLGU193	glaucous gull	11.9	20.0	0.76	5.85	3.19	35.1	59.9	8.42	0.93	2.43	3.17	48.0
GLGU254	glaucous gull	7.73	25.4	0.31	3.84	2.07	38.8	102	7.46	0.88	4.41	5.48	81.9
GLGU265	glaucous gull	5.85	35.6	0.16	4.14	1.78	67.6	242	14.7		8.08	9.02	144
IVGU080	ivory gull	3.37	16.5	0.69	1.30	1.15	36.3	89.4	9.01		2.13	5.64	70.5
IVGU081	ivory gull	4.56	12.6	0.60	2.01	1.73	29.9	74.1	6.81		2.41	4.48	55.0
IVGU182	ivory gull	4.48	16.0	0.51	2.21	2.24	35.3	92.3	9.46		2.76	5.26	70.2
IVGU191	ivory gull	4.80	13.3	0.53	2.23	4.31	26.5	60.8	8.02	0.41	2.32	3.31	49.8
IVGU210	ivory gull	2.38	2.05	0.17	0.69	0.59	5.85	10.2	1.48		0.34	0.47	7.89
BLKI113	black-legged kittiwake	2.25	4.48	0.15	1.46	0.61	8.83	22.2	2.65	0.13	0.62	1.20	19.7
BLKI144	black-legged kittiwake	2.29	4.34	0.19	1.43	0.79	10.6	24.3	3.59	0.11	0.90	1.45	21.9
BLKI145	black-legged kittiwake	3.15	5.66	0.25	1.41	0.39	12.4	29.9	3.32	0.24	0.86	1.72	25.8
BLKI148	black-legged kittiwake	3.27	4.85	0.16	1.90	0.25	12.3	24.6	3.51	0.12	0.94	1.41	23.2
BLKI149	black-legged kittiwake	1.66	2.30	0.13	0.68	0.23	5.56	13.4	1.52	0.10	0.40	0.65	11.3
TBMU120	thick-billed murre	1.00	0.45	0.04	0.07	0.16	3.36	4.21	1.68		0.36	0.05	3.50
TBMU128	thick-billed murre	1.14	1.54	0.04	0.15	0.16	4.76	8.14	2.08		0.29	0.19	6.47
TBMU129	thick-billed murre	0.44	0.80	0.01	0.12	0.08	2.26	3.97	0.67		0.12	0.09	3.16
TBMU135	thick-billed murre	0.77	0.59	0.03	0.10	0.18	2.34	2.80	0.18		0.13	0.06	2.38
TBMU142	thick-billed murre	1.35	2.00	0.08	0.12	0.25	5.76	10.31	2.73		0.37	0.24	8.39

File name	Common name	PCB concentration (ng/g wet weight)											
		158	178	187	183	128	156	200/157	172	180	170/190	196/203	208
GLGU088	glaucous gull	5.94	5.23	20.8	16.8	12.0	14.2	2.04	4.31	58.2	25.9	9.11	0.83
GLGU101	glaucous gull	3.36	2.94	13.4	10.7	8.02	9.00	0.98	2.50	38.2	15.3	8.53	0.43
GLGU192	glaucous gull	2.18	1.49	7.46	6.48	4.27	4.68	0.41	1.64	18.8	7.22	3.69	0.16
GLGU193	glaucous gull	3.18	2.65	11.4	6.75	6.11	6.90	0.68	1.43	18.4	8.06	3.44	0.23
GLGU254	glaucous gull	5.13	3.19	20.2	17.0	10.3	11.4	1.06	3.70	51.4	19.9	11.2	0.57
GLGU265	glaucous gull	8.20	3.25	33.5	43.5	24.5	40.7	4.02	7.59	178	74.0	39.6	0.95
IVGU080	ivory gull	6.20	1.71	12.3	18.8	5.54	14.9	0.67	3.28	52.4	26.7	16.4	0.73
IVGU081	ivory gull	4.60	2.77	11.4	12.2	4.02	10.6	0.50	2.38	40.0	17.6	10.0	0.43
IVGU182	ivory gull	5.73	2.50	13.9	15.2	5.26	13.0	0.60	2.69	46.2	21.4	10.6	0.36
IVGU191	ivory gull	3.39	2.97	11.6	9.40	3.22	6.97	0.33	1.60	28.0	13.3	6.65	0.33
IVGU210	ivory gull	0.54	0.49	2.01	1.25	0.56	1.15	0.08	0.53	3.87	1.72	0.78	0.05
BLKI113	black-legged kittiwake	0.90	0.64	4.81	3.67	2.72	3.22	0.11	1.15	11.9	4.75	2.62	0.16
BLKI144	black-legged kittiwake	1.10	0.89	7.19	5.05	3.60	4.00	0.34	1.41	13.3	5.70	3.38	0.38
BLKI145	black-legged kittiwake	1.70	1.09	6.41	5.19	3.36	4.42	0.34	1.44	17.0	7.01	3.79	0.21
BLKI148	black-legged kittiwake	1.65	0.96	7.54	4.79	3.68	3.96	0.33	1.29	13.2	5.67	3.53	0.38
BLKI149	black-legged kittiwake	0.48	0.31	2.95	2.21	1.47	1.72	0.14	0.57	7.34	2.99	1.77	0.13
TBMU120	thick-billed murre	0.23	0.22	2.84	0.76	0.87	0.76	0.28	0.28	1.35	1.33	0.71	0.09
TBMU128	thick-billed murre	0.23	0.17	2.59	0.75	0.94	0.95	0.29	0.29	2.30	1.28	0.69	0.07
TBMU129	thick-billed murre	0.16	0.09	1.19	0.22	0.45	0.45	0.16	0.13	1.06	0.57	0.33	0.05
TBMU135	thick-billed murre	0.08	0.19	2.38	0.40	0.20	0.38	0.11	0.20	0.47	0.42	0.36	0.06
TBMU142	thick-billed murre	0.31	0.26	3.59	0.97	1.24	1.03	0.41	0.35	3.31	1.54	1.18	0.15

File name	Common name	PCB concentration (ng/g wet weight)			
		195	207	194	206
GLGU088	glaucous gull	2.00	0.61	11.65	3.45
GLGU101	glaucous gull	1.52	0.59	7.26	2.01
GLGU192	glaucous gull	0.68	0.28	3.08	0.65
GLGU193	glaucous gull	0.74	0.30	2.72	0.78
GLGU254	glaucous gull	2.16	1.00	8.88	2.48
GLGU265	glaucous gull	9.81	2.61	36.0	10.7
IVGU080	ivory gull	3.99	1.35	13.2	5.48
IVGU081	ivory gull	2.10	0.61	8.03	2.98
IVGU182	ivory gull	1.98	0.67	7.79	2.29
IVGU191	ivory gull	1.25	0.39	4.97	1.81
IVGU210	ivory gull	0.20	0.14	0.56	0.23
BLKI113	black-legged kittiwake	0.46	0.24	1.84	0.68
BLKI144	black-legged kittiwake	0.44	0.23	2.14	0.75
BLKI145	black-legged kittiwake	0.77	0.35	2.76	1.40
BLKI148	black-legged kittiwake	0.75	0.35	2.39	1.23
BLKI149	black-legged kittiwake	0.33	0.14	1.22	0.64
TBMU120	thick-billed murre	0.25	0.11	0.82	0.33
TBMU128	thick-billed murre	0.23	0.09	0.71	0.26
TBMU129	thick-billed murre	0.17	0.08	0.34	0.32
TBMU135	thick-billed murre	0.17	0.05	0.45	0.20
TBMU142	thick-billed murre	0.31	0.14	1.20	0.51

File name	Common name	PCB concentration (ng/g wet weight)											
		31	28	52	49	47/48	44	42	64	74	70/76	95/66	56/60
NORS002	ringed seal	5.20	10.6	125	12.4	32.4	4.31	2.15	2.20	53.4	1.91	26.6	6.69
NORS007	ringed seal	3.76	8.42	19.0	3.80	6.74	2.53	0.82	1.75	16.4	4.04	33.2	5.16
NORS010	ringed seal	2.71	4.60	33.8	6.20	12.6	2.69		1.58	23.1	2.17	17.1	3.95
NORS014	ringed seal		0.85	4.21	0.79	1.33	0.26		0.00	2.06	0.25	1.43	0.40
NORS019	ringed seal		17.6	89.8	16.0	42.0	4.12	0.98	1.79	92.4	2.03	23.2	5.33
NORS020	ringed seal	1.05	4.17	16.9	2.60	5.71	1.22	2.31	0.78	16.5	1.19	29.3	3.66
NORS026	ringed seal	2.66	10.9	21.2	3.74	6.92	1.76	0.46	1.05	25.1	4.66	25.4	3.79
NORS029	ringed seal	1.34	4.50	14.6	1.63	2.03	0.82	0.00	0.42	4.78	1.00	4.74	0.85
NORS033	ringed seal	7.94	15.5	27.8	5.61	6.96	26.9	0.69	1.81	15.1	4.77	19.0	3.27
NORS035	ringed seal	4.73	17.4	62.3	11.0	22.6	3.27	0.99	2.39	52.6	2.49	23.8	5.58
NORS045	ringed seal	3.69	9.80	26.5	4.37	10.3	1.34	0.23	1.54	25.5	1.53	17.0	4.23
NORS048	ringed seal	4.67	16.7	98.8	20.6	40.0	3.43	1.27	2.48	43.0	1.60	22.7	5.76
NORS055	ringed seal		3.74	4.76	0.92	1.64	0.74	0.00	0.36	5.60	0.96	4.49	1.22

File name	Common name	PCB concentration (ng/g wet weight)											
		92	**101/90**	**99**	**97**	**87**	**85**	**110**	**151**	**149**	**118**	**146**	**153**
NORS002	ringed seal	34.0	229	408	3.20	24.9	77.3	13.6	21.6	41.8	106	160	1030
NORS007	ringed seal	11.2	43.6	52.6	1.16	12.3	10.0	8.72	5.75	13.1	54.2	27.1	160
NORS010	ringed seal	18.2	128	222	1.96	16.4	22.4	12.9	5.40	26.5	97.1	99.7	709
NORS014	ringed seal	1.71	7.32	10.9	0.00	1.28	2.93	0.91	1.28	1.46	4.07	3.28	19.9
NORS019	ringed seal	23.1	169.	482	2.74	15.8	49.7	11.4	8.45	28.0	87.7	119	890
NORS020	ringed seal	12.0	65.1	83.5	0.61	12.8	9.71	10.1	2.63	12.8	77.7	39.2	260
NORS026	ringed seal	9.90	45.5	63.9	0.86	10.8	8.98	9.46	3.44	11.1	52.0	25.5	179
NORS029	ringed seal	2.53	12.54	12.52	0.00	2.58	2.72	2.96	1.60	3.43	8.08	2.59	24.40
NORS033	ringed seal	11.0	45.3	46.4	1.21	11.5	10.8	10.5	6.54	14.8	37.4	17.9	107
NORS035	ringed seal	22.5	160	247	1.37	21.2	26.8	15.4	8.64	31.6	141	117	820
NORS045	ringed seal	12.8	72.6	106	0.48	13.04	11.8	8.82	3.56	14.4	66.7	55.0	374
NORS048	ringed seal	20.6	153	231	1.90	23.0	50.5	15.1	16.3	23.1	101	69.0	466
NORS055	ringed seal	2.01	9.64	11.6	0.37	2.14	1.58	1.99	0.55	2.32	9.33	3.28	19.3

File name	Common name	PCB concentration (ng/g wet weight)											
		105	**179**	**141**	**130/176**	**137**	**138**	**158**	**178**	**187**	**183**	**128**	**174**
NORS002	ringed seal	57.0		5.48	5.47	28.0	770	32.8	47.9	161	78.0	31.8	4.79
NORS007	ringed seal	19.0		5.87	0.86	4.69	113	5.35	14.1	35.3	15.1	4.51	1.80
NORS010	ringed seal	52.5		6.53	4.42	15.3	477	17.9	31.4	67.5	49.20	10.7	3.88
NORS014	ringed seal	1.73		0.56	0.73	0.54	13.6	0.89	0.92	2.03	0.81	1.01	0.19
NORS019	ringed seal	46.7		2.79	34.9	16.6	616	22.6	23.2	58.8	51.5	22.0	3.49
NORS020	ringed seal	24.0		5.57	8.18	3.83	138	5.25	12.1	30.1	19.1	3.66	1.17
NORS026	ringed seal	19.6		2.94	6.22	3.46	116	3.73	9.15	19.9	9.98	2.94	1.00
NORS029	ringed seal	3.03					17.2		0.83	2.22	0.89	0.65	
NORS033	ringed seal	13.7		3.42	4.36	2.44	86.8	3.96	8.07	23.4	9.11	4.89	1.30
NORS035	ringed seal	51.6		4.92	27.4	11.1	413	17.4	23.2	55.5	39.0	8.62	2.14
NORS045	ringed seal	44.0		5.00	17.0	5.84	247	9.12	20.2	37.0	25.1	5.53	1.92
NORS048	ringed seal	49.0		4.11	17.6	11.4	370	18.7	14.3	56.2	28.3	26.4	2.01
NORS055	ringed seal	4.02	0.63	0.44	0.74	0.53	14.0	0.56	0.98	1.84	0.95	0.59	0.29

File name	Common name	PCB concentration (ng/g wet weight)											
		177	202	171	156	200/157	172	180	170/190	201	196/203	208	195
NORS002	ringed seal	22.0	32.5	13.1	33.6	2.73	17.7	222	82.3	27.7	32.2	9.95	4.27
NORS007	ringed seal	3.31	8.19	2.69	8.93	0.69	4.44	46.6	17.61	9.74	8.85	4.34	1.51
NORS010	ringed seal	5.53	17.2	9.29	32.5	3.44	16.0	220	85.0	20.2	25.7	8.52	4.45
NORS014	ringed seal	0.35	0.36	0.25	0.27	4.24	0.00	2.44	1.16	0.33	0.37		
NORS019	ringed seal	6.46	25.7	10.4	34.5	9.86	14.0	208	85.1	12.8	19.4		2.95
NORS020	ringed seal	3.07	10.6	3.02	13.2	3.63	6.05	78.0	29.6	9.99	11.8		1.49
NORS026	ringed seal	1.13	4.56	1.37	6.84	2.36	2.47	37.9	14.6	3.53	3.25		
NORS029	ringed seal				0.75			3.73	1.69				
NORS033	ringed seal	1.26	4.23	1.15	4.29	1.42	2.03	26.1	9.53	3.55	3.58		
NORS035	ringed seal	2.39	17.7	6.23	25.5	7.59	8.91	122	49.3	11.3	13.8	6.08	2.34
NORS045	ringed seal	1.12	12.3	3.59	16.4	4.67	6.26	84.3	31.5	9.11	9.91	3.98	1.21
NORS048	ringed seal	6.49	9.43	4.38	18.3	5.32	4.45	67.8	29.3	5.88	7.04	2.20	1.22
NORS055	ringed seal	0.27	0.32	0.32	0.87	0.18	0.35	2.68	0.90	0.25	0.26		

File name	Common name	PCB concentration (ng/g wet weight)		
		207	194	206
NORS002	ringed seal	51.4	46.7	48.4
NORS007	ringed seal		19.4	24.5
NORS010	ringed seal		50.1	52.4
NORS014	ringed seal		0.84	
NORS019	ringed seal		33.1	33.7
NORS020	ringed seal		18.2	24.6
NORS026	ringed seal		10.0	
NORS029	ringed seal			
NORS033	ringed seal		6.23	9.78
NORS035	ringed seal		20.5	26.1
NORS045	ringed seal		15.2	18.0
NORS048	ringed seal		8.87	8.38
NORS055	ringed seal		0.49	

Appendix 3

Enantiomer fractions for PCBs detected within subset of biota from the Northwater Polynya

Appendix 3. Congeners with enantiomer fractions presented were below the limit of detection (0.02 ng/g)

Biota	File name	Enantiomer Fractions					
		PCB 91	PCB 95	PCB 149	PCB 174	PCB 176	PCB 183
Calanus hyperboreus	nzp 305	0.516	0.491	0.486			
Calanus hyperboreus	nzp 345	0.513	0.489	0.496			
Calanus hyperboreus	nzp 417	0.493	0.489	0.496			
Arctic cod	NFW005	0.525	0.462	0.514			
Arctic cod	NFW006	0.524	0.463	0.471			
Arctic cod	NFW008		0.463	0.542			
Dovekie			0.508				
Dovekie			0.498				
Dovekie				0.111			
Black guillemot	BLGU180			0.169			
Black guillemot	BLGU183	0.191	0.613	0.176			
Black guillemot	BLGU184		0.560	0.226			
Black guillemot	BLGU189			0.190			
Black guillemot	BLGU190			0.241			
Northern fulmar	NUFU112			0.463			0.294
Northern fulmar	NUFU130	0.624	0.744	0.348			
Northern fulmar	NUFU136			0.450			
Northern fulmar	NUFU140	0.613	0.809	0.412			
Northern fulmar	NUFU141	0.631	0.734	0.418			
Glaucous gull	GLGU008	0.138	0.386	0.258			
Glaucous gull	GLGU009	0.143	0.482	0.299			
Glaucous gull	GLGU037	0.106	0.833	0.304	0.828		0.443
Glaucous gull	GLGU192	0.125	0.695	0.327			
Glaucous gull	GLGU193	0.172	0.648	0.195			
Ivory gull	IVGU080	0.497	0.829	0.169			
Ivory gull	IVGU081			0.186			
Ivory gull	IVGU182		0.850	0.321			
Ivory gull	IVGU191			0.379			
Ivory gull	IVGU210			0.255			
Black-legged kittiwake	BLKI113	0.306	0.435	0.402			
Black-legged kittiwake	BLKI144	0.650	0.826	0.391			
Black-legged kittiwake	BLKI145	0.643	0.799	0.415			

Biota	File name	Enantiomer Fractions					
		PCB 91	PCB 95	PCB 149	PCB 174	PCB 176	PCB 183
Black-legged kittiwake	BLKI148	0.568	0.718	0.403			
Black-legged kittiwake	BLKI149			0.404			
Thick-billed murre	TBMU120		0.781	0.115			
Thick-billed murre	TBMU128		0.721	0.102			
Thick-billed murre	TBMU129		0.614	0.167			
Thick-billed murre	TBMU135	0.676	0.792	0.103			
Thick-billed murre	TBMU142		0.800	0.270			
Ringed seal	NORS026	0.040	0.881	0.473	0.597		0.420
Ringed seal	NORS029		0.886	0.446			0.540
Ringed seal	NORS033	0.122	0.840	0.501	0.572		0.474
Ringed seal	NORS035	0.051	0.900	0.445	0.588		0.424
Ringed seal	NORS045	0.065	0.872	0.491	0.573		0.407
Ringed seal	NORS048	0.073	0.803	0.464	0.692	0.490	0.512
Ringed seal	NORS055	0.085	0.848	0.413	0.514		
Ringed seal	NORS014	0.120	0.637	0.579	0.584	0.416	0.490
Ringed seal	NORS020	0.056	0.903	0.429	0.555		0.437
Ringed seal	NORS007		0.863	0.515	0.539		0.472
Ringed seal	NORS010	0.031	0.893	0.480	0.551	0.398	0.421
Ringed seal	NORS019	0.067	0.860	0.455	0.667		0.443
Ringed seal	NORS002	0.048		0.526	0.647		0.488

Appendix 4

Operating procedures for *Mysis relicta* Husbandry

Appendix 4: Operating procedures for *Mysis relicta* husbandry

- Collected organisms were stored in a large 60 L aquarium containing non-chlorinated water to and sediment for approximately 2 days for acclimation purposes before introduced into experimental aquaria containing control and spiked sediment
- Non-chlorinated water was used in all experimental aquaria
- All sediment used within control and spiked exposure aquaria was sieved to a size of 500 μm
- Water within experimental aquaria was aerated through activated carbon filters help maintain water quality
- Weekly monitoring of pH, nitrate, nitrite and ammonia levels to assess water quality
- To maintain water quality throughout the timeline of the experiment, 10% of water volume was changed within experimental aquaria weekly
- Organisms were fed krill flakes to introduce another source of nutrients into the organisms diet and to help prevent cannibalism
- Krill flakes were only given after 3 days from previous feeding to maximize feeding on the sediment

Appendix 5

Incubation and extraction protocols for PCBs and OH-PCBs for rat and human CYP incubations

Appendix 5: Incubation and extraction protocols for PCBs and OH-PCBs for rat and human CYP incubations

- Solutions for the NADPH regeneration system (Solution A and B) along with the CYP enzymes was thawed in a water bath at 37°C.
- Once thawed, 50 µl of solution A and 10 ul of solution B was mixed within a test tube with 740 µl of K_2PO_4 buffer (pH 7.4) and incubated for 5 minutes at 37°C
- 25 µl of thawed enzymes was combined with 75 µl of K_2PO_4 buffer and incubated in 500 µl centrifuge tube for 5 min at 37°C
- 5 µl of 5 µg/ml individual PCB congener solutions was added to the test tube containing our NADPH regeneration solution
- Enzyme mixture was added to the test tube using 100 µl to quantitatively rinse out the centrifuge tube
- Test tube was vortexed briefly and incubated at 37°C for the desired amount of time
- Incubations were terminated using 1 ml of ice cold methanol and stored under ice until ready to be extracted
- PCB and mass labeled OH-PCBs were added to the test tube, vortexed for 2 minutes, followed by a addition of 1 ml 6 M HCl, and 2 ml of 2-propanol, then vortexed again briefly
- Contents of test tube were transferred to a 50 ml centrifuge tube using 6 ml of 1:1 methyl-*t*-butyl ether (MTBE)/hexane for quantitative transfer
- The centrifuge tube was vortexed for 1 minute and then centrifuged for 30 minutes

- The top organic layer was removed from the centrifuge tube and transferred to a 125 ml separatory funnel
- The extraction of the aqueous layer with MTBE/hexane was repeated twice more with the organic layer transferred to the separatory funnel
- 6 ml of 1% KCl was added to the separatory funnel and shaken for 1 minute
- The aqueous layer was discarded and the organic layer was drained into a 250 ml round bottom flask and roto-evaporated to approximately 1 ml
- The organic layer was quantitatively transferred to at 125 ml separatory funnel 3 x 1 ml washes with hexane
- 6 ml of 1M KOH in 50% ethanol was added to the separatory funnel and shaken for 1 minute
- The aqueous layer (metabolite fraction) was drained into 50 ml centrifuge tube
- Extraction of the organic layer with 1 M KOH in 50% ethanol was repeated twice more with the aqueous phase being combined in a 50 ml centrifuge tube
- The collected aqueous phase was re-washed with hexane to remove any co-extracted PCBs with hexane washes being added to the original organic layer
- The aqueous fraction was acidified to a pH of approximately 2 using a drop wise addition of H_2SO_4
- 6 ml of 1:1 MTBE/hexane was added to the centrifuge tube containing the aqueous fraction, vortexed for 1 minute to re-extract the metabolites from the aqueous phase, and centrifuged for 30 minutes to remove any precipitate that formed
- The organic layer was collected and transferred to a 250 ml round bottom flask

- The re-extraction of the aqueous fraction followed by centrifugation was repeated twice more with the organic layer containing the metabolites being combined in a 250 ml round bottom flask
- The organic fraction containing the metabolites was dried over ashed Na_2SO_4, roto-evaporated down to approximately 1 ml, and quantitatively transferred to a test tube using hexane to be derivatized using diazomethane
- Diazomethane was generated by adding nitrsomethylurea in excess to a 25 ml conical flask containing 10 ml of hexane and 10 ml of 50% NaOH solution
- The diazomethane is formed in the hexane layer and reaches a sufficient concentration when the hexane layer has obtained a strong yellow color
- Diazomethane was added to the test tubes containing the metabolite fraction and allowed to sit in the fridge overnight for the reaction to go to completion
- If the solution color goes clear overnight, then more diazomethane should be generated and added to the test tube and allowed to react for another 4 hours
- Test tubes containing the metabolite fraction mixed with diazomethane were nitrogen evaporated down to approximately 1 ml and purified on an acidified silica gel column (22%, 5 grams) using 50 ml of 1:1 DCM/hexane as our mobile phase
- The purified metabolite fraction underwent roto-evaporation followed by nitrogen evaporation, and was quantitatively transferred to an GC vial insert followed by the addition of our volume correction standard
- The original organic layer containing the parent PCB congeners was dried over ashed Na_2SO_4 and roto-evaporated to approximately 1 ml

- The parent congener fraction was then purified on an acidified silica gel column (22%, 3 grams) using 20 ml of 15% DCM in hexane as our mobile phase
- The purified parent congener fraction underwent roto-evaporation followed by nitrogen evaporation and quantitatively transferred to a GC vial insert followed by the addition of our volume correction standard

References

1. Eduljee, G. H., Budget and Source Inventories. In *Persistent Organic Pollutants: Environmental Behaviour and Pathways for Human Exposure*, Harrad, S. J., Ed. Kluwer Academic Publishers: Norwell, Massachusetts, 2001, p 1-29.
2. Baird, C., *Environmental Chemistry*. 2nd ed.; W. H. Freeman and Company: New York, NY, 1998; p 557.
3. Schwarzenbach, R. P.; Gschwend, P. M.; Imboden, D. M. *Environmental Organic Chemistry*. 2 ed.; John Wiley & Sons: Hoboken, NJ, 2003, p 1313.
4. Rappe, C.; Marklund, S.; Kjeller, L. O.; Lindskog, A. Long-range transport of PCDDs and PCDFs on airborne particles. *Chemosphere* **1989**, *18*, 1283-1290.
5. Wania, F.; Mackay, D. Global fractionation and cold condensation of low volatility organochlorine compounds in polar regions. *Ambio* **1993,** *22*, 10-18.
6. Wassermann, M.; Wassermann, D.; Cucos, S.; Miller, H. J. World PCBs map: Storage and effects in man and his biologic environment. *Annals of the New York Academy of Sciences* **1979,** 69-124.
7. Jensen, S.; Johnels, A. G.; Olsson, M.; Otterlin, G. DDT and PCB in marine animals from Swedish waters. *Nature* **1969**, *224*, 247-250.
8. Kaiser, K. L. E. On the optical activity of polychlorinated biphenyls. *Environmental Pollution* **1974**, *7*, 93-101.
9. Vetter, W.; Schurig, V. Enantioselective determination of chiral organochlorine compounds in biota by gas chromatography on modified cyclodextrins. *Journal of Chromatography A* **1997**, *774*, 143-175.
10. Puttmann, M.; Mannschreck, A.; Oesch, F.; Robertson, L. W. Chiral effects in the induction of drug-metabolizing enzymes using synthetic atropisomers of polychlorinated biphenyls (PCBs). *Biochemical Pharmacology* **1989**, *38*, 1345-1352.
11. Rodman, L. E.; Shedlofsky, S. I.; Mannschrek, A.; Puttmann, M.; Swim, A. T.; Robertson, L. W. Differential potency of atropisomers of polychlorinated biphenyls on cytochrome P450 induction and uroporphyrin accumulation in the chick embryo hepatocyte culture. *Biochemical Pharmacology* **1991**, *41*, 915-922.

12. Hoekstra, P. F.; Burnison, B. K.; Neheli, T.; Muir, D. C. G. Enantiomer-specific activity of *o,p'*-DDT with the human estrogen receptor. *Toxicology Letters* **2001**, *125*, 75-81.

13. Ulrich, E. M.; Willett, K. L.; Caperell-Grant, A.; Bigsby, R. M.; Hites, R. A. Understanding enantioselective processes: A laboratory rat model for alpha-hexachlorocyclohexane accumulation. *Environmental Science & Technology* **2001**, *35*, 1604-1609.

14. Hühnerfuss, H.; Kallenborn, R. Chromatographic separation of marine organic pollutants. *Journal of Chromatography-Biomedical Applications* **1992**, *580*, 191-214.

15. Mossner, S.; Spraker, T. R.; Becker, P. R.; Ballschmiter, K. Ratios of enantiomers of alpha-HCH and determination of alpha-HCH, beta-HCH, and gamma-HCH isomers in brain and other tissues of neonatal Northern Fur seals (*Callorhinus ursinus*). *Chemosphere* **1992**, *24*, 1171-1180.

16. Buser, H.; Müller, M. D. Enantioselective determination of chlordane components, metabolites and photoconversion products in envrionmental samples using chiral high resolution gas chromatogrpahy and mass spectrometry. *Environmental Science & Technology* **1993**, *27*, 1211-1220.

17. Glausch, A.; Hahn, J.; Schurig, V. Enantioselective determination of chiral 2,2',3,3',4,6'-hexachlorobiphenyl (PCB 132) in human milk samples by multidimensional gas chromatography electron capture detection and by mass spectrometry. *Chemosphere* **1995**, *30*, 2079-2085.

18. Blanch, G. P.; Glausch, A.; Schurig, V.; Serrano, R.; Gonzalez, M. J. Quantification and determination of enantiomeric ratios of chiral PCB 95, PCB 132, and PCB 149 in shark liver samples (*Coelolepis*) from the Atlantic Ocean. *HRC-Journal of High Resolution Chromatography* **1996**, *19*, 392-396.

19. Mills III, S. A.; Thal, D. I.; Barney, J. A summary of the 209 PCB congener nomenclature. *Chemosphere* **2007**, *68*, 1603-1612.

20. Ballschmiter, K.; Zell, M. Analysis of polychlorinated biphenyls (PCB) by glass-capillary gas chromatography - Composition of technical Aroclor-PCB and Clophen-PCB mixtures. *Fresenius Zeitschrift Fur Analytische Chemie* **1980**, *302*, 20-31.

21. Durfee, R. L.; Contos, G.; Whitmore, J. D.; Barden, E. E.; Hackman, I.; Westin, R. A. *PCBs in the United States - Industrial Use and Environmental Distributions*; Office of Toxic Substances, U. S. Environmental Protection Agency: 1976, p 488.

22. Mackay, D. Finding fugacity feasible. *Environmental Science & Technology* **1979**, *13*, 1218-1223.

23. Mackay, D.; Paterson, S. Evaluating the multimedia fate of organic chemicals - A level-III fugacity model. *Environmental Science & Technology* **1991**, *25*, 427-436.

24. Falconer, R. L.; Bidleman, T. F. Vapor pressures and predicted particle gas distributions of polychlorinated biphenyl congeners as functions of temperature and *ortho*-chlorine substitution. *Atmospheric Environment* **1994**, *28*, 547-554.

25. Jensen, S.; Renberg, L.; Olsson, M. PCB contamination from boat bottom paint and levels of PCB in plankton outside a polluted area. *Nature* **1972**, *240*, 358-360.

26. Shiu, W. Y.; Mackay, D. A critical review of aqueous solubilities, vapor pressures, Henry's Law constants, and octanol-water partition coefficients of the polychlorinated biphenyls. *Journal of Physical and Chemical Reference Data* **1986**, 911-929.

27. Mackay, D. Correlation of bioconcentration factors. *Environmental Science & Technology* **1982**, *16*, 274-278.

28. Clark, K. E.; Gobas, F.; Mackay, D. Model of organic chemical uptake and clearance by fish from food and water. *Environmental Science & Technology* **1990**, *24*, 1203-1213.

29. Safe, S. H. Polychlorinated biphenyls (PCBs) - Environmental impact, biochemical and toxic responses, and implications for risk assessment. *Critical Reviews in Toxicology* **1994**, *24*, 87-149.

30. Schurig, V.; Reich, S. Determination of the rotational barriers of atropisomeric polychlorinated biphenyls (PCBs) by a novel stopped-flow multidimensional gas chromatographic technique. *Chirality* **1998**, *10*, 316-320.

31. Harju, M. T.; Haglund, P., Determination of the rotational energy barriers of atropisomeric polychlorinated biphenyls. *Fresenius Journal of Analytical Chemistry* **1999**, *364*, 219-223.

32. Frame, G. M.; Wagner, R. E.; Carnahan, J. C.; Brown, J. F.; May, R. J.; Smullen, L. A.; Bedard, D. L. Comprehensive, quantitative, congener-specific analyses of eight

Aroclors and complete PCB congener assignments on DB-1 capillary GC columns. *Chemosphere* **1996**, *33*, 603-623.

33. Hansen, L. G. *The Ortho Side of PCBs: Occurrence and Disposition*. Kluwer Academic Publishers: Boston, 1999.
34. Garcia-Ruiz, C.; Martin-Biosca, Y.; Crego, A. L.; Marina, M. L. Rapid enantiomeric separation of polychlorinated biphenyls by electrokinetic chromatography using mixtures of neutral and charged cyclodextrin derivatives. *Journal of Chromatography A* **2001**, *910*, 157-164.
35. Hühnerfuss, H.; Pfaffenberger, B.; Gehrcke, B.; Karbe, L.; Konig, W. A.; Landgraff, O., Stereochemical effects of PCBs in the marine environment: Seasonal variation of coplanar and atropisomeric PCBs in blue mussels (*Mytilus edulis L.*) of the German Bight. *Marine Pollution Bulletin* **1995**, *30*, 332-340.
36. Benicka, E.; Novakovsky, R.; Hrouzek, J.; Krupcik, J.; Sandra, P.; deZeeuw, J., Multidimensional gas chromatographic separation of selected PCB atropisomers in technical formulations and sediments. *HRC-Journal of High Resolution Chromatography* **1996**, *19*, 95-98.
37. Glausch, A.; Blanch, G. P.; Schurig, V. Enantioselective analysis of chiral polychlorinated biphenyls in sediment samples by multidimensional gas chromatography electron-capture detection after steam distillation-solvent extraction and sulfur removal. *Journal of Chromatography A* **1996**, *723*, 399-404.
38. Klobes, U.; Vetter, W.; Luckas, B.; Skirnisson, K.; Plotz, J. Levels and enantiomeric ratios of alpha-HCH, oxychlordane, and PCB 149 in blubber of Harbour seals (*Phoca vitulina)* and grey seals (*Halichoerus grypus*) from Iceland and further species. *Chemosphere* **1998**, *37*, 2501-2512.
39. Reich, S.; Jimenez, B.; Marsili, L.; Hernandez, L. M.; Schurig, V.; Gonzalez, M. J. Congener specific determination and enantiomeric ratios of chiral polychlorinated biphenyls in striped dolphins (*Stenella coeruleoalba*) from the Mediterranean Sea. *Environmental Science & Technology* **1999**, *33*, 1787-1793.
40. Jimenez, O.; Jimenez, B.; Gonzalez, M. J. Isomer-specific polychlorinated biphenyl determination in cetaceans from the Mediterranean Sea: Enantioselective occurrence

of chiral polychlorinated biphenyl congeners. *Environmental Toxicology and Chemistry* **2000**, *19*, 2653-2660.

41. Serrano, R.; Fernandez, M.; Rabanal, R.; Hernandez, M.; Gonzalez, M. J. Congener specific determination of polychlorinated biphenyls in shark and grouper livers from the northwest African Atlantic Ocean. *Archives of Environmental Contamination and Toxicology* **2000**, *38*, 217-224.
42. Wong, C. S.; Garrison, A. W. Enantiomer separation of polychlorinated biphenyl atropisomers and polychlorinated biphenyl retention behavior on modified cyclodextrin capillary gas chromatography columns. *Journal of Chromatography A* **2000**, *866*, 213-220.
43. Wong, C. S.; Garrison, A. W.; Smith, P. D.; Foreman, W. T. Enantiomeric composition of chiral polychlorinated biphenyl atropisomers in aquatic and riparian biota. *Environmental Science & Technology* **2001**, *35*, 2448-2454.
44. Wong, C. S.; Garrison, A. W.; Foreman, W. T. Enantiomeric composition of chiral polychlorinated biphenyl atropisomers in aquatic bed sediment. *Environmental Science & Technology* **2001**, *35*, 33-39.
45. Hoekstra, P. F.; Wong, C. S.; O'Hara, T. M.; Solomon, K. R.; Mabury, S. A.; Muir, D. C. G. Enantiomer specific accumulation of PCB atropisomers in the bowhead whale (*Balaena mysticetus*). *Environmental Science & Technology* **2002**, *36*, 1419-1425.
46. Chu, S.; Covaci, A.; Van De Vijver, K.; De Coen, W.; Blust, R.; Schepens, P. Enantiomeric signatures of chiral polychlorinated biphenyl atropisomers in livers of harbour porpoises (*Phocoena phocoena*) from the sourthern North Sea. *Journal of Environmental Monitoring* **2003**, 521-526.
47. Chu, S. G.; Covaci, A.; Schepens, P. Levels and chiral signatures of persistent organochlorine pollutants in human tissues from Belgium. *Environmental Research* **2003**, *93*,167-176.
48. Hoekstra, P. F.; Braune, B. M.; Wong, C. S.; Williamson, M.; Elkin, B.; Muir, D. C. G. Profile of persistent chlorinated contaminants including selected chiral compounds in wolverine livers from the Canadian Arctic. *Chemosphere* **2003**, *53*, 551-560.

49. Robson, M.; Harrad, S. Chiral PCB signatures in air and soil: Implications for atmospheric source apportionment. *Environmental Science & Technology* **2004**, *38*, 1662-1666.

50. Wong, C. S.; Mabury, S. A.; Whittle, D. M.; Backus, S. M.; Teixeira, C.; DeVault, D. S.; Bronte, C. R.; Muir, D. C. G. Organochlorine compounds in Lake Superior: Chiral polychlorinated biphenyls and biotransformation in the aquatic food web. *Environmental Science & Technology* **2004**, *38*, 84-92.

51. Warner, N. A.; Norstrom, R. J.; Wong, C. S.; Fisk, A. T. Enantiomer fractions of chiral polychlorinated biphenyls provide insights on biotransformation capacity of arctic biota. *Environmental Toxicology and Chemistry* **2005**, *24*, 2763-2767.

52. Bucheli, T. D.; Brandli, R. C. Two-dimensional gas chromatography coupled to triple quadrupole mass spectrometry for the unambiguous determination of atropisomeric polychlorinated biphenyls in environmental samples. *Journal of Chromatography A* **2006**, *1110*, 156-164.

53. Gomara, B.; Gonzalez, M. J., Enantiomeric fractions and congener specific determination of polychlorinated biphenyls in eggs of predatory birds from Donana National Park (Spain). *Chemosphere* **2006**, *63*, 662-669.

54. Harrad, S.; Ren, J. Z.; Hazrati, S. Chiral signatures of PCB#s 95 and 149 in indoor air, grass, duplicate diets and human faeces. *Chemosphere* **2006**, *63*, 1368-1376.

55. Asher, B. J.; Wong, C. S.; Rodenburg, L. A. Chiral source apportionment of polychlorinated biphenyls to the Hudson River estuary atmosphere and food web. *Environmental Science & Technology* **2007**, *41*, 6163-6169.

56. Wong, C. S.; Pakdeesusuk, U.; Morrissey, J. A.; Lee, C. M.; Coates, J. T.; Garrison, A. W.; Mabury, S. A.; Marvin, C. H.; Muir, D. C. G. Enantiomeric composition of chiral polychlorinated biphenyl atropisomers in dated sediment cores. *Environmental Toxicology and Chemistry* **2007**, *26*, 254-263.

57. Blanch, G. P.; Glausch, A.; Schurig, V. Determination of the enantiomeric ratios of chiral PCB 95 and 149 in human milk samples by multidimensional gas chromatography with ECD and MS (SIM) detection. *European Food Research and Technology* **1999**, *209*, 294-296.

58. Wong, C. S.; Lau, F.; Clark, M.; Mabury, S. A.; Muir, D. C. G. Rainbow trout (*Oncorhynchus mykiss*) can eliminate chiral organochlorine compounds enantioselectively. *Environmental Science & Technology* **2002**, *36*, 1257-1262.

59. Mannschreck, A.; Pustet, N.; Robertson, L. W.; Oesch, F.; Puttmann, M. Enantiomers of polychlorinated-biphenyls semipreparative enrichment by liquid-chromatography. *Liebigs Annalen Der Chemie* **1985**, 2101-2103.

60. Haglund, P. Enantioselective separation of polychlorinated biphenyl atropisomers using chiral high-performance liquid chromatography. *Journal of Chromatography A* **1996**, *724*, 219-228.

61. Reich, S.; Schurig, V. Enantiomerentrennung atropisomerer PCB mittels HPLC. *GIT Spezial* **1999**, *1*, 15-16.

62. Haglund, P.; Wiberg, K. Determination of the gas chromatographic elution sequences of the (+)- and (-)-enantiomers of stable atropisomeric PCBs on Chirasil-Dex. *HRC-Journal of High Resolution Chromatography* **1996**, *19*, 373-376.

63. Konig, W. A. Enantioselective gas-chromatography. *TRAC-Trends in Analytical Chemistry* **1993**, *12*, 130-137.

64. Vetter, W. Enantioselective fate of chiral chlorinated hydrocarbons and their metabolites in environmental samples. *Food Reviews International* **2001**, *17*, 113-182.

65. Konig, W. A.; Gehrcke, B.; Icheln, D.; Evers, P.; Donnecke, J.; Wang, W. C. New selectively substituted cyclodextrins as stationary phases for the analysis of chiral constituents of essential oils. *HRC-Journal of High Resolution Chromatography* **1992**, *15*, 367-372.

66. Konig, W. A.; Gehrcke, B.; Runge, T.; Wolf, C. Gas chromatographic separation of atropisomeric alkylated and polychlorinated biphenyls using modified cyclodextrins. *HRC-Journal of High Resolution Chromatography* **1993**, *16*, 376-378.

67. Schurig, V.; Glausch, A. Enantiomer separation of atropisomeric polychlorinated-biphenyls (PCBs) by gas chromatography on Chirasil-Dex. *Naturwissenschaften* **1993**, *80*, 468-469.

68. Larsen, B. R. HRGC separation of PCB congeners. *HRC-Journal of High Resolution Chromatography* **1995**, *18*, 141-151.

69. Ramos, L.; Hernandez, L. M.; Gonzalez, M. J. Simultaneous separation of coplanar and chiral polychlorinated biphenyls by off-line pyrenyl-silica liquid chromatography and gas chromatography. Enantiomeric ratios of chiral congeners. *Analytical Chemistry* **1999**, *71*, 70-77.

70. Harner, T.; Wiberg, K.; Norstrom, R. J. Enantiomer fractions are prefered to enantiomer raios for describing chiral signatures in environmental analysis. *Environmental Science & Technology* **2000**, *34*, 218-220.

71. Ulrich, E. M.; Helsel, D. R.; Foreman, W. T. Complications with using ratios for environmental data: Comparing enantiomeric ratios (ERs) and enantiomer fractions (EFs). *Chemosphere* **2003**, *53*, 531-538.

72. Glausch, A.; Nicholson, G. J.; Fluck, M.; Schurig, V. Separation of the enantiomers of stable atropisomeric polychlorinated biphenyls (PCBs) by multidimensional gas-chromatography on Chirasil-Dex. *HRC-Journal of High Resolution Chromatography* **1994**, *17*, 347-349.

73. Frame, G. M. A collaborative study of 209 PCB congeners and 6 Aroclors on 20 different HRGC columns. *Fresenius' Journal of Analytical Chemistry* **1997**, *357*, 701-713.

74. Morrissey, J. A.; Bleackley, D. S.; Warner, N. A.; Wong, C. S. Enantiomer fractions of polychlorinated biphenyls in three selected Standard Reference Materials. *Chemosphere* **2007**, *66*, 326-331.

75. Wong, C. S.; Hoestra, P. F.; Karlsson, H.; Backus, S. M.; Mabury, S. A.; Muir, D. C. G. Enantiomer fractions of chiral organochlorine pesticides and polychlorinated biphenyls in standard and certified reference materials. *Chemosphere* **2002**, *49*, 1339-1347.

76. Pakdeesusuk, U.; Jones, W. J.; Lee, C. M.; Garrison, A. W.; O'Niell, W. L.; Freedman, D. L.; Coates, J. T.; Wong, C. S. Changes in enantiomeric fractions during microbial reductive dechlorination of PCB132, PCB149, and Aroclor 1254 in Lake Hartwell sediment microcosms. *Environmental Science & Technology* **2003**, *37*, 1100-1107.

77. Farley, K. J.; Germann, G. G.; Elzerman, A. W. *Environmental Chemistry of Lakes and Reservoirs*. American Chemical Society: Washington, DC., 1994; p 575-600.

78. Quensen, J. F.; Tiedje, J. M.; Boyd, S. A. Reductive dechlorination of polychlorinated-biphenyls by anaerobic microorganisms from sediments. *Science* **1988**, *242*, 752-754.

79. Quensen, J. F.; Boyd, S. A.; Tiedje, J. M. Dechlorination of 4 commercial polychlorinated biphenyl mixtures (Aroclors) by anaerobic microorganisms from sediments. *Applied and Environmental Microbiology* **1990**, *56*, 2360-2369.

80. Brown, J. F.; Wagner, R. E.; Feng, H.; Bedard, D. L.; Brennan, M. J.; Carnahan, J. C.; May, R. J. Environmental dechlorination of PCBs. *Environmental Toxicology and Chemistry* **1987**, *6*, 579-593.

81. Brown, J. F.; Bedard, D. L.; Brennan, M. J.; Carnahan, J. C.; Feng, H.; Wagner, R. E. Polychlorinated biphenyl dechlorination in aquatic sediments. *Science* **1987**, *236*, 709-712.

82. Garcia-Ruiz, C.; Andres, R.; Valera, J. L.; Laborda, F.; Marina, M. L. Monitoring the stereoselectivity of biodegradation of chiral polychlorinated biphenyls using electrokinetic chromatography. *Journal of Separation Science* **2002**, *25*, 17-22.

83. Singer, A. C.; Wong, C. S.; Crowley, D. E. Differential enantioselective transformation of atropisomeric polychlorinated biphenyls by multiple bacterial strains with different inducing compounds. *Applied and Environmental Microbiology* **2002**, *68*, 5756-5759.

84. Alcock, R. E.; Johnston, A. E.; McGrath, S. P.; Berrow, M. L.; Jones, K. C. Long-term changes in the polychlorinated biphenyl content of United Kingdom soils. *Environmental Science & Technology* **1993**, *27*, 1918-1923.

85. Harner, T.; Mackay, D.; Jones, K. C. Model of the long-term exchange of PCBs between soil and the atmosphere in the southern UK. *Environmental Science & Technology* **1995**, *29*, 1200-1209.

86. Harrad, S. J.; Sewart, A. P.; Alcock, R.; Boumphrey, R.; Burnett, V.; Duartedavidson, R.; Halsall, C.; Sanders, G.; Waterhouse, K.; Wild, S. R.; Jones, K. C. Polychlorinated biphenyls (PCBs) in the British environment - Sinks, sources and temporal trends. *Environmental Pollution* **1994**, *85*, 131-146.

87. Jeremiason, J. D.; Hornbuckle, K. C.; Eisenreich, S. J. PCBs in Lake Superior, 1978-1992 - Decreases in water concentrations reflect loss by volatilization. *Environmental Science & Technology* **1994**, *28*, 903-914.

88. Currado, G. M.; Harrad, S. Factors influencing atmospheric concentrations of polychlorinated biphenyls in Birmingham, UK. *Environmental Science & Technology* **2000**, *34*, 78-82.

89. Halsall, C. J.; Lee, R. G. M.; Coleman, P. J.; Burnett, V.; Harding-Jones, P.; Jones, K. C. PCBs in UK urban air. *Environmental Science & Technology* **1995**, *29*, 2368-2376.

90. Bidleman, T. F.; Jantunen, L. M. M.; Wiberg, K.; Harner, T.; Brice, K. A.; Su, K.; Falconer, R. L.; Leone, A. D.; Aigner, E. J.; Parkhurst, W. J. Soil as a source of atmospheric heptachlor epoxide. *Environmental Science & Technology* **1998**, *32*, 1546-1548.

91. Bidleman, T. F.; Falconer, R. L. Enantiomer ratios for apportioning two sources of chiral compounds. *Environmental Science & Technology* **1999**, *33*, 2299-2301.

92. Shen, L.; Wania, F.; Lei, Y. D.; Teixeira, C.; Muir, D. C. G.; Bidleman, T. F. Hexachlorocyclohexanes in the North American atmosphere. *Environmental Science & Technology* **2004**, *38*, 965-975.

93. Harrad, S.; Hazrati, S.; Ibarra, C. Concentrations of polychlorinated biphenyls in indoor air and polybrominated diphenyl ethers in indoor air and dust in Birmingham, United Kingdom: Implications for human exposure. *Environmental Science & Technology* **2006**, *40*, 4633-4638.

94. Jamshidi, A.; Hunter, S.; Hazrati, S.; Harrad, S. Concentrations and chiral signatures of polychlorinated biphenyls in outdoor and indoor air and soil in a major UK conurbation. *Environmental Science & Technology* **2007**, *41*, 2153-2158.

95. Bamford, H. A.; Ko, F. C.; Baker, J. E. Seasonal and annual air-water exchange of polychlorinated biphenyls across Baltimore Harbor and the Northern Chesapeake Bay. *Environmental Science & Technology* **2002**, *36*, 4245-4252.

96. Totten, L. A.; Brunciak, P. A.; Gigliotti, C. L.; Dachs, J.; Glenn, T. R.; Nelson, E. D.; Eisenreich, S. J. Dynamic air-water exchange of polychlorinated biphenyls in the

New York - New Jersey Harbor Estuary. *Environmental Science & Technology* **2001**, *35*, 3834-3840.

97. Gobas, F.; McCorquodale, J. R.; Haffner, G. D. Intestinal absorption and biomagnification of organochlorines. *Environmental Toxicology and Chemistry* **1993**, *12*, 567-576.

98. Grossnickle, N. E. Feeding habits of *Mysis relicta* - An overview. *Hydrobiologia* **1982**, *93*, 101-107.

99. Lester, D. C.; McIntosh, L. Accumulation of polychlorinated biphenyl congeners from Lake Champlain sediments by *Mysis relicta*. *Environmental Toxicology and Chemistry* **1994**, *13*, 1825-1841.

100. Harkey, G. A.; Lydy, M. J.; Kukkonen, J.; Landrum, P. F. Feeding selectivity and assimilation of PAH and PCB in *Diporeia Spp*. *Environmental Toxicology and Chemistry* **1994**, *13*, 1445-1455.

101. Warner, N. A.; Wong, C. S. The freshwater invertebrate *Mysis relicta* can eliminate chiral organochlorine compounds enantioselectively. *Environmental Science & Technology* **2006**, *40*, 4158-4164.

102. Buckman, A. H.; Wong, C. S.; Chow, E. A.; Brown, S. B.; Solomon, K. R.; Fisk, A. T. Biotransformation of polychlorinated biphenyls (PCBs) and bioformation of hydroxylated PCBs in fish. *Aquatic Toxicology* **2006**, *78*, 176-185.

103. Harju, M.; Bergman, A.; Olsson, M.; Roos, A.; Haglund, P. Determination of atropisomeric and planar polychlorinated biphenyls, their enantiomeric fractions and tissue distribution in Grey seals using comprehensive 2D gas chromatography. *Journal of Chromatography A* **2003**, *1019*, 127-142.

104. Lehmler, H. J.; Price, D. J.; Garrison, A. W.; Birge, W. J.; Robertson, L. W. Distribution of PCB 84 enantiomers in C57BL/6 mice. *Fresenius Environmental Bulletin* **2003**, *12*, 254-260.

105. Kania-Korwel, I.; Garrison, A. W.; Avants, J. K.; Hornbuckle, K. C.; Robertson, L. W.; Sulkowski, W. W.; Lehmler, H. J. Distribution of chiral PCBs in selected tissues in the laboratory rat. *Environmental Science & Technology* **2006**, *40*, 3704-3710.

106. Norstrom, K.; Eriksson, J.; Haglund, J.; Silvari, V.; Bergman, A. Enantioselective formation of methyl sulfone metabolites of 2,2',3,3',4,6'-hexachlorobiphenyl in rat. *Environmental Science & Technology* **2006**, *40*, 7649-7655.

107. Kania-Korwel, I.; Shaikh, N. S.; Hornbuckle, K. C.; Robertson, L. W.; Lehmler, H. J. Enantioselective disposition of PCB 136 (2,2 ',3,3 ',6,6 '-hexachlorobiphenyl) in C57BL/6 mice after oral and intraperitoneal administration. *Chirality* **2007**, *19*, 56-66.

108. Livingstone, D. R.; Kirchin, M. A.; Wiseman, A. Cytochrome-P-450 and oxidative-metabolism in mollusks. *Xenobiotica* **1989**, *19*, 1041-1062.

109. Klump, J. V.; Kaster, J. L.; Sierszen, M. E. *Mysis relicta* assimilation of hexachlorobiphenyl from sediments. *Canadian Journal of Fisheries and Aquatic Sciences* **1991**, *48*, (2), 284-289.

110. Landrum, P. F.; Frez, W. A.; Simmons, M. S. The effect of food consumption on the toxicokinetics of benzo(*a*)pyrene and 2,2',4,4',5,5'-hexachlorobiphenyl in *Mysis relicta*. *Chemosphere* **1992**, *25*, 397-415.

111. Landrum, P. F.; Nalepa, T. F. A review of the factors affecting the ecotoxicology of *Diporeia* spp. *Journal of Great Lakes Research* **1998**, *24*, 889-904.

112. Gooch, J. W.; Elskus, A. A.; Kloeppersams, P. J.; Hahn, M. E.; Stegeman, J. J. Effects of *ortho*-substituted and non-*ortho*-substituted polychlorinated biphenyl congeners on the hepatic monooxygenase system in Scup (*Stenotomus-chrysops*). *Toxicology and Applied Pharmacology* **1989**, *98*, 422-433.

113. Kleinow, K. M.; Melancon, M. J.; Lech, J. J. Biotransformation and induction - Implications for toxicity, bioaccumulation and monitoring of environmental xenobiotics in fish. *Environmental Health Perspectives* **1987**, *71*, 105-119.

114. Stegeman, J. J.; Kloeppersams, P. J. Cytochrome P-450 isozymes and monooxygenase activity in aquatic animals. *EnvironmentalHealthPerspectives* **1987**, *71*, 87-95.

115. Stapleton, H. M.; Letcher, R. J.; Baker, J. E. Metabolism of PCBs by the deepwater sculpin (*Myoxocephalus thompsoni*). *Environmental Science & Technology* **2001**, *35*, 4747-4752.

116. Campbell, L. M.; Muir, D. C. G.; Whittle, D. M.; Backus, S.; Norstrom, R. J.; Fisk, A. T. Hydroxylated PCBs and other chlorinated phenolic compounds in lake trout (*Salvelinus namaycush*) blood plasma from the Great Lakes Region. *Environmental Science & Technology* **2003**, *37*, 1720-1725.

117. Bright, D. A.; Grundy, S. L.; Reimer, K. J. Differential bioaccumulation of non-ortho-substituted and other PCB congeners in coastal arctic invertebrates and fish. *Environmental Science & Technology* **1995**, *29*, 2504-2512.

118. Larsson, C.; Ellerichmann, T.; Hühnerfuss, H.; Bergman, A. Chiral PCB methyl sulfones in rat tissues after exposure to technical PCBs. *Environmental Science & Technology* **2002**, *36*, 2833-2838.

119. Wiberg, K.; Letcher, R. J.; Sandau, C. D.; Duffe, J.; Norstrom, R. J.; Haglund, P.; Bidleman, T. F., Enantioselective gas chromatography/mass spectrometry of methylsulfonyl PCBs with application to arctic marine mammals. *Analytical Chemistry* **1998**, *70*, 3845-3852.

120. Larsson, C.; Norstrom, K.; Athanansiadis, I.; Bignert, A.; Konig, W. A.; Bergman, A. Enantiomeric specificity of methylsulfonyl-PCBs and distribution of bis(4-chlorophenyl) sulfone in Grey seal tissues. *Environmental Science & Technology* **2004**, *38*, 4950-4955.

121. Karasek, L.; Hajslova, J.; Rosmus, J.; Huhnerfuss, H. Methylsulfonyl PCB and DDE metabolites and their enantioselective gas chromatographic separation in human adipose tissues, seal blubber and pelican muscle. *Chemosphere* **2007**, *67*, S22-S27.

122. Chu, S. G.; Covaci, A.; Haraguchi, K.; Voorspoels, S.; Van de Vijver, K.; Das, K.; Bouquegneau, J. M.; De Coen, W.; Blust, R.; Schepens, P. Levels and enantiomeric signatures of methyl sulfonyl PCB and DDE metabolites in livers of harbor porpoises (*Phocoena phocoena*) from the southern North Sea. *Environmental Science & Technology* **2003**, *37*, 4573-4578.

123. Ellerichmann, T.; Bergman, A.; Franke, S.; Huhnerfuss, H.; Jakobsson, E.; Konig, W. A.; Larsson, C., Gas chromatographic enantiomer separations of chiral PCB methyl sulfones and identification of selectively retained enantiomers in human liver. *Fresenius Environmental Bulletin* **1998**, *7*, 244-257.

124. Jacobson, J. L.; Fein, G. G.; Jacobson, S. W.; Schwartz, P. M.; Dowler, J. K. Transfer of polychlorinated biphenyls (PCBs) and polybrominated biphenyls (PBBs) across the human placenta and into maternal milk. *American Journal of Public Health* **1984**, *74*, 378-379.

125. Karlsson, H.; Oehme, M.; Skopp, S.; Burkow, I. C., Enantiomer ratios of chlordane congeners are gender specific in cod (*Gadus morhua*) from the Barents Sea. *Environmental Science & Technology* **2000**, *34*, 2126-2130.

126. Boon, J. P.; Eijgenraam, F.; Everaarts, J. M.; Duinker, J. C., A structure activity relationship (SAR) approach towards metabolism of PCBs in marine animals from different trophic levels. *Marine Environmental Research* **1989**, *27*, 159-176.

127. McFarland, V. A.; Clarke, J. U. Environmental occurrence, abundance, and potential toxicity of polychlorinated biphenyl congeners - Considerations for a congener specific analysis. *Environmental Health Perspectives* **1989**, *81*, 225-239.

128. Letcher, R. J.; Klasson-Wehler, E.; Bergman, A. Methyl sulfone and hydroxylated metabolites of polychlorinated biphenyls. In *The Handbook of Environmental Chemistry*, J., P., Ed. Springer-Verlag: Berlin Heidelberg, 2000; Vol. 3, pp 315-359.

129. Lewis, D. F. V. The CYP2 family: models, mutants and interactions. *Xenobiotica* **1998**, *28*, 617-661.

130. Haraguchi, K.; Kuroki, H.; Masuda, Y.; Koga, N.; Kuroki, J.; Hokama, Y.; Yoshimura, H. Toxicological evaluation of sulfur-containing metabolites of 2,5,2',5'-tetrachlorobiphenyl in rats. *Chemosphere* **1985**, *14*, 1755-1762.

131. Koga, N.; Kikuichinishimura, N.; Hara, T.; Harada, N.; Ishii, Y.; Yamada, H.; Oguri, K.; Yoshimura, H., Purification and characterization of a newly identified isoform of cytochrome P-450 responsible for 3-hydroxylation of 2,5,2',5'-tetrachlorobiphenyl in hamster liver. *Archives of Biochemistry and Biophysics* **1995**, *317*, 464-470.

132. Bakke, J. E.; Bergman, A. L.; Larsen, G. L. Metabolism of 2,4', 5-trichlorobiphenyl by the mercapturic acid pathway. *Science* **1982**, *217*, 645-647.

133. Letcher, R. J.; Norstrom, R. J.; Muir, D. C. G. Biotransformation versus bioaccumulation: Sources of methyl sulfone PCB and 4,4 '-DDE metabolites in the polar bear food chain. *Environmental Science & Technology* **1998**, *32*, 1656-1661.

134. Haraguchi, K.; Kuroki, H.; Masuda, Y. Occurrence and distribution of chlorinated aromatic methylsulfones and sulfoxides in biological samples. *Chemosphere* **1989**, *19*, 487-492.

135. Klasson-Wehler, E.; Bergman, A.; Athanasiadou, M.; Ludwig, J. P.; Auman, H. J.; Kannan, K.; Van Den Berg, M.; Murk, A. J. Hydroxylated and methylsulfonyl polychlorinated biphenyl metabolites in albatrosses from Midway Atoll, North Pacific Ocean. *Environmental Toxicology and Chemistry* **1998**, *17*, 1620-1625.

136. Letcher, R. J.; Norstrom, R. J.; Bergman, A. An integrated analytical method for determination of polychlorinated aryl methyl sulfone metabolites and polychlorinated hydrocarbon contaminants in biological matrices. *Analytical Chemistry* **1995**, *67*, 4155-4163.

137. Haraguchi, K.; Athanasiadou, M.; Bergman, A.; Hovander, L.; Jensen, S. PCB and PCB methyl sulfones in selected groups of seals from Swedish waters. *Ambio* **1992**, *21*, 546-549.

138. Janak, K.; Becker, G.; Colmsjo, A.; Ostman, C.; Athanasiadou, M.; Valters, K.; Bergman, A. Methyl sulfonyl polychlorinated biphenyls and 2,2-bis(4-chlorophenyl)-1,1-dichlorethene in gray seal tissues determined by gas chromatography with electron capture detection and atomic emission detection. *Environmental Toxicology and Chemistry* **1998**, *17*, 1046-1055.

139. Troisi, G. M.; Haraguchi, K.; Simmonds, M. P.; Mason, C. F. Methyl sulfone metabolites of polychlorinated biphenyls (PCBs) in cetaceans from the Irish and the Aegean Seas. *Archives of Environmental Contamination and Toxicology* **1998**, *35*, 121-128.

140. Letcher, R. J.; Norstrom, R. J.; Bergman, A., Geographical distribution and identification of methyl sulfone PCB and DDE metabolites in pooled polar bear (*Ursus-maritimus*) adipose tissue from Western Hemisphere Arctic and sub-Arctic Regions. *Science of the Total Environment* **1995**, *161*, 409-420.

141. Weistrand, C.; Noren, K. Methylsulfonyl metabolites of PCBs and DDE in human tissues. *Environmental Health Perspectives* **1997**, *105*, 644-649.

142. Bergman, A.; Norstrom, R. J.; Haraguchi, K. PCB and DDE methyl sulfones in mammals from Canada and Sweden. *Environmental Toxicology and Chemistry* **1994**, *13*, 121-128.

143. Brandt, I.; Bergman, A. PCB methyl sulfones and related compounds - identification of target cells and tissues in different species. *Chemosphere* **1987**, *16*, 1671-1676.

144. Noren, K.; Lunden, A.; Pettersson, E.; Bergman, A. Methylsulfonyl metabolites of PCBs and DDE in human milk in Sweden, 1972-1992. *Environmental Health Perspectives* **1996**, *104*, 766-772.

145. Lund, J.; Nordlund, L.; Devereux, T.; Glaumann, H.; Gustafsson, J. A. Physicochemical and immunochemical characterization of a binding protein for PCB methyl sulfones. *Chemosphere* **1987**, *16*, 1677-1680.

146. Lund, J.; Brandt, I.; Poellinger, L.; Bergman, A.; Klassonwehler, E.; Gustafsson, J. A. Target cells for the polychlorinated biphenyl metabolite 4,4'-Bis(Methylsulfonyl)-2,2',5,5'-tetrachlorobiphenyl - Characterization of high affinity binding in rat and mouse lung cytosol. *Molecular Pharmacology* **1985**, *27*, 314-323.

147. Bergman, A.; Brandt, I.; Darnerud, P. O.; Wachtmeister, C. A. Metabolism of 2,2',5,5'-tetrachlorobiphenyl - Formation of monomethyl and bis-methyl sulfone metabolites with a selective affinity for the lung and kidney tissues in mice. *Xenobiotica* **1982**, *12*, 1-7.

148. Letcher, R. J.; Norstrom, R. J.; Muir, D. C. G.; Sandau, C. D.; Koczanski, K.; Michaud, R.; De Guise, S.; Beland, P. Methylsulfone polychlorinated biphenyl and 2,2-bis(chlorophenyl)-1,1-dichloroethylene metabolites in beluga whale (*Delphinapterus leucas*) from the St. Lawrence River estuary and Western Hudson Bay, Canada. *Environmental Toxicology and Chemistry* **2000**, *19*, 1378-1388.

149. Karlson, K.; Ishaq, R.; Becker, G.; Berggren, P.; Broman, D.; Colmsjo, A. PCBs, DDTs and methyl sulfone metabolites in various tissues of Harbour porpoises from Swedish waters. *Environmental Pollution* **2000**, *110*, 29-46.

150. Huhnerfuss, H.; Bergman, A.; Larsson, C.; Peters, N.; Westendorf, J. Enantioselective transformation of atropisomeric PCBs or of their methylsulfonyl metabolites by rat hepatocytes? *Organohalogen Compounds* **2003**, *62*, 265-268.

151. Sandau, C. D.; Ayotte, P.; Dewailly, E.; Duffe, J.; Norstrom, R. J. Analysis of hydroxylated metabolites of PCBs (OH-PCBs) and other chlorinated phenolic compounds in whole blood from Canadian Inuit. *Environmental Health Perspectives* **2000**, *108*, 611-616.

152. Bergman, A.; Klassonwehler, E.; Kuroki, H., Selective retention of hydroxylated PCB metabolites in blood. *Environmental Health Perspectives* **1994**, *102*, 464-469.

153. Berger, U.; Herzke, D.; Sandanger, T. M. Two trace analytical methods for determination of hydroxylated PCBs and other halogenated phenolic compounds in eggs from Norwegian birds of prey. *Analytical Chemistry* **2004**, *76*, 441-452.

154. Hoekstra, P. F.; Letcher, R. J.; O'Hara, T. M.; Backus, S. M.; Solomon, K. R.; Muir, D. C. G. Hydroxylated and methylsulfone containing metabolites of polychlorinated biphenyls in the plasma and blubber of bowhead whales (*Balaena mysticetus*). *Environmental Toxicology and Chemistry* **2003**, *22*, 2650-2658.

155. Sandala, G. M.; Sonne-Hansen, C.; Dietz, R.; Muir, D. C. G.; Valters, K.; Bennett, E. R.; Born, E. W.; Letcher, R. J. Hydroxylated and methyl sulfone PCB metabolites in adipose and whole blood of polar bear (*Ursus maritimus*) from East Greenland. *Science of the Total Environment* **2004**, *331*, 125-141.

156. Houde, M.; Pacepavicius, G.; Wells, R. S.; Fair, P. A.; Letcher, R. J.; Alaee, M.; Bossart, G. D.; Hohn, A. A.; Sweeney, J.; Solomon, K. R.; Muir, D. C. G. Polychlorinated biphenyls and hydroxylated polychlorinated biphenyls in plasma of Bottlenose dolphins (*Tursiops truncatus*) from the Western Atlantic and the Gulf of Mexico. *Environmental Science & Technology* **2006**, *40*, 5860-5866.

157. Kunisue, T.; Sakiyama, T.; Yamada, T. K.; Takahashi, S.; Tanabe, S. Occurrence of hydroxylated polychlorinated biphenyls in the brain of cetaceans stranded along the Japanese coast. *Marine Pollution Bulletin* **2007**, *54*, 963-973.

158. Ueno, D.; Darling, C.; Alaee, M.; Campbell, L.; Pacepavicius, G.; Teixeira, C.; Muir, D. C. G. Detection of hydroxylated polychlorinated biphenyls (OH-PCBs) in the abiotic environment: Surface water and precipitation from Ontario, Canada. *Enviromental. Science &. Technology* **2007**, *41*, 1841-1848.

159. Guvenius, D. M.; Hassanzadeh, P.; Bergman, A.; Noren, K. Metabolites of polychlorinated biphenyls in human liver and adipose tissue. *Environmental Toxicology and Chemistry* **2002**, *21*, 2264-2269.

160. Brouwer, A.; Klassonwehler, E.; Bokdam, M.; Morse, D. C.; Traag, W. A. Competitive inhibition of thyroxine binding to transthyretin by monohydroxy metabolites of 3,4,3',4'-tetrachlorobiphenyl. *Chemosphere* **1990**, *20*, 1257-1262.

161. Haraguchi, K.; Kato, Y.; Kimura, R.; Masuda, Y. Comparative study on formation of hydroxy and sulfur-containing metabolites from different chlorinated biphenyls with 2,5-substitution in rats. *Drug Metabolism and Disposition* **1997**, *25*, 845-852.

162. Hovander, L.; Malmberg, T.; Athanasiadou, M.; Athanassiadis, I.; Rahm, S.; Bergman, A.; Klasson-Wehler, E. Identification of hydroxylated PCB metabolites and other phenolic halogenated pollutants in human blood. *Archives of Environmental Contamination and Toxicology* **2002**, *42*, 105-117.

163. Shigematsu, N.; Ishimaru, S.; Saito, R.; Ikeda, T.; Matsuba, K.; Sugiyama, K.; Masuda, Y. Respiratory involvement in polychlorinated biphenyls poisoning. *Environmental Research* **1978**, *16*, 92-100.

164. Kato, Y.; Haraguchi, K.; Shibahara, T.; Masuda, Y.; Kimura, R. Reduction of thyroid hormone levels by methylsulfonyl metabolites of polychlorinated biphenyl congeners in rats. *Archives of Toxicology* **1998**, *72*, 541-544.

165. Letcher, R. J.; van Holsteijn, I.; Drenth, H. J.; Norstrom, R. J.; Bergman, A.; Safe, S.; Pieters, R.; van den Berg, M. Cytotoxicity and aromatase (CYP19) activity modulation by organochlorines in human placental JEG-3 and JAR choriocarcinoma cells. *Toxicology and Applied Pharmacology* **1999**, *160*, 10-20.

166. Lund, B. O.; Orberg, J.; Bergman, A.; Larsson, C.; Backlin, B. M.; Hakansson, H.; Madej, A. Chronic and reproductive toxicity of a mixture of 15 methylsulfonyl-polychlorinated biphenyls and 3-methylsulfonyl-2,2-bis-(4-chlorophenyl)-1,1-dichloroethene in mink (*Mustela vison*). *Environmental Toxicology and Chemistry* **1999**, *18*, 292-298.

167. Brouwer, A.; Morse, D. C.; Lans, M. C.; Schuur, A. G.; Murk, A. J.; Klasson-Wehler, E.; Beroman, A.; Visser, T. J. Interactions of persistent environmental organohalogens with the thyroid hormone system: Mechanisms and possible

consequences for animal and human health. *Toxicology & Industrial Health* **1998**, *14*, 59-84.

168. Kitamura, S.; Jinno, N.; Suzuki, T.; Sugihara, K.; Ohta, S.; Kuroki, H.; Fujimoto, N. Thyroid hormone-like and estrogenic activity of hydroxylated PCBs in cell culture. *Toxicology* **2005**, *208*, 377-387.
169. Sinjari, T.; Darnerud, P. O. Hydroxylated polychlorinated biphenyls: placental transfer and effects on thyroxine in the foetal mouse. *Xenobiotica* **1998**, *28*, 21-30.
170. Meerts, I.; Assink, Y.; Cenijn, P. H.; van den Berg, J. H. J.; Weijers, B. M.; Bergman, A.; Koeman, J. H.; Brouwer, A. Placental transfer of a hydroxylated polychlorinated biphenyl and effects on fetal and maternal thyroid hormone homeostasis in the rat. *Toxicological Sciences* **2002**, *68*, 361-371.
171. Halldin, K.; Bergman, A.; Brandt, I.; Brunstrom, B. Developmental toxicity in Japanese quail exposed to hydroxylated metabolites of PCBs in ovo. *Avian and Poultry Biology Reviews* **2005**, *16*, 11-17.
172. Connor, K.; Ramamoorthy, K.; Moore, M.; Mustain, M.; Chen, I.; Safe, S.; Zacharewski, T.; Gillesby, B.; Joyeux, A.; Balaguer, P. Hydroxylated polychlorinated biphenyls (PCBs) as estrogens and antiestrogens: Structure-activity relationships. *Toxicology and Applied Pharmacology* **1997**, *145*, 111-123.
173. Machala, M.; Blaga, L.; Lehmler, H. J.; Pliskova, M.; Majkova, Z.; Kapplova, P.; Sovadinova, I.; Vondracek, J.; Malmberg, T.; Robertson, L. W. Toxicity of hydroxylated and quinoid PCB metabolites: Inhibition of gap junctional intercellular communication and activation of aryl hydrocarbon and estrogen receptors in hepatic and mammary cells. *Chemical Research in Toxicology* **2004**, *17*, 340-347.
174. Martinez, J. M.; Stephens, L. C.; Jones, L. A., Long-term effects of neonatal exposure to hydroxylated polychlorinated biphenyls in the BALB/CCRGL mouse. *Environmental Health Perspectives* **2005**, *113*, 1022-1026.
175. James, M. O.; Kleinow, K. M.; Zhang, Y. B.; Zheng, R.; Wang, L. Q.; Faux, L. R. Increased toxicity of benzo(*a*)pyrene-7,8-dihydrodiol in the presence of polychlorobiphenylols. *Marine Environmental Research* **2004**, *58*, 343-346.
176. Sterling, I. The biological importance of polynyas in the Canadian Arctic. *Arctic* **1980**, *33*, 303-315.

177. Fisk, A. T.; Hobson, K. A.; Norstrom, R. J. Influence of chemical and biological factors on trophic transfer of persistent organic pollutants in the Northwater Polynya marine food web. *Environmental Science & Technology* **2001**, *35*, 732-738.

178. Moisey, J.; Fisk, A. T.; Hobson, K. A.; Norstrom, R. J. Hexachlorocyclohexane (HCH) isomers and chiral signatures of alpha-HCH in the arctic marine food web of the Northwater Polynya. *Environmental Science & Technology* **2001**, *35*, 1920-1927.

179. Hoekstra, P. F.; O'Hara, T. M.; Karlsson, H.; Solomon, K. R.; Muir, D. C. G. Enantiomer specific biomagnification of alpha hexachlorocyclohexane and selected chiral chlordane related compounds within an arctic marine food web. *Environmental Toxicology and Chemistry* **2003**, *22*, 2482-2491.

180. Borga, K.; Fisk, A. T.; Hoekstra, P. F.; Muir, D. C. G. Biological and chemical factors of importance in the bioaccumulation and trophic transfer of persistent organochlorine contaminants in arctic marine food webs. *Environmental Toxicology and Chemistry* **2004**, *23*, 2367-2385.

181. Fisk, A. T.; Holst, M.; Hobson, K. A.; Duffe, J.; Moisey, J.; Norstrom, R. J. Persistent organochlorine contaminants and enantiomeric signatures of chiral pollutants in ringed seals (*Phoca hispida*) collected on the east and west side of the Northwater Polynya, Canadian Arctic. *Archives of Environmental Contamination and Toxicology* **2002**, *42*, 118-126.

182. Buckman, A. H.; Norstrom, R. J.; Hobson, K. A.; Karnovsky, N. J.; Duffe, J.; Fisk, A. T. Organochlorine contaminants in seven species of Arctic seabirds from Northern Baffin Bay. *Environmental Pollution* **2004**, *128*, 327-338.

183. Wiberg, K.; Letcher, R. J.; Sandau, C. D.; Norstrom, R. J.; Tysklind, M.; Bidleman, T. F. The enantioselective bioaccumulation of chiral chlordane and alpha-HCH contaminants in the polar bear food chain. *Environmental Science & Technology* **2000**, *34*, 2668-2674.

184. Fisk, A. T.; Moisey, J.; Hobson, K. A.; Karnovsky, N. J.; Norstrom, R. J. Chlordane components and metabolites in seven species of Arctic seabirds from the Northwater Polynya: Relationships with stable isotopes of nitrogen and enantiomeric fractions of chiral components. *Environmental Pollution* **2001**, *113*, 225-238.

185. Chu, S.; Covaci, A.; Haraguchi, K.; Voorspoels, S.; Van De Vijver, K.; Das, K.; Bouquegneau, J. M.; De Coen, W.; Blust, R.; Schepens, P., Levels and enantiomeric signatures of methyl sulfonyl PCB and DDE metabolites in livers of Harbor porpoises from the Southern North Sea. *Environmental Science & Technology* **2003**, *37*, 4573-4578.

186. Michener, R. H.; Schell, D. M. Stable isotope ratios as tracers in marine and aquatic food webs. In *Stable Isotopes in Ecology and Environmental Science*, Lajtha, K.; Michener, R. H., Eds. Blackwell Scientific Publications: Oxford, 1994; pp 138-157.

187. Borga, K.; Bidleman, T. F. Enantiomer fractions of organic chlorinated pesticides in arctic marine lee fauna, zooplankton, and benthos. *Environmental Science & Technology* **2005**, *39*, 3464-3473.

188. Hobson, K. A.; Fisk, A. T.; Karnovsky, N.; Holst, M.; Gagnon, J. M.; Fortier, M. A stable isotope (13C, 15N) model for the North Water food web: Implications for evaluating trophodynamics and the flow of energy and contaminants. *Deep-Sea Research II* **2002**, *49*, 5131-5150.

189. Drouillard, K. G.; Fernie, K. J.; Smits, J. E.; Bortolotti, G. R.; Bird, D. M.; Norstrom, R. J. Bioaccumulation and toxicolkinetics of 42 polychlorinated biphenyl congeners in American kestrels. *Environmental Toxicology and Chemistry* **2001**, *20*, 2514-2522.

190. Walker, C. H. Persistent pollutants in fish-eating sea birds - Bioaccumulation, metabolism and effects. *Aquatic Toxicology* **1990**, *17*, 293-324.

191. Matthews, H. B.; Dedrick, R. L. Pharmacokinetics of PCBs. *Annual Review of Pharmacology and Toxicology* **1984**, *24*, 85-103.

192. Wolkers, J.; Witkamp, R. F.; Nijmeijer, S. M.; Burkow, I. C.; de Groene, E. M.; Lydersen, C.; Dahle, S.; Monshouwer, M. Phase I and phase II enzyme activities in Ringed seals (*Phoca hispida*): Characterization of hepatic cytochrome P-450 by activity patterns, inhibitions studies, mRNA analyses, and western blotting. *Aquatic Toxicology* **1998**, 103-115.

193. Van Duyn-Henderson, J. A.; Lasenby, D. C. Zinc and cadmium transport by the vertically migrating opossum shrimp, *Mysis relicta*. *Canadian Journal of Fisheries and Aquatic Sciences* **1986**, *43*, 1726-1732.

194. Foreman, W. T.; Conner, B. F.; T., F. E.; Vaught, D. G.; Merten, L. M. *Methods of analysis by the U.S. Geological Survey National Water Quality Laboratory - Determination of organochlorine pesticides and polychlorinated biphenyls in sediment by dual capillary column gas chromatography with electron capture detector.* U.S. Geological Survey Open-File Report: 1995, p 95-140.

195. Adare, K. I.; Lasenby, D. C. Seasonal changes in the total lipid content of the opossum shrimp, *Mysis relicta* (*Malacostraca, Mysidacea*). *Canadian Journal of Fisheries and Aquatic Sciences* **1994**, *51*, 1935-1941.

196. Matthews, H. B.; Anderson, M. W., Effect of chlorination on the distributin and excretion of polychlorinated biphenyls. *Drug Metabolism and Disposition* **1975**, *3*, 371-380.

197. Lutz, R. J.; Dedrick, R. L.; Matthews, H. B.; Eling, T. E.; Anderson, M. W. Preliminary pharmacokinetic model for several chlorinated biphenyls in rat. *Drug Metabolism and Disposition* **1977**, *5*, 386-396.

198. Bachmann, A.; Walet, P.; Wijnen, P.; de Bruin, W.; Huntjens, J. L.; Roelofsen, W.; Zehnder, A. J. Biodegradation of alpha- and beta-hexachlorocyclohexane in a soil slurry under different redox conditions. *Applied and Environmental Microbiology.* **1988**, *54*, 143-149.

199. Willett, K. L.; Ulrich, E. M.; Hites, R. A. Differential toxicity and environmental fates of hexachlorocyclohexane isomers. *Environmental Science & Technology* **1998**, *32*, 2197-2207.

200. Degraeve, G. M.; Reynolds, J. B. Feeding behavior and temperature and light tolerance of *Mysis relicta* in laboratory. *Transactions of the American Fisheries Society* **1975**, *104*, 394-397.

201. Lasenby, D. C.; Langford, R. R. Growth, life-history, and respiration of *Mysis relicta* in an arctic and temperate lake. *Journal of theFisheries Research Board of Canada* **1972**, *29*, 1701-.

202. Hawker, D. W.; Connell, D. W. Octanol water partition coefficients of polychlorinated biphenyl congeners. *Environmental Science & Technology* **1988**, *22*, 382-387.

203. Evans, M. S.; Landrum, P. F., Toxicokinetics of DDE, benzo(*a*)pyrene, and 2, 4, 5, 2', 4', 5'-hexachlorobiphenyl in *Pontoporeia hoyi* and *Mysis relicta*. *Journal of Great Lakes Research* **1989**, *15*, 589-600.

204. Parker, J. I. Predation by *Mysis relicta* on *Pontoporeia hoyi*: A food chain link to potential importance in the Great Lakes. *Journal of Great Lakes Research* **1980**, *6*, 164-166.

205. Cooper, S. D.; Goldman, C. R. Opossum shrimp (*Mysis relicta*) Predation on zooplankton. *Canadian Journal of Fisheries and Aquatic Sciences* **1980**, *37*, 909-919.

206. Clark, K. E.; Mackay, D. Dietary uptake and biomagnification of 4 chlorinated hydrocarbons by guppies. *Environmental Toxicology and Chemistry* **1991**, *10*, 1205-1217.

207. Evans, M. S.; Noguchi, G. E.; Rice, C. P. The biomagnification of polychlorinated-biphenyls, toxaphene, and DDT compounds in a Lake Michigan offshore food web. *Archives of Environmental Contamination and Toxicology* **1991**, *20*, 87-93.

208. Gobas, F. A. P. C.; Zhang, X.; Wells, R. Gastrointestinal magnification: The mechanism of biomagnification and food chain accumulation of organic chemicals. *Environmental Science & Technology* **1993**, *27*, 2855-2863.

209. Fisk, A. T.; Norstrom, R. J.; Cymbalisty, C. D.; Muir, D. C. G. Dietary accumulation and depuration of hydrophobic organochlorines: Bioaccumulation parameters and their relationship with the octanol/water partition coefficient. *Environmental Toxicology and Chemistry* **1998**, *17*, 951-961.

210. Li, H. X.; Boon, J. P.; Lewis, W. E.; van den Berg, M.; Nyman, M.; Letcher, R. J. Hepatic microsomal cytochrome P-450 enzyme activity in relation to in vitro metabolism/inhibition of polychlorinated biphenyls and testosterone in Baltic grey seal (*Halichoerus grypus*). *Environmental Toxicology and Chemistry* **2003**, *22*, 636-644.

211. Müller, T. A.; Kohler, H. P. E. Chirality of pollutants-effects on metabolism and fate. *Applied Microbiology and Biotechnology* **2004**, *64*, 300-316.